

Supplementary Information

Site-specific substitution in atomically precise carboranethiol-protected nanoclusters and concomitant changes in electronic properties

Vivek Yadav¹, Arijit Jana¹, Swetashree Acharya¹, Sami Malola², Harshita Nagar¹, Ankit Sharma³, Amoghavarsha R. Kini¹, Sudhadevi Antharjanam⁴, Jan Machacek⁵, Kumaran Nair Valsala Devi Adarsh^{*3}, Tomas Base^{*5}, Hannu Häkkinen^{*2}, and Thalappil Pradeep^{*1}

1 DST Unit of Nanoscience (DST UNS) and Thematic Unit of Excellence (TUE), Department of Chemistry, Indian Institute of Technology, Madras, Chennai – 600036, India

2 Department of Physics and Chemistry, Nanoscience Center, University of Jyväskylä, FI 40014 Jyväskylä, Finland

3 Department of Physics, Indian Institute of Science Education, and Research Bhopal, Bhopal-462066, India

4 Sophisticated Analytical Instruments Facility (SAIF), Indian Institute of Technology, Madras, Chennai – 600036, India

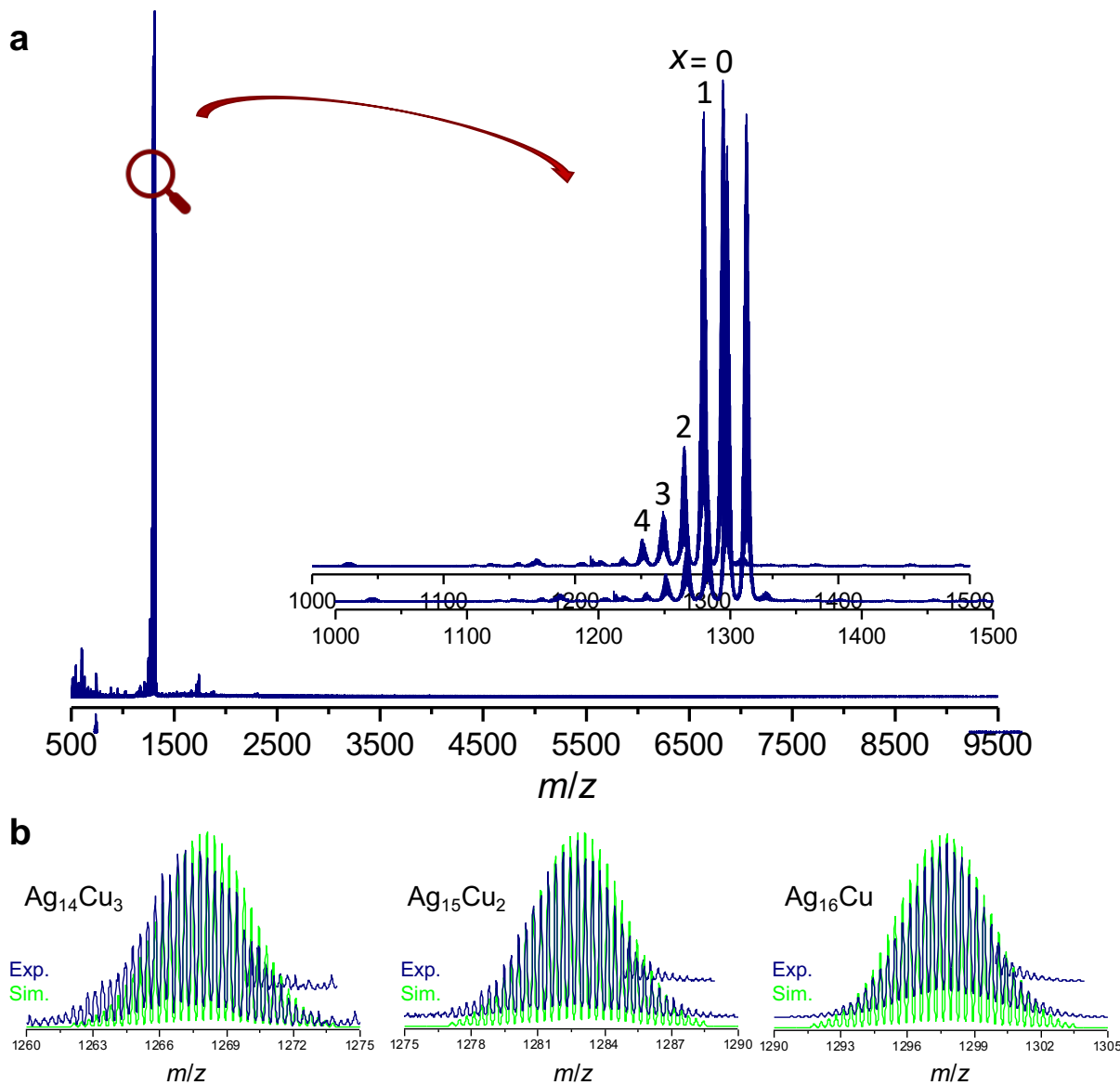
5 Department of Synthesis, Institute of Inorganic Chemistry, The Czech Academy of Science, 1001 Husinec-Rez, 25068, Czech Republic

*Corresponding authors email: pradeep@iitm.ac.in, hannu.j.hakkinen@jyu.fi, tbase@iic.acs.cz, adarsh@iiserb.ac.in

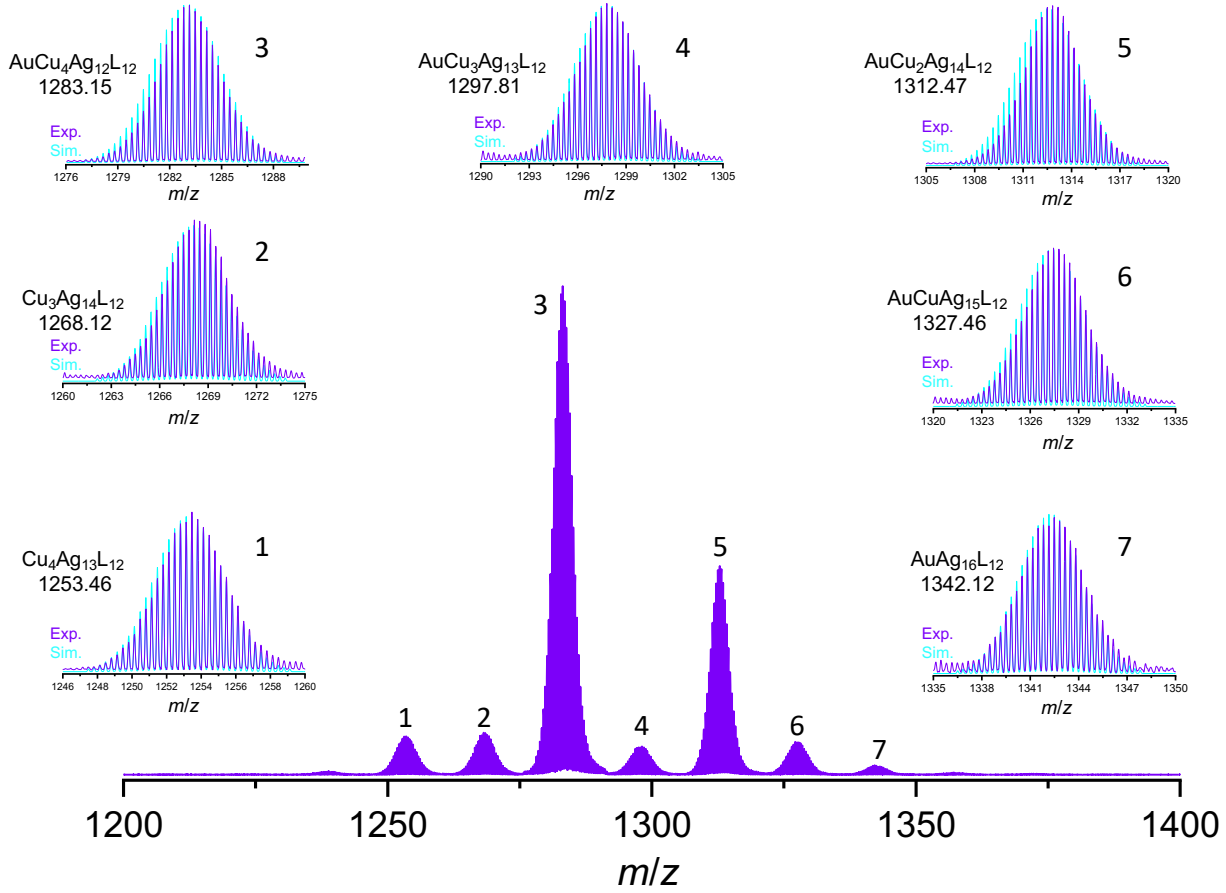
Table of Contents

Supplementary Figures	S2-S42
Supplementary Tables	S43-S66

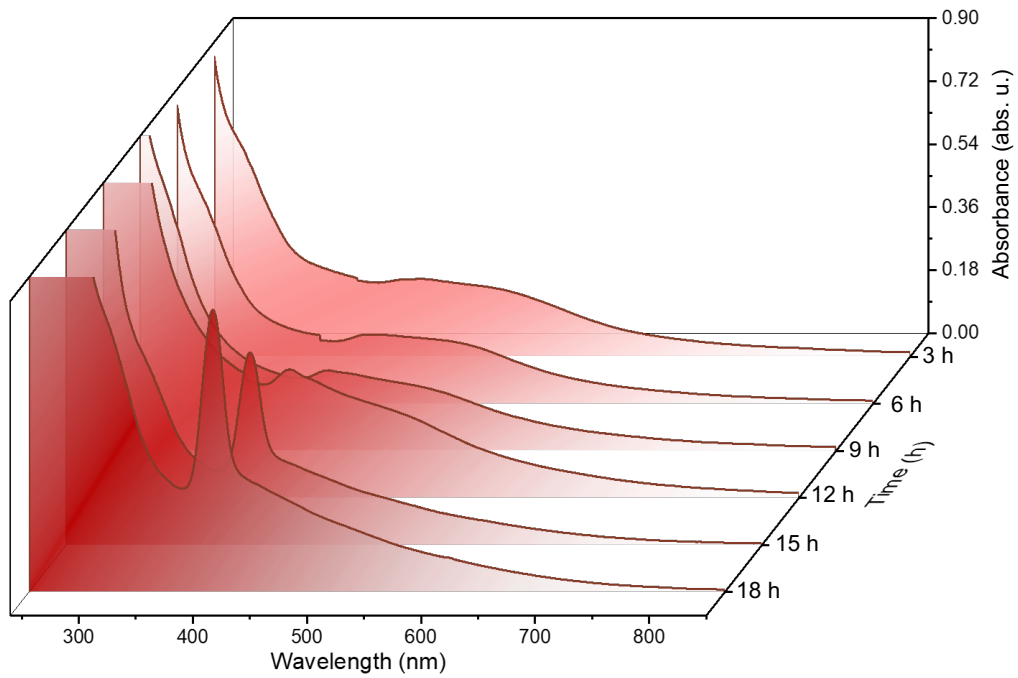
Supplementary Figures



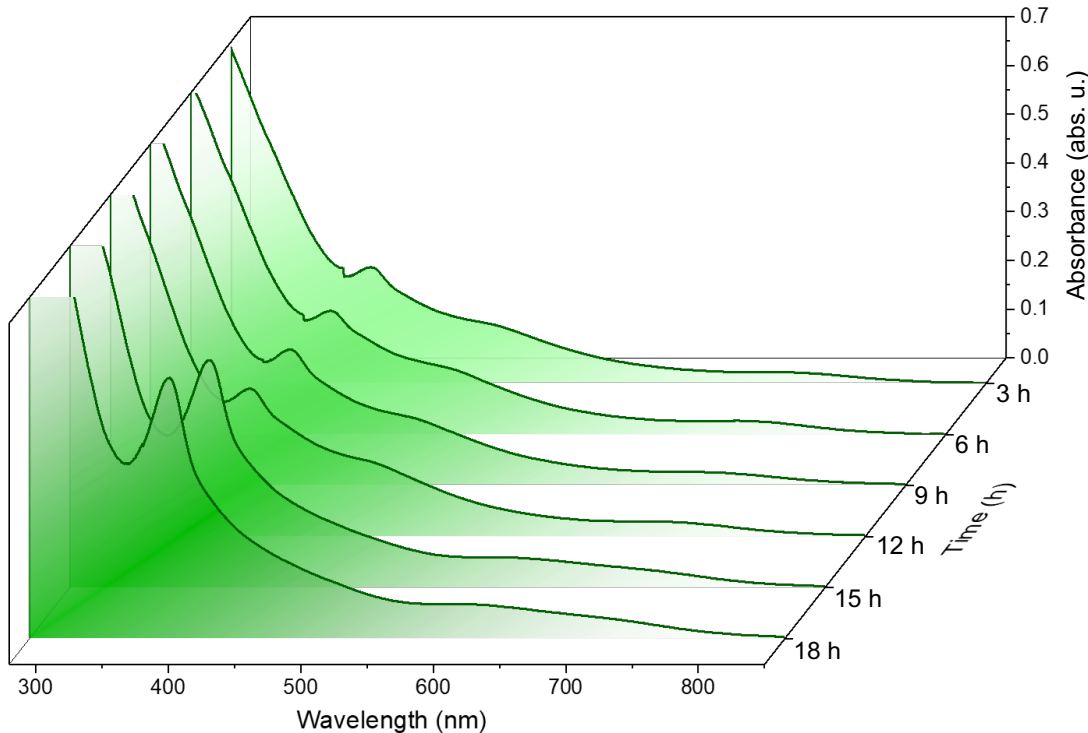
Supplementary Fig. 1 | a Mass Spectrum of the initial synthesis trial for incorporating Cu in Ag_{17} NC showing a mixture of products as $\text{Ag}_{17-x}\text{Cu}_x$ ($x = 0-4$). **b** Exact matching of the isotopic distributions of the experimental (dark blue) and simulated spectra (light green) of $\text{Ag}_{14}\text{Cu}_3$, $\text{Ag}_{15}\text{Cu}_2$ and Ag_{16}Cu NCs.



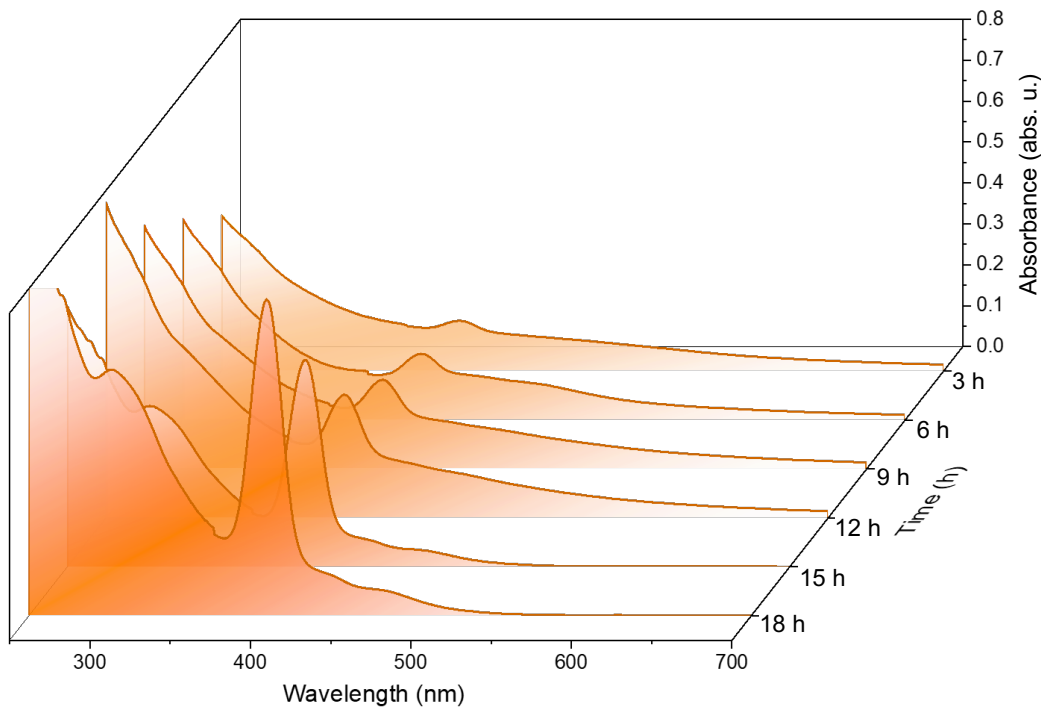
Supplementary Fig. 2 | Mass spectrum of $\text{AuAg}_{12}\text{Cu}_4$ showing multiple peaks assigned and their exact matching of the isotopic distributions of the experimental (deep purple) and simulated (cyan) spectra.



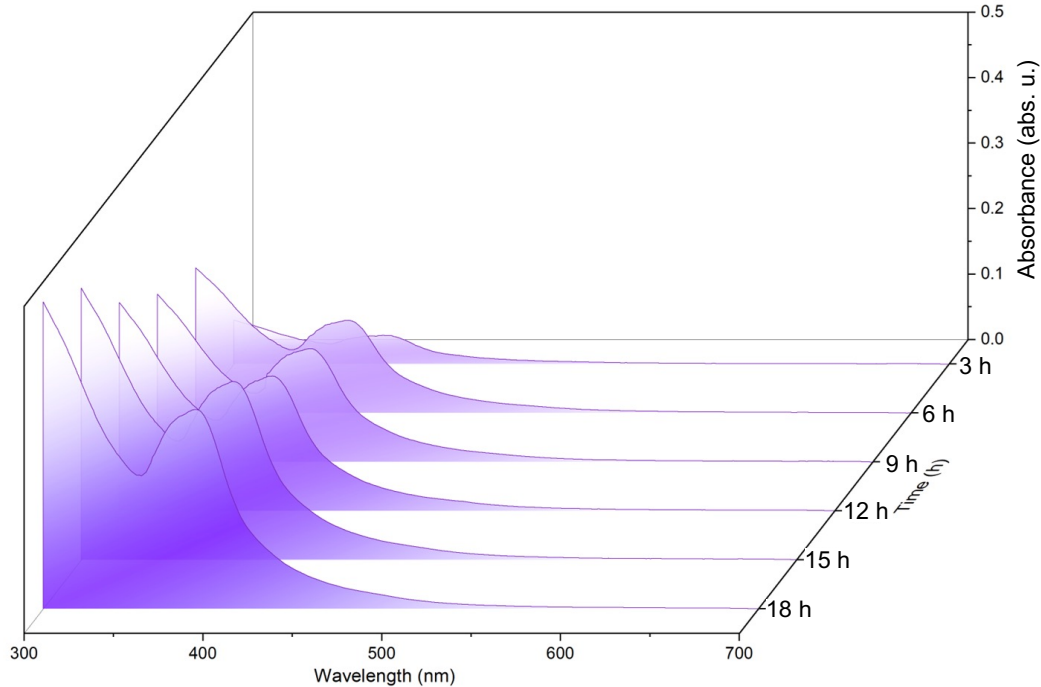
Supplementary Fig. 3 | Time dependent UV-Vis absorption spectra of the Ag_{17} , after the addition of NaBH_4 during the synthesis. The cluster Ag_{17} started forming after 15 h of reaction.



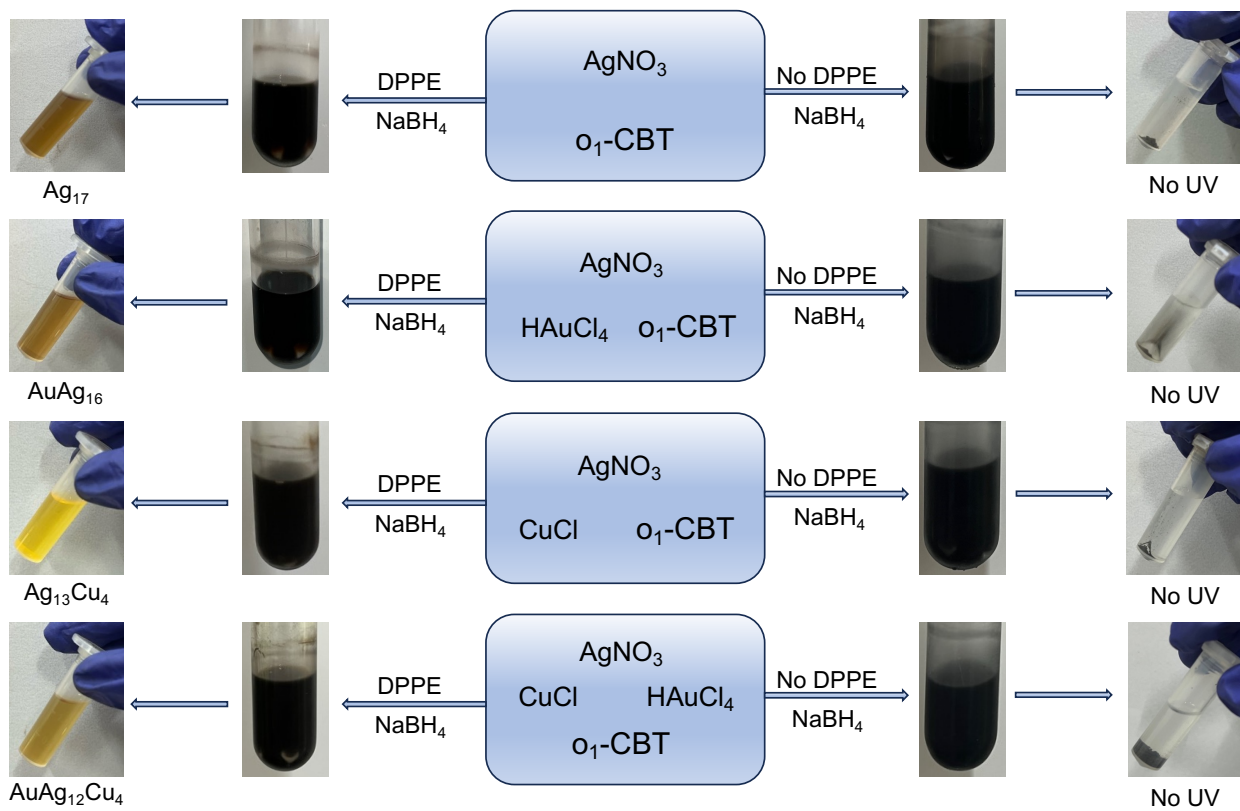
Supplementary Fig. 4 | Time sequence UV-Vis absorption spectra of the AuAg_{16} , after the addition of NaBH_4 during the synthesis. The AuAg_{16} started forming after 15 h of reaction.



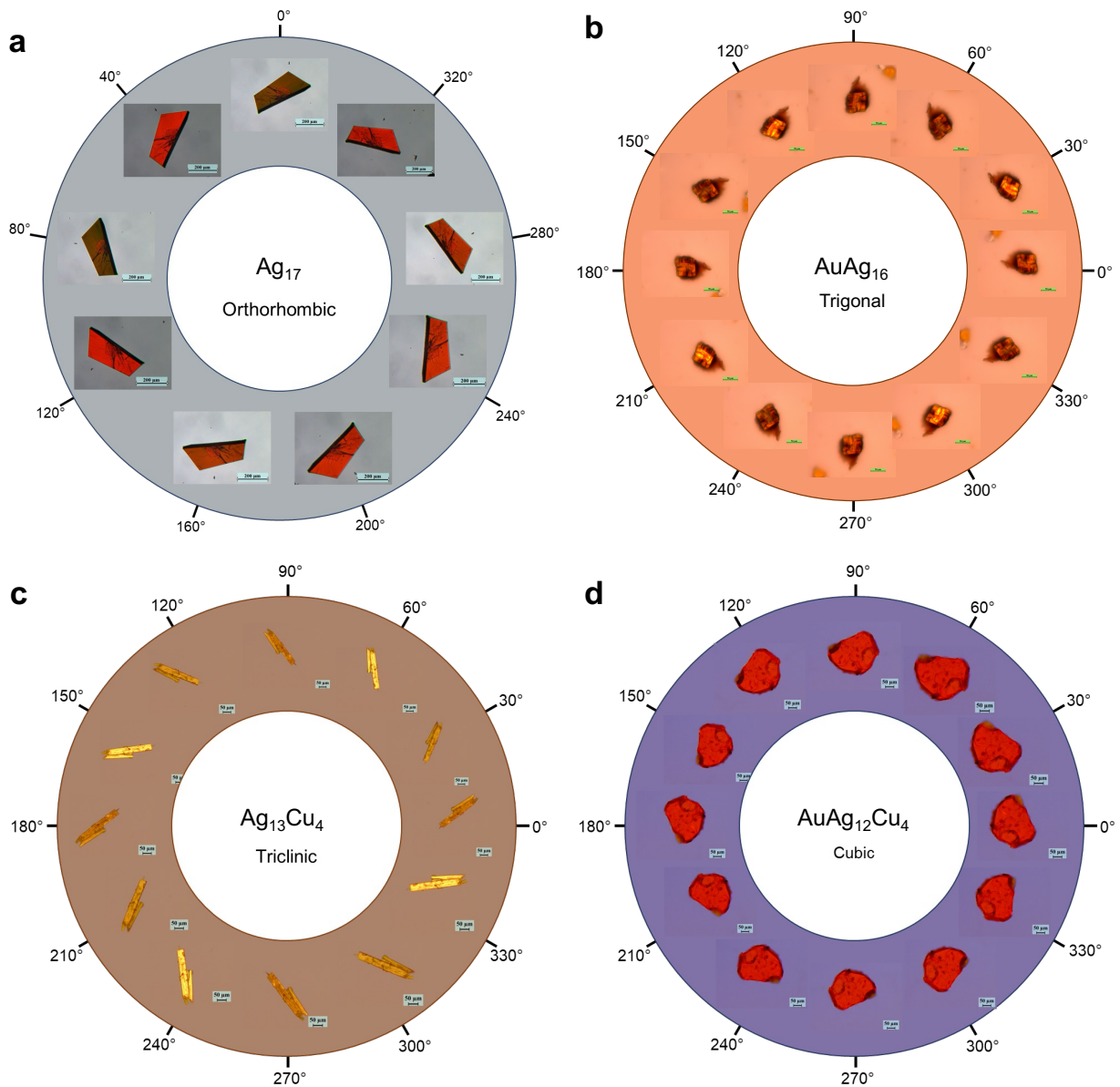
Supplementary Fig. 5 | Time dependent UV-Vis absorption spectra of $\text{Ag}_{13}\text{Cu}_4$, after the addition of NaBH_4 during the synthesis. The $\text{Ag}_{13}\text{Cu}_4$ started forming after 12 h of reaction.



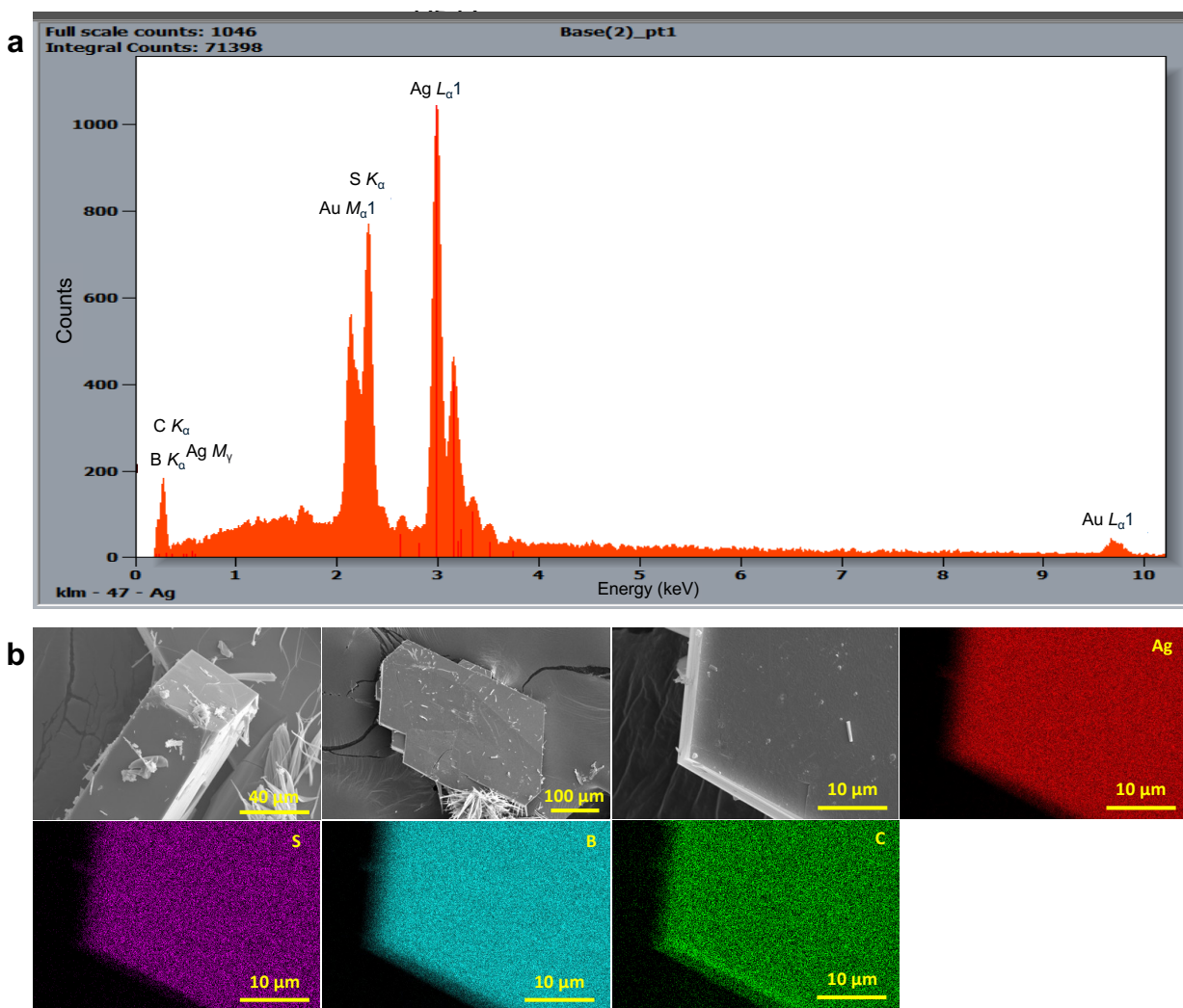
Supplementary Fig. 6 | Time sequence UV-Vis absorption spectra of $\text{AuAg}_{12}\text{Cu}_4$, after the addition of NaBH_4 during the synthesis. The $\text{AuAg}_{12}\text{Cu}_4$ started forming after 12 h of reaction.



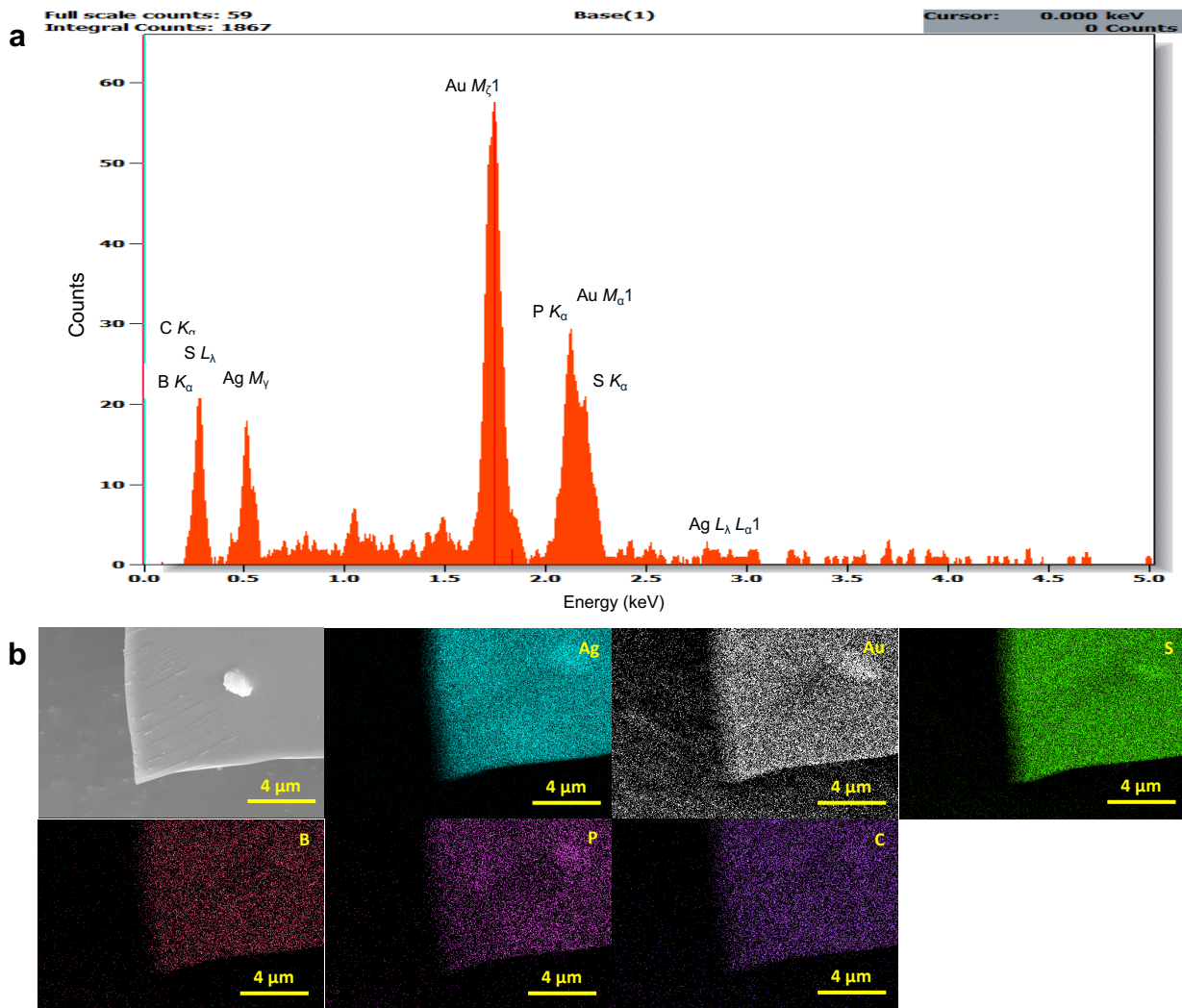
Supplementary Fig. 7 | Photographic images of the different synthetic steps of all the four clusters with and without DPPE. No product was formed without DPPE as a supporting ligand.



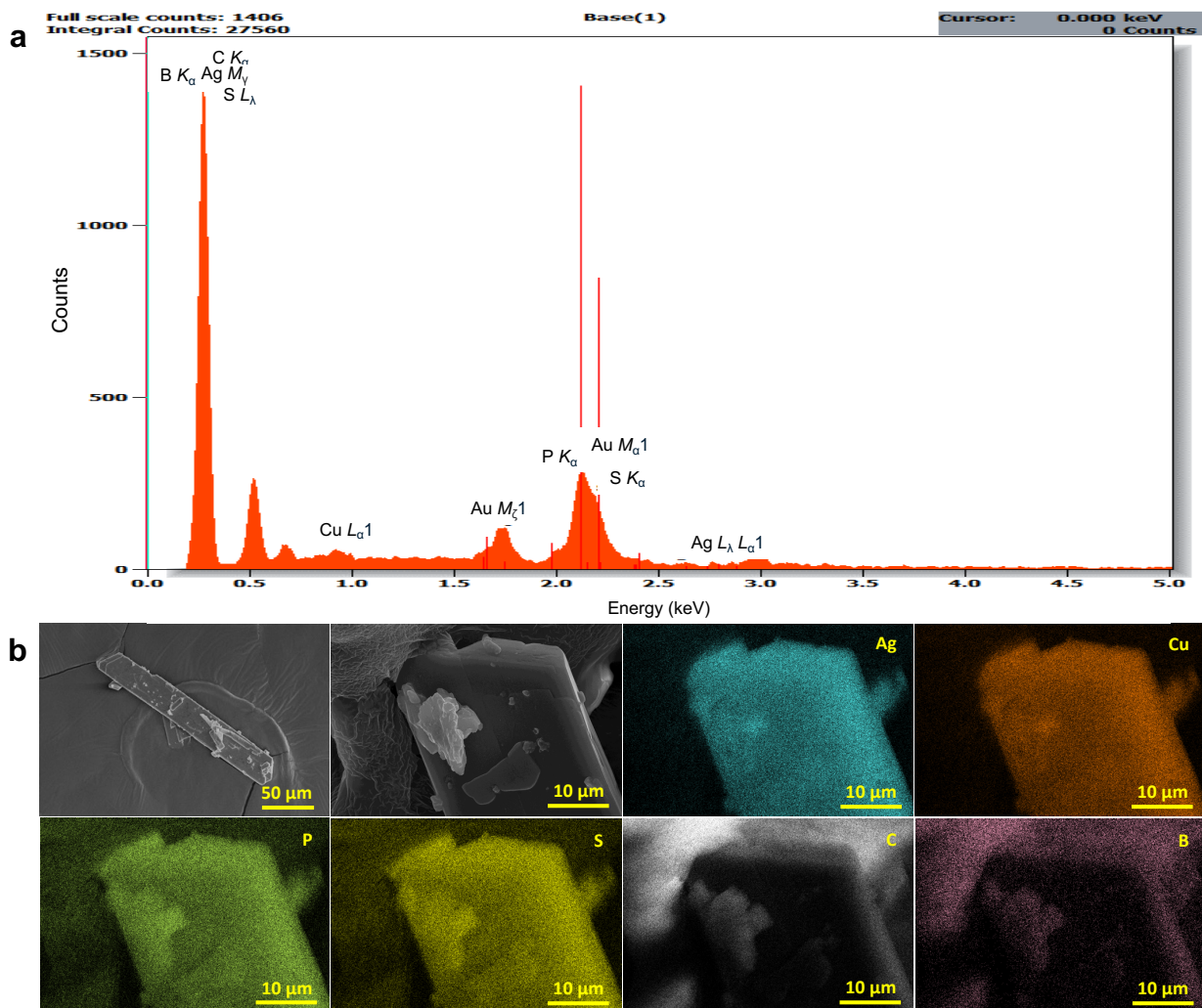
Supplementary Fig. 8 | Optical microscopic images of **a** Ag_{17} , (Scale bar: 200 μm) **b** AuAg_{16} , (Scale bar: 50 μm) **c** $\text{Ag}_{13}\text{Cu}_4$ (Scale bar: 50 μm) and **d** $\text{AuCu}_4\text{Ag}_{12}$ (Scale bar: 50 μm) single crystal under the polarizer at various rotation. Distinct optical polarization was observed for Ag_{17} , AuAg_{16} and $\text{Ag}_{13}\text{Cu}_4$ cluster crystals. Such polarization was absent for trimetallic $\text{AuCu}_4\text{Ag}_{12}$ cluster.



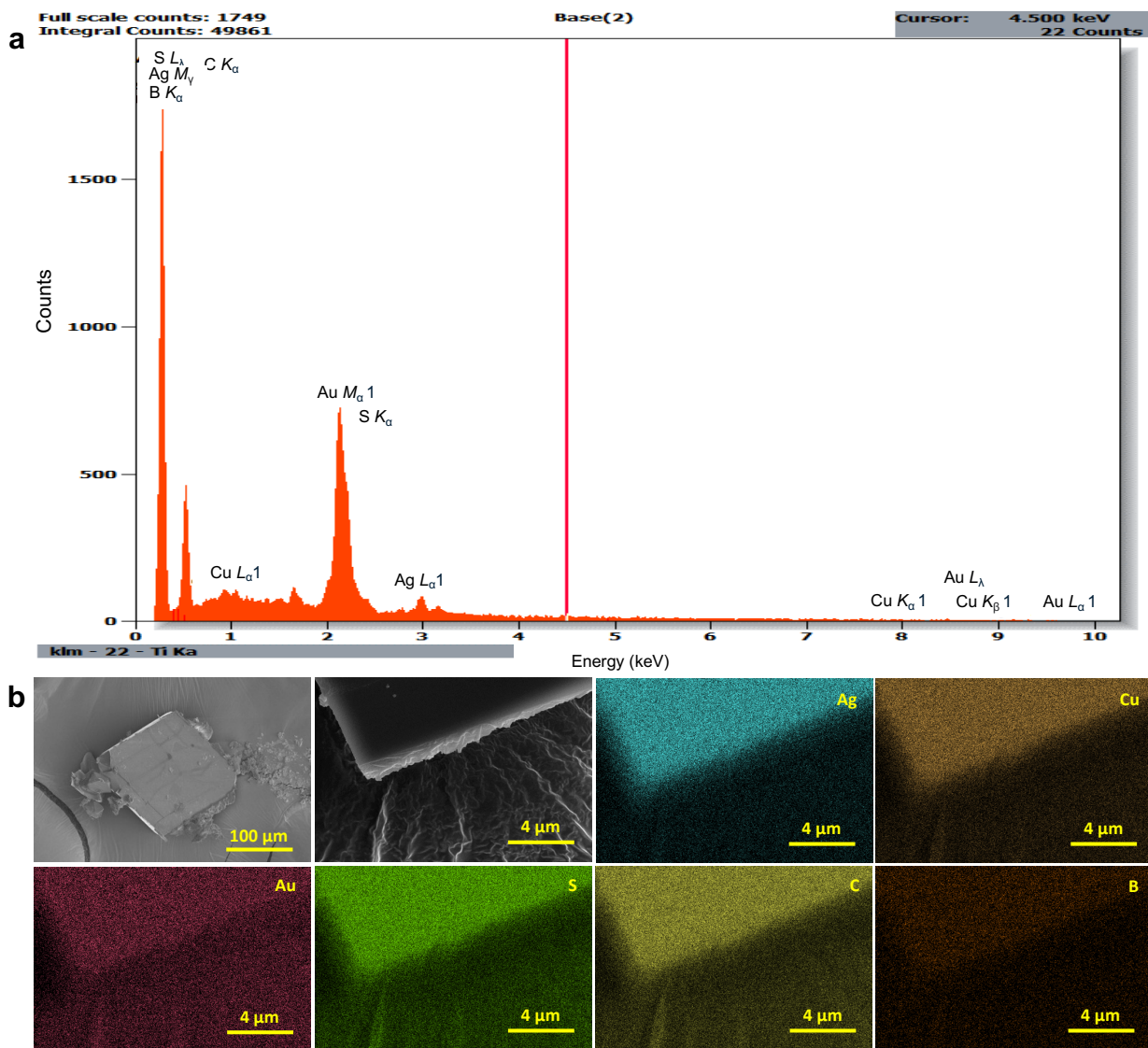
Supplementary Fig. 9 | FESEM images of the crystals and EDS mapping of Ag₁₇. **a** The EDS spectrum indicates the presence of respective elements. **b** The FESEM image of a single crystal and the collected EDS elemental mapping of the same crystal, showing Ag, S, C and B elements.



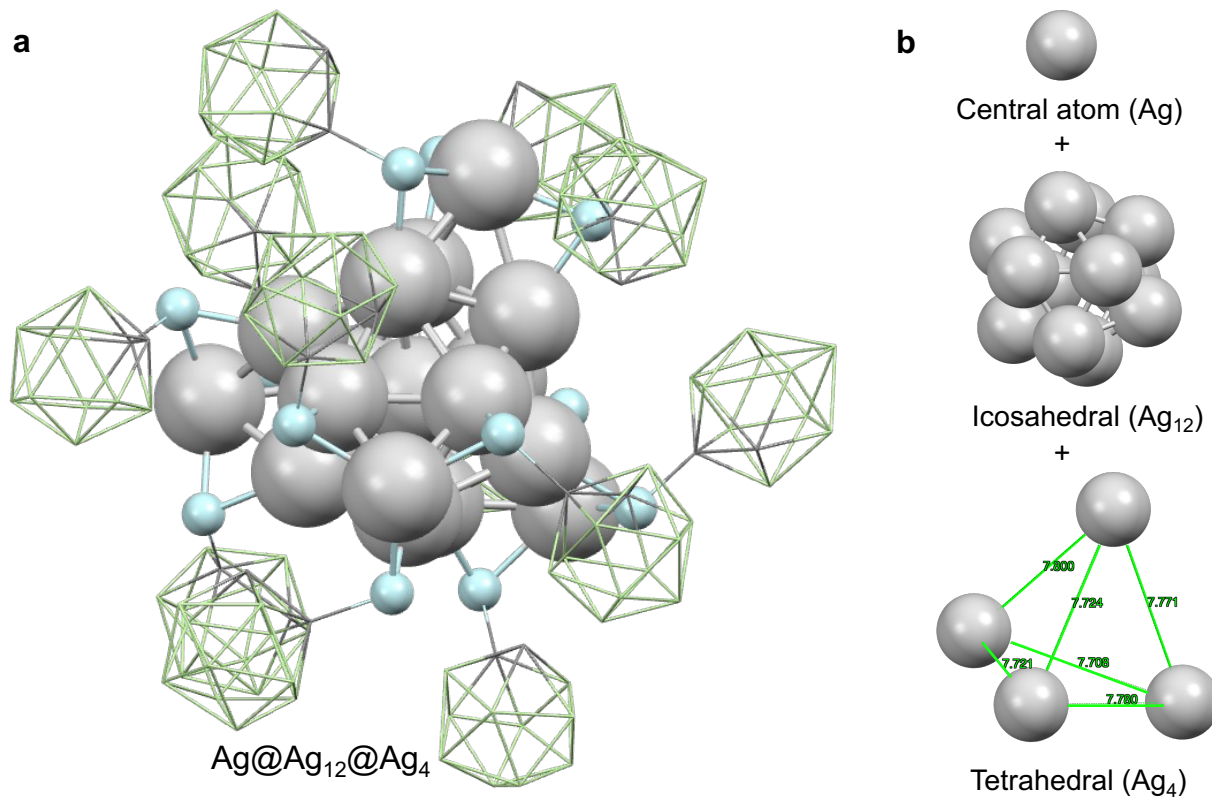
Supplementary Fig. 10 | FESEM images of the crystals and EDS mapping of AuAg_{16} . **a** The EDS spectrum indicates the presence of respective elements. **b** The FESEM image of a single crystal and the collected EDS elemental mapping of the same crystal, showing Ag, Au, S, P, C and B elements.



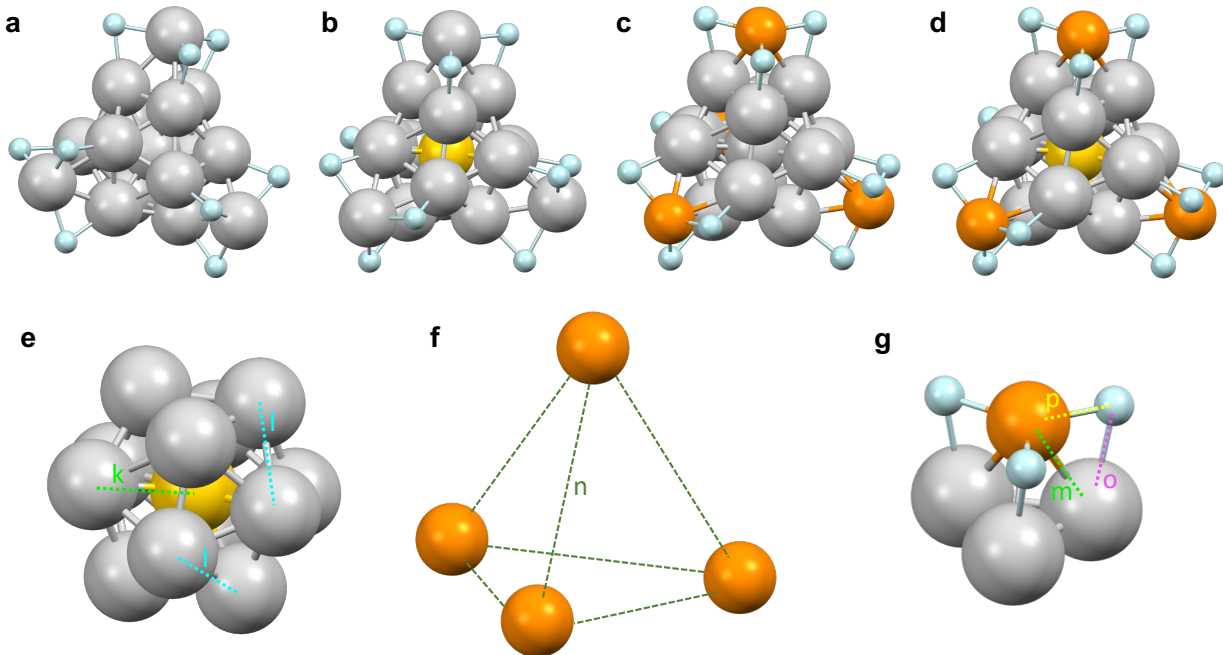
Supplementary Fig. 11 | FESEM images of the crystals and EDS mapping of $\text{Ag}_{13}\text{Cu}_4$. **a** The EDS spectrum indicates the presence of respective elements. **b** The FESEM image of a single crystal and the collected EDS elemental mapping of the same crystal, showing Ag, Cu, S, P, C and B elements.



Supplementary Fig. 12 | FESEM images of the crystals and EDS mapping of $\text{AuAg}_{12}\text{Cu}_4$. a The EDS spectrum indicates the presence of respective elements. **b** The FESEM image of a single crystal and the collected EDS elemental mapping of the same crystal, showing Ag, Cu, Au, S, C and B elements.

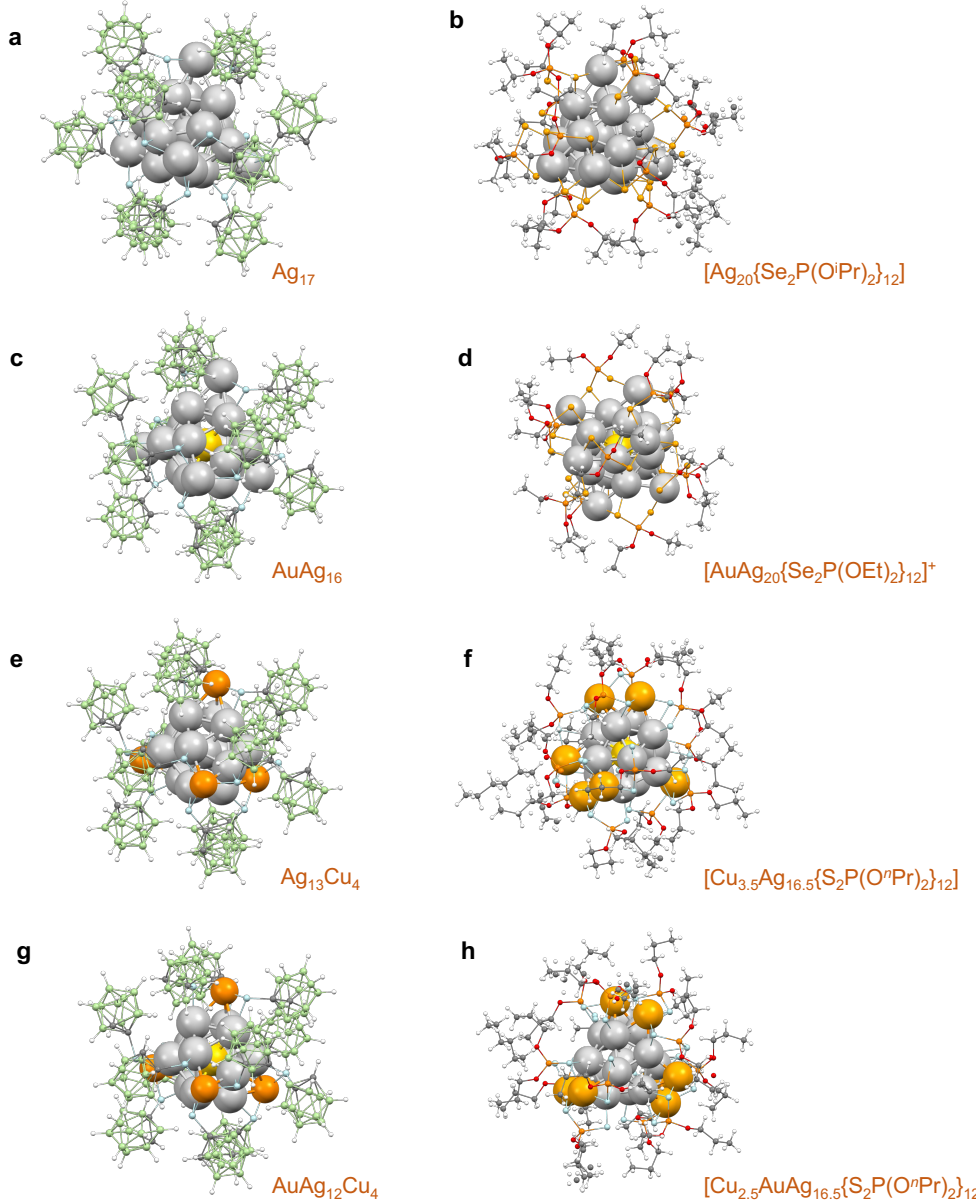


Supplementary Fig. 13 | Structural composition of the Ag_{17} . **a** Full structure of Ag_{17} shows the 17-silver core binded with sulphur of o_1 -CBT (Hydrogen has been removed for clarity). **b** Composition of silver core with central atom (Ag) covered with an icosahedral (Ag_{12}) capped with tetrahedral (Ag_4) for overall core to become $\text{Ag}@\text{Ag}_{12}@ \text{Ag}_4$. Color codes: metallic gray: silver, cyan: sulphur, green: boron and dark grey: carbon.

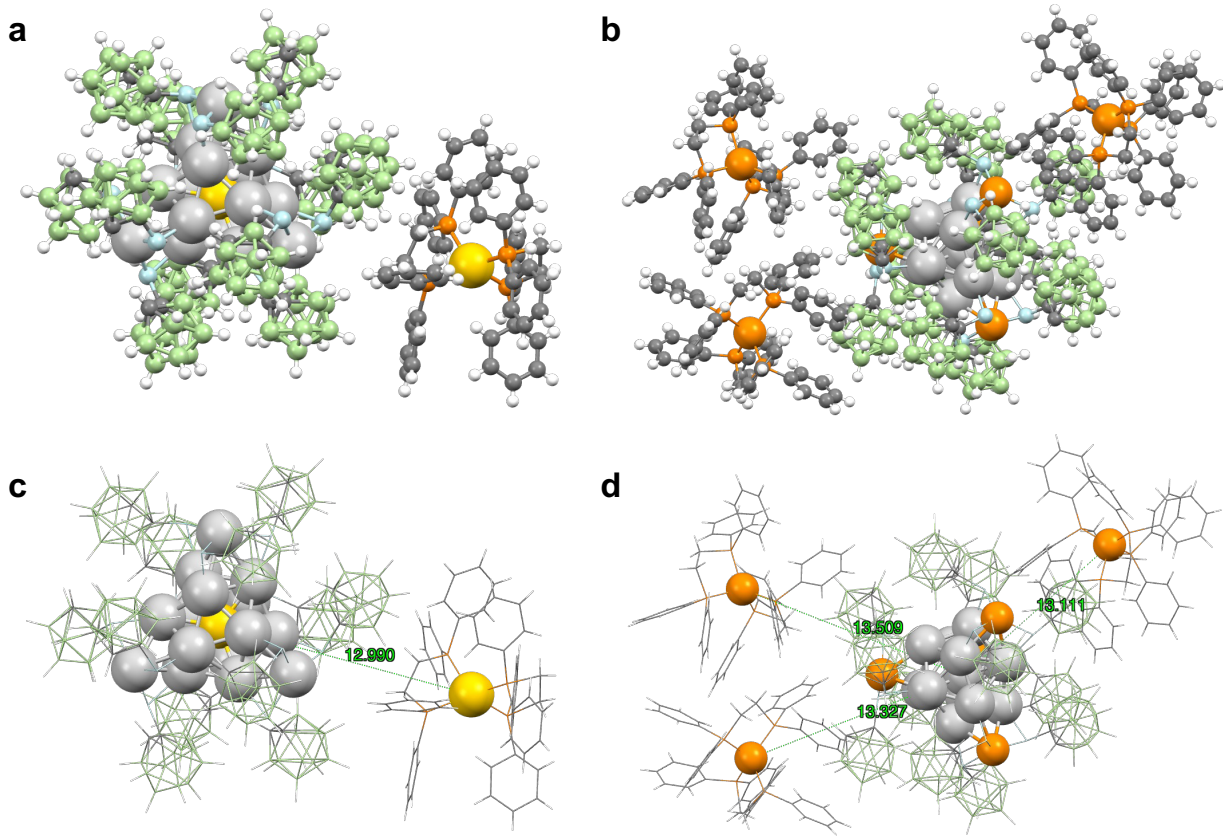


Nanocluster	Average distance (Å) between central atom to Icosahedral atoms (k)	Average distance (Å) among the bonds of Icosahedral atoms (l)	Average distance (Å) between capped tetrahedral metal atom to Icosahedral atoms (m)	Average distance (Å) among capped tetrahedral atoms (n)	Average distance (Å) between Sulphur of ligand to Icosahedral atoms (o)	Average distance (Å) between Sulphur of ligand to capped tetrahedral atoms (p)
Ag₁₇	2.792	2.938	3.061	7.750	2.492	2.498
AuAg₁₆	2.785	2.931	3.054	7.776	2.481	2.548
Ag₁₃Cu₄	2.785	2.930	2.986	7.611	2.493	2.277
AuAg₁₂Cu₄	2.759	2.902	2.958	7.580	2.491	2.186

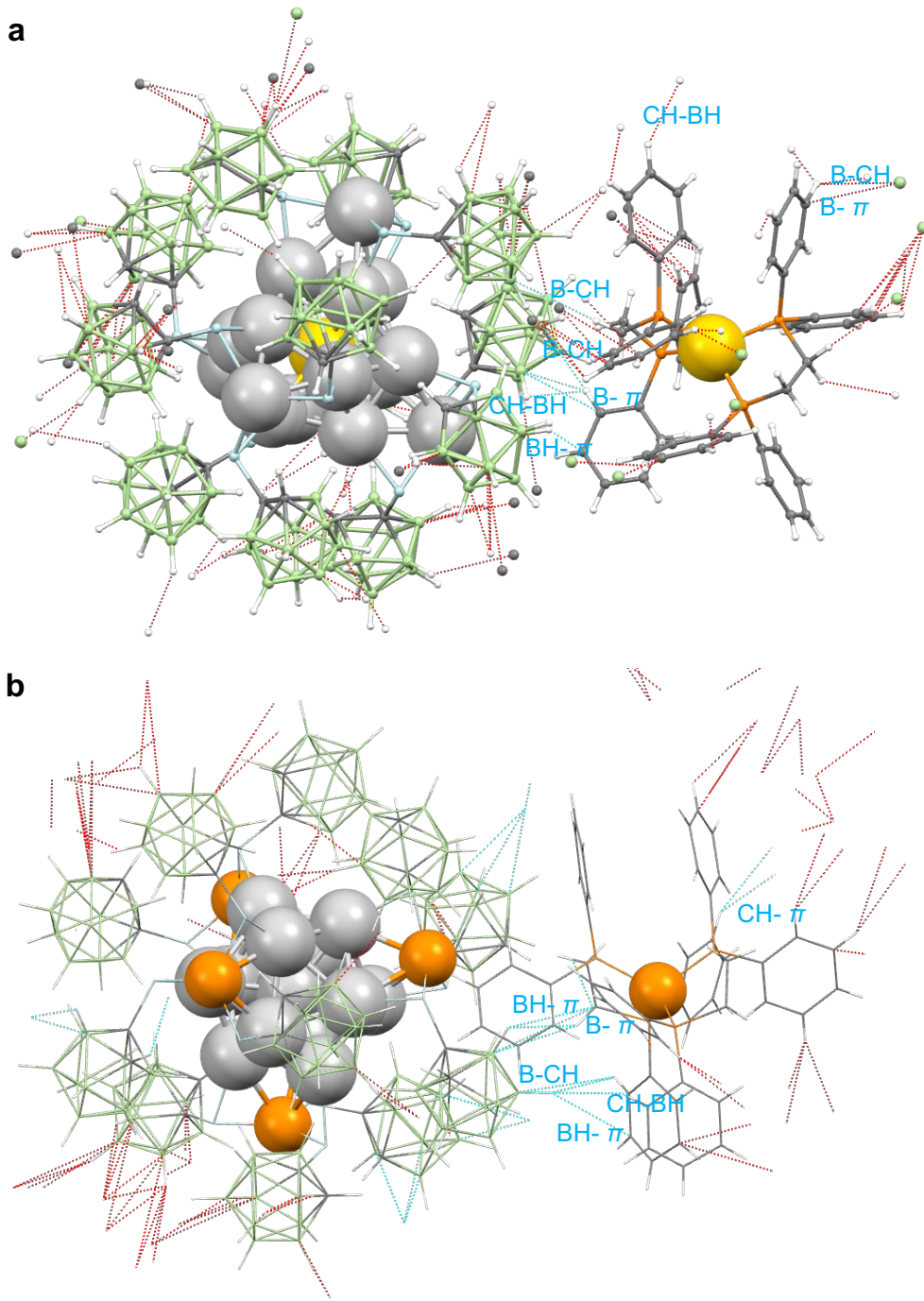
Supplementary Fig. 14 | Metal sulphur core of **a** Ag₁₇, **b** AuAg₁₆, **c** Ag₁₃Cu₄ and **d** AuAg₁₂Cu₄ shows the site-specific doping of Au and Cu in the desired NCs. **e,f** shows the inner icosahedral core and the capped tetrahedral units i.e. M₁₃ having two different metal sites (Central M₁ and icosahedral M₁₂) and M₄ respectively. **g** shows the binding of S with the metal core. Table shows all the average bond distances associated with the NCs.



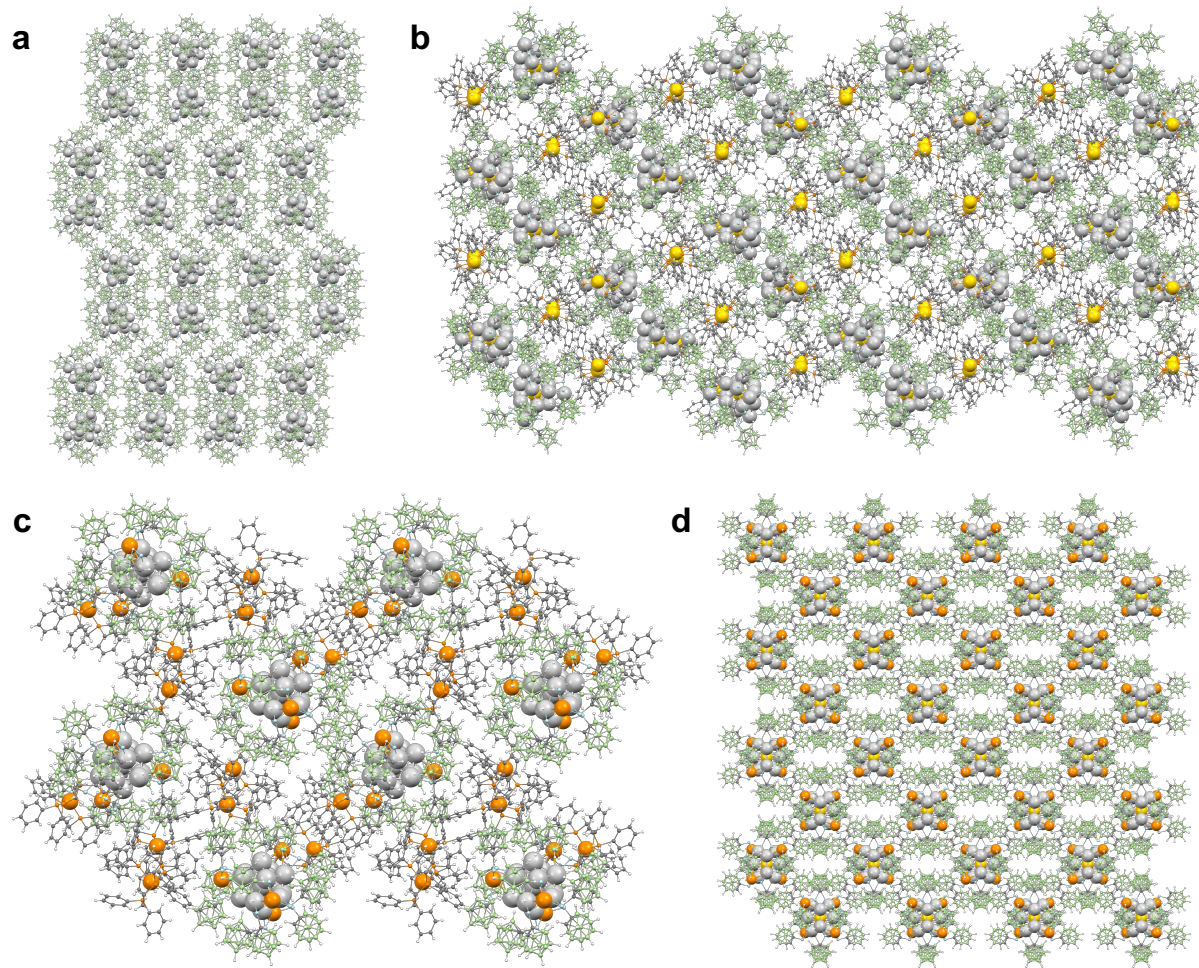
Supplementary Fig. 15 | Structural comparison of different doped systems of M_{20} and M_{21} with M_{17} systems showing site specificity of the M_{17} system. Structures **a,b** represent the similar icosahedra-centred structures of Ag_{17} and $[Ag_{20}\{Se_2P(O^iPr)_2\}_{12}]$. Structures **c,d** represent $AuAg_{16}$ and $[AuAg_{20}\{Se_2P(OEt)_2\}_{12}]^+$ clusters where the incorporation of Au is possible with the selenium based ligand, increasing the nuclearity to M_{21} . Structures **e,f** show $Ag_{13}Cu_4$ and $[Cu_{3.5}Ag_{16.5}\{S_2P(O^nPr)_2\}_{12}]$ clusters where the position of Cu is fixed at the four peripheral sites for $Ag_{13}Cu_4$ whereas it is randomly distributed at the capping positions for $[Cu_{3.5}Ag_{16.5}\{S_2P(O^nPr)_2\}_{12}]$. Structures **g,h** show the trimetallic $AuAg_{12}Cu_4$ and $[Cu_{2.5}AuAg_{16.5}\{S_2P(O^nPr)_2\}_{12}]$ clusters where the position of Cu is not definite for the M_{20} system.



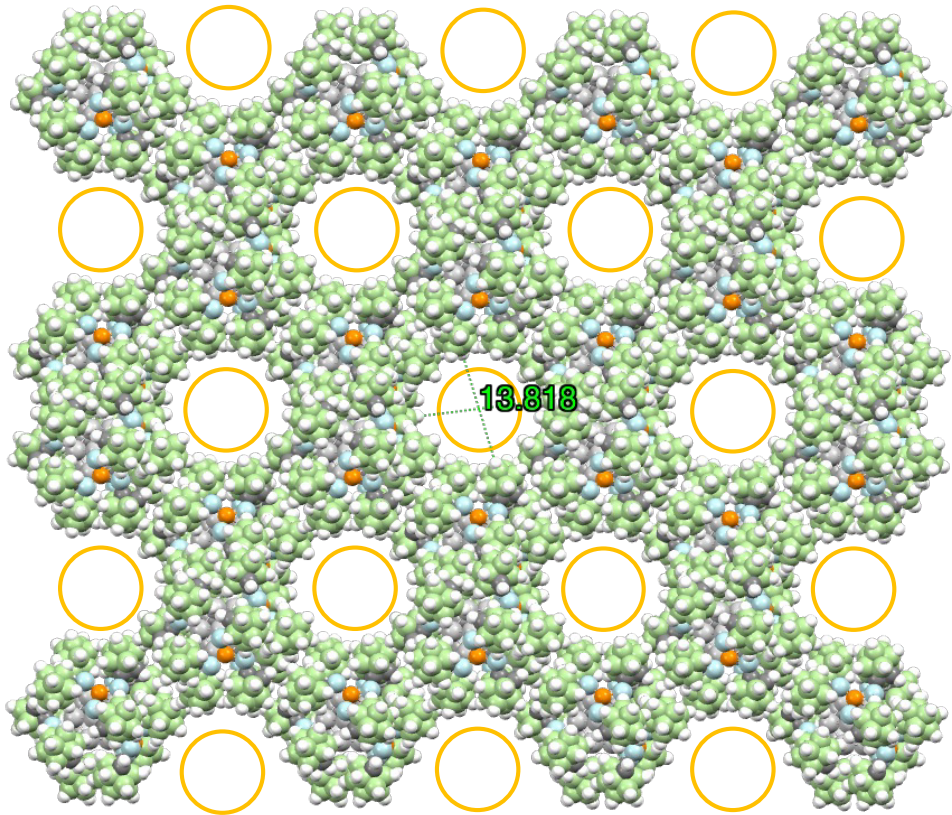
Supplementary Fig. 16 | Structure of **a** AuAg_{16} and **b** $\text{Ag}_{13}\text{Cu}_4$ show $[\text{Au}(\text{DPPE})_2]^+$ and $[\text{Cu}(\text{DPPE})_2]^+$ units surrounding the AuAg_{16} and $\text{Ag}_{13}\text{Cu}_4$ NC respectively; **c,d** show the distance of $[\text{Au}(\text{DPPE})_2]^+$ and $[\text{Cu}(\text{DPPE})_2]^+$ units from the centre of AuAg_{16} and $\text{Ag}_{13}\text{Cu}_4$ respectively.



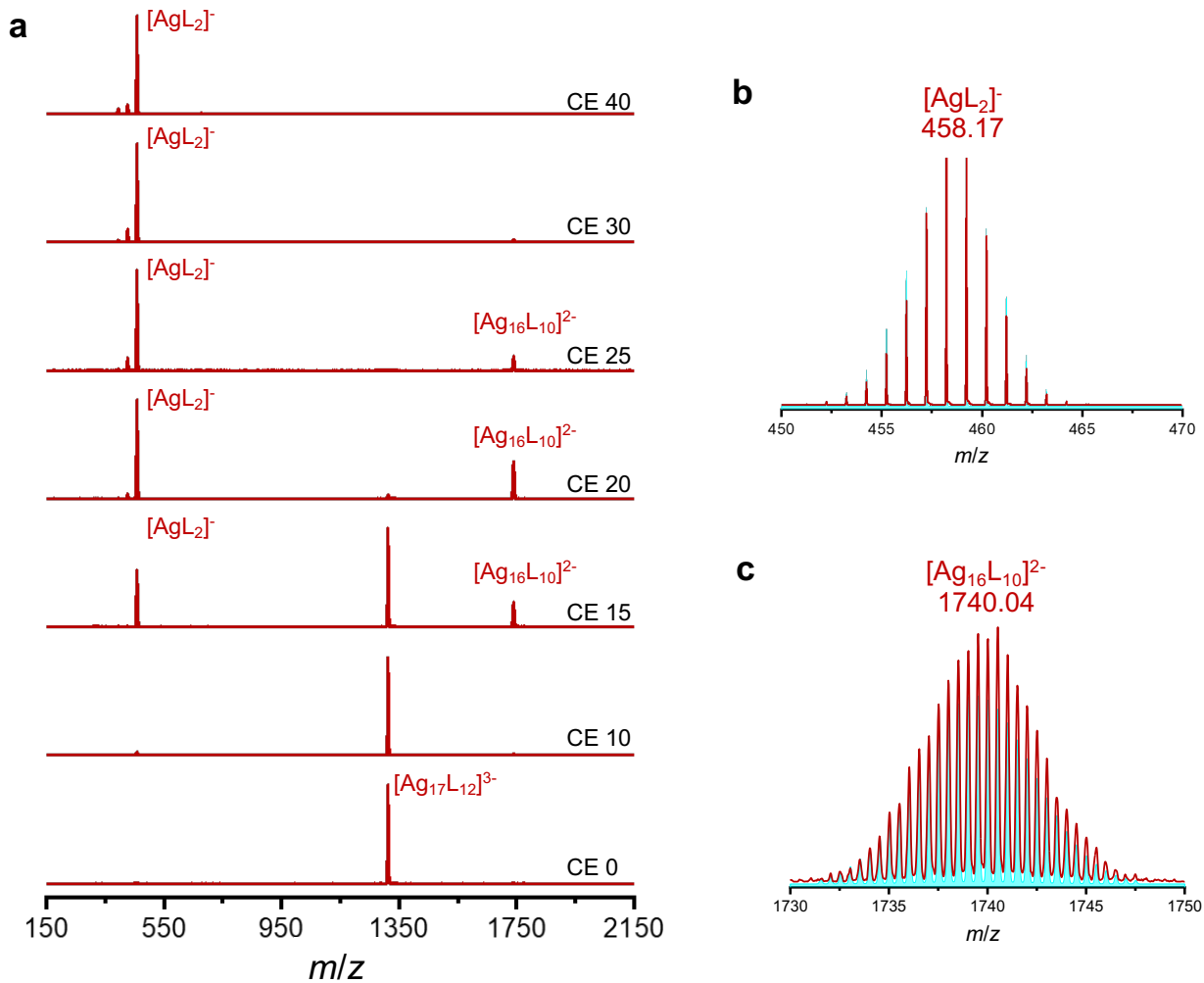
Supplementary Fig. 17 | Intermolecular interaction such as CH- π , BH- π , B-CH, BH-CH, CH-CH, B- π of **a** AuAg₁₆ with [Au(DPPE)₂]⁺ and **b** Ag₁₃Cu₄ with [Cu(DPPE)₂]⁺ units.



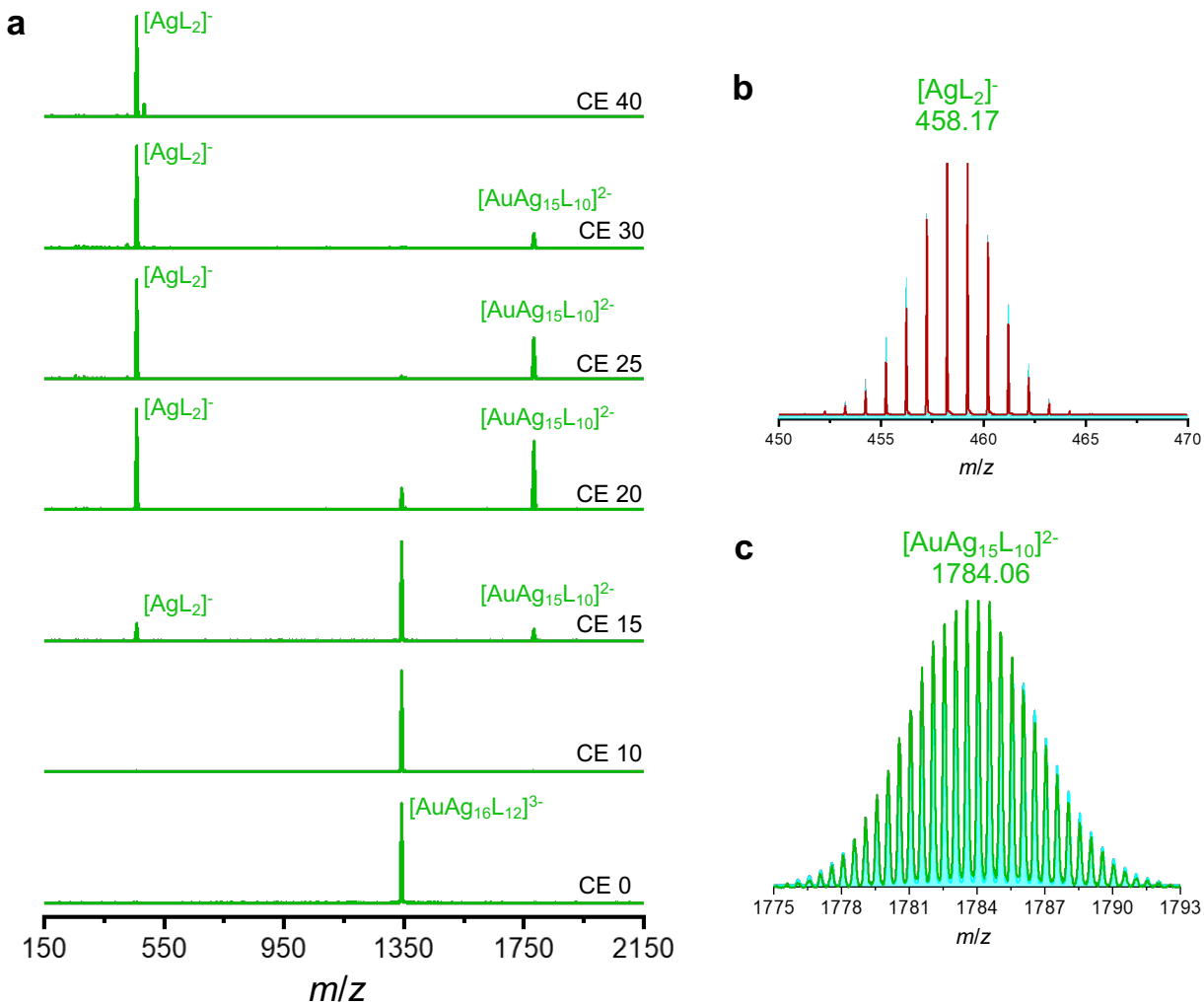
Supplementary Fig. 18 | Extended molecular packing of **a** Ag_{17} , **b** AuAg_{16} along with $[\text{Au}(\text{DPPE})_2]^+$ units, **c** $\text{Ag}_{13}\text{Cu}_4$ along with $[\text{Cu}(\text{DPPE})_2]^+$ units and **d** $\text{AuAg}_{12}\text{Cu}_4$ NCs.



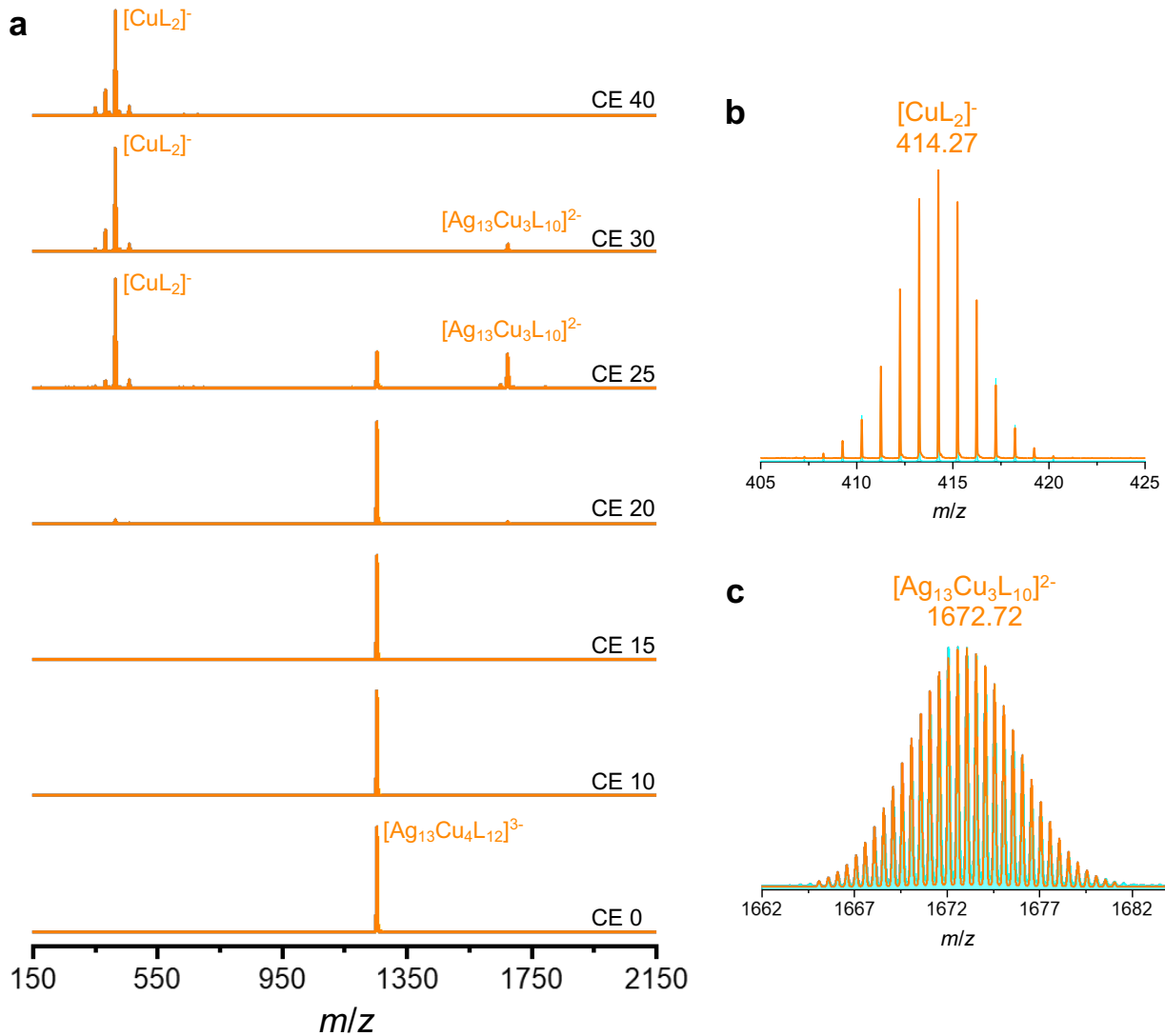
Supplementary Fig. 19 | The space-filled molecular packing of AuAg₁₂Cu₄, highlighting its (011) plane, reveals packing pores represented by saffron circles. However, due to the unresolved counter ions and the diffuse electron densities likely to be originating from solvent molecules (which were squeezed out during analysis), the void size (13.818 Å) and porosity of the region marked by saffron circles remain undefined.



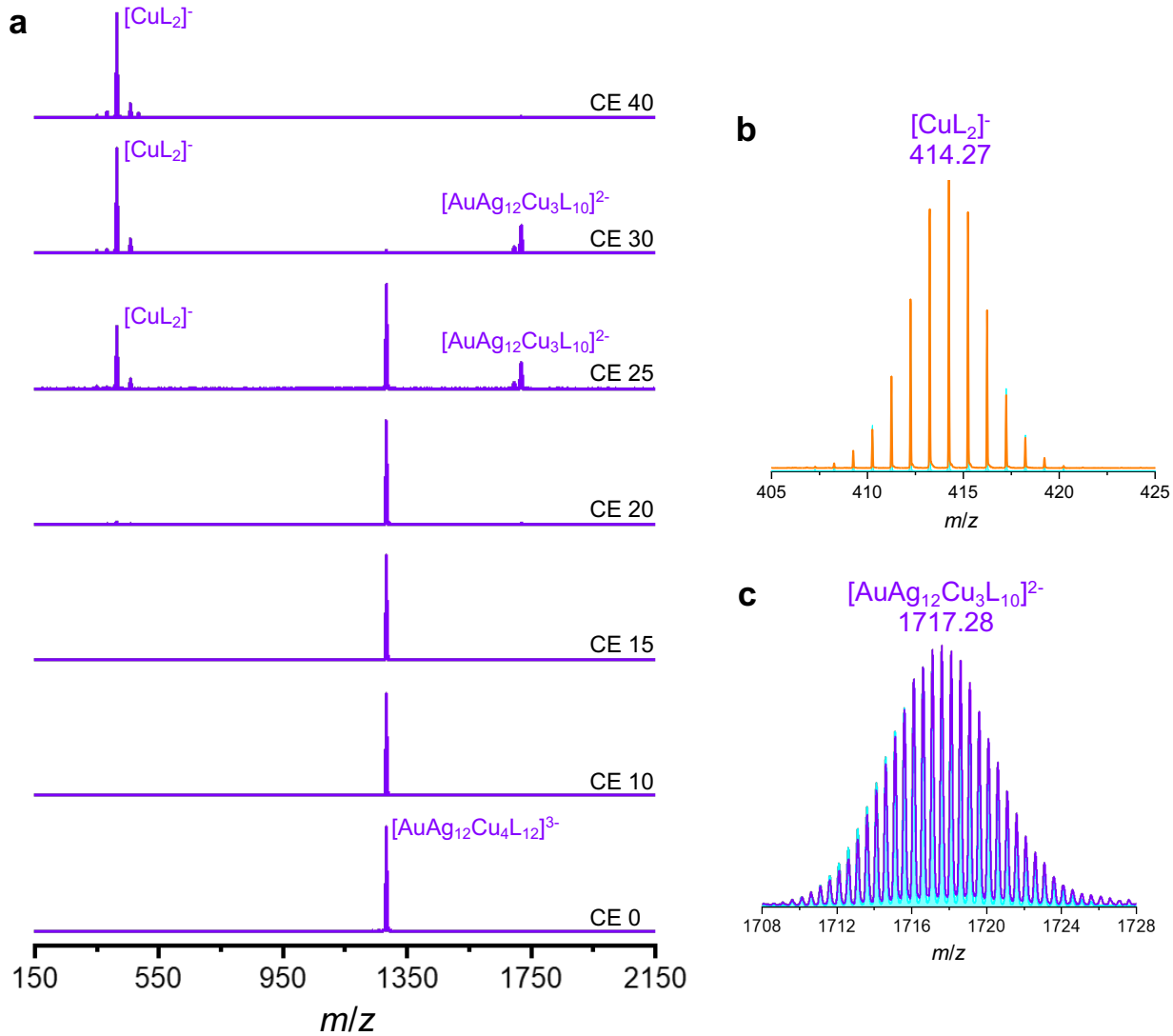
Supplementary Fig. 20 | a Collision energy dependent MS/MS fragmentation spectra of Ag_{17} ($\text{L}: o_1\text{-CBT}$). Fragmentation studies were performed upon selecting the molecular ion peak at 1312.42, having a charge state of 3-. **b,c** Comparative isotopic distribution of the experimental and simulated (Cyan) peaks for **b** $[\text{AgL}_2]^-$ and **c** $[\text{Ag}_{16}\text{L}_{10}]^{2-}$ fragments.



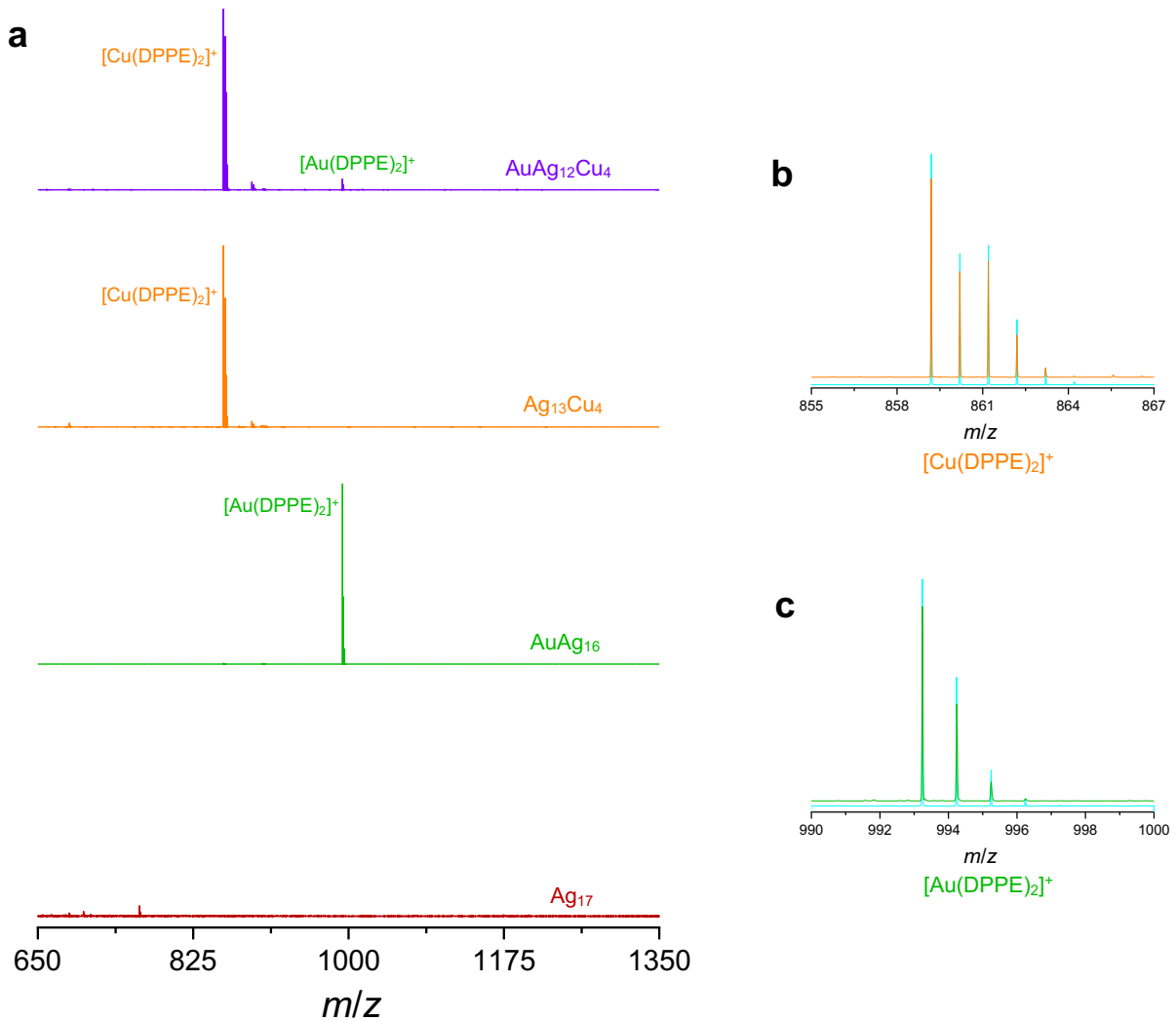
Supplementary Fig. 21 | a Collision energy dependent MS/MS fragmentation spectra of AuAg_{16} (L : σ_1 -CBT). Fragmentation studies were performed upon selecting the molecular ion peak at 1342.11, having a charge state of 3-. **b,c** Comparative isotopic distribution of the experimental and simulated (Cyan) peaks for **b** $[\text{AgL}_2\text{}^-]$ and **c** $[\text{AuAg}_{15}\text{L}_{10}\text{}}^{2-}$ fragments.



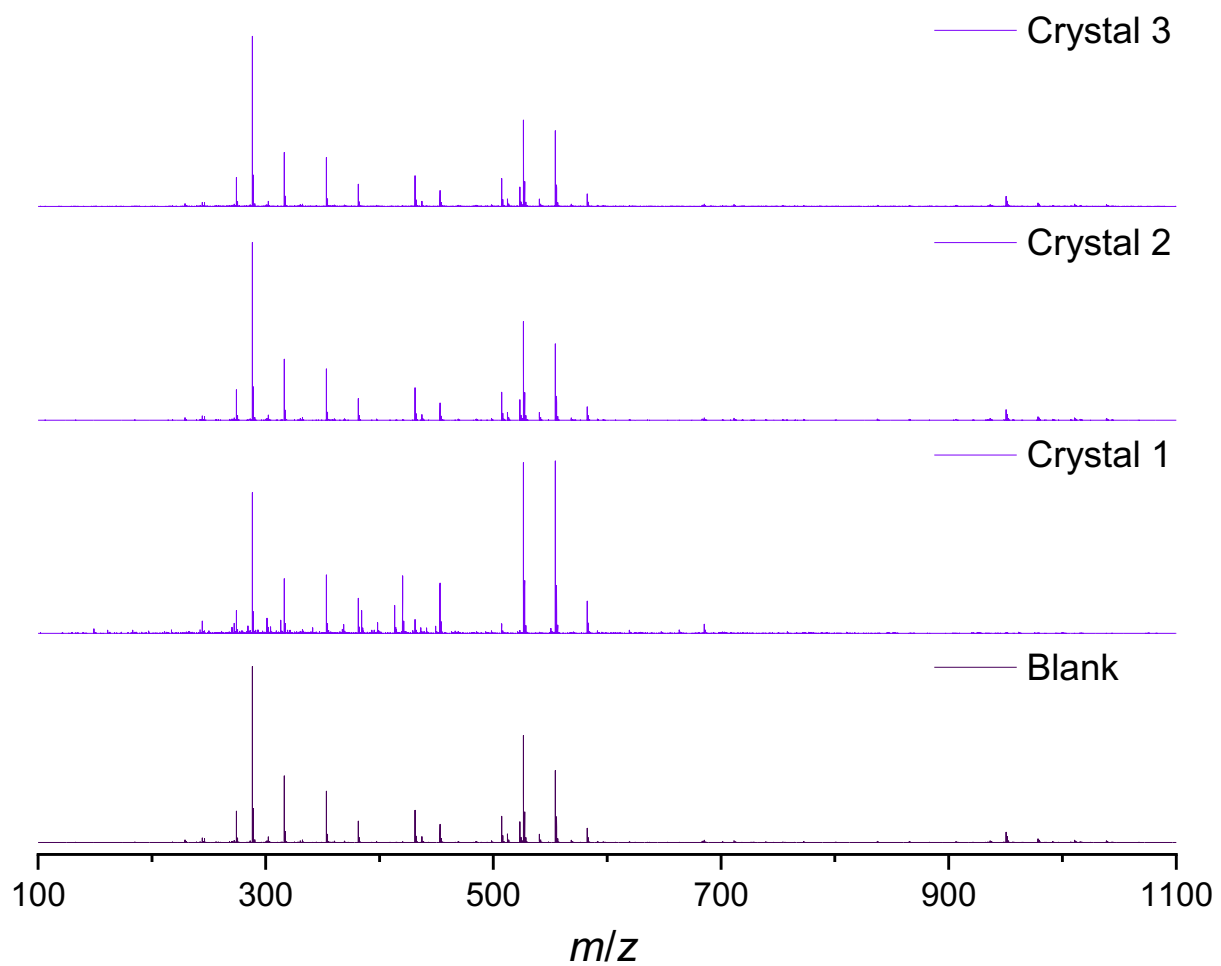
Supplementary Fig. 22 | a Collision energy dependent MS/MS fragmentation spectra of $\text{Ag}_{13}\text{Cu}_4$ (L : *o*₁-CBT). Fragmentation studies were performed upon selecting the molecular ion peak at 1253.46, having a charge state of 3-. **b,c** Comparative isotopic distribution of the experimental and simulated (Cyan) peaks for **b** $[\text{CuL}_2]^-$ and **c** $[\text{Ag}_{13}\text{Cu}_3\text{L}_{10}]^{2-}$ fragments.



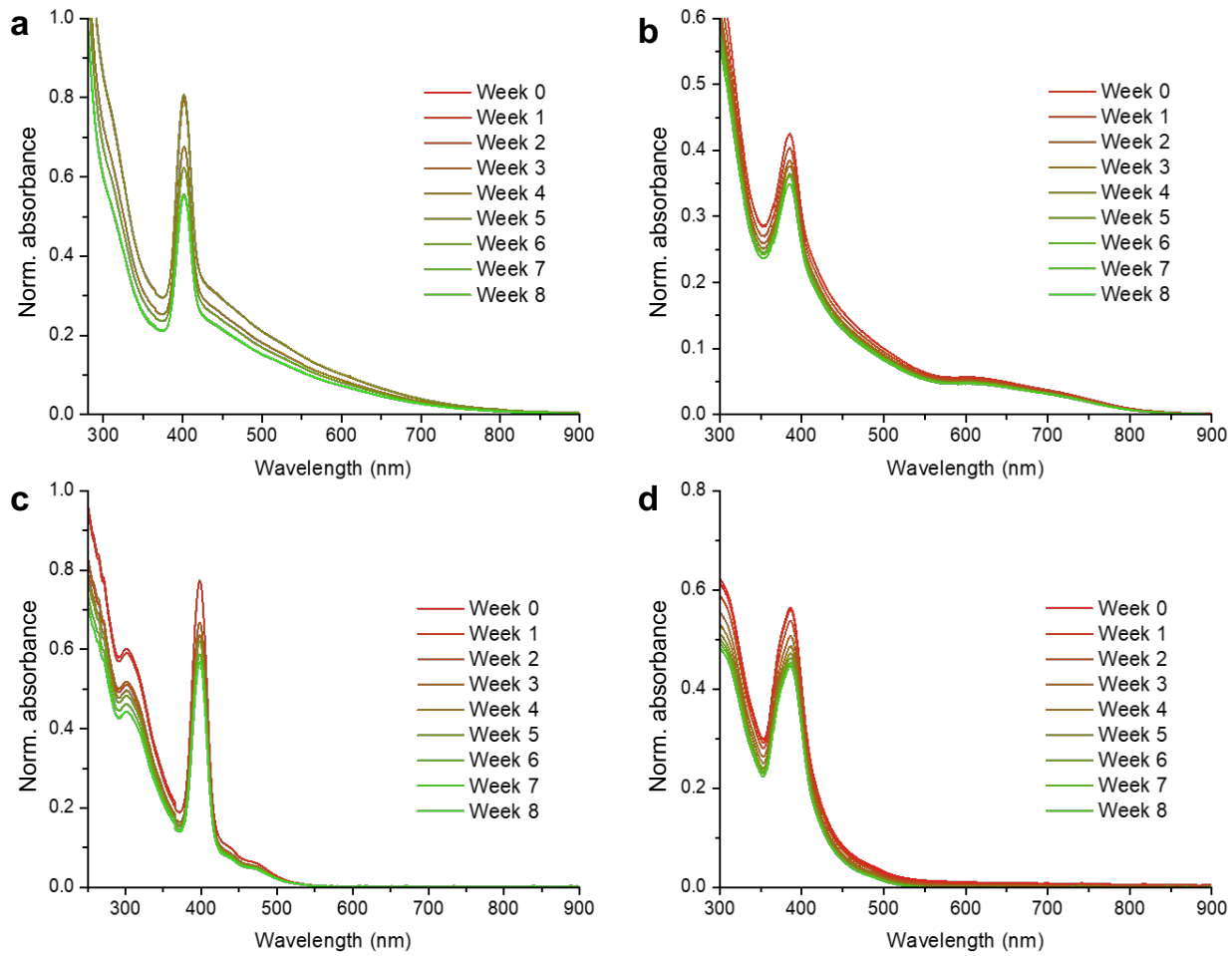
Supplementary Fig. 23 | a Collision energy dependent MS/MS fragmentation spectra of $\text{AuAg}_{12}\text{Cu}_4$ (L : σ_1 -CBT). Fragmentation studies were performed upon selecting the molecular ion peak at 1283.15, having a charge state of 3-. **b,c** Comparative isotopic distribution of the experimental and simulated (Cyan) peaks for **b** $[\text{CuL}_2\text{-}]$ and **c** $[\text{AuAg}_{12}\text{Cu}_3\text{L}_{10}]^{2-}$ fragments.



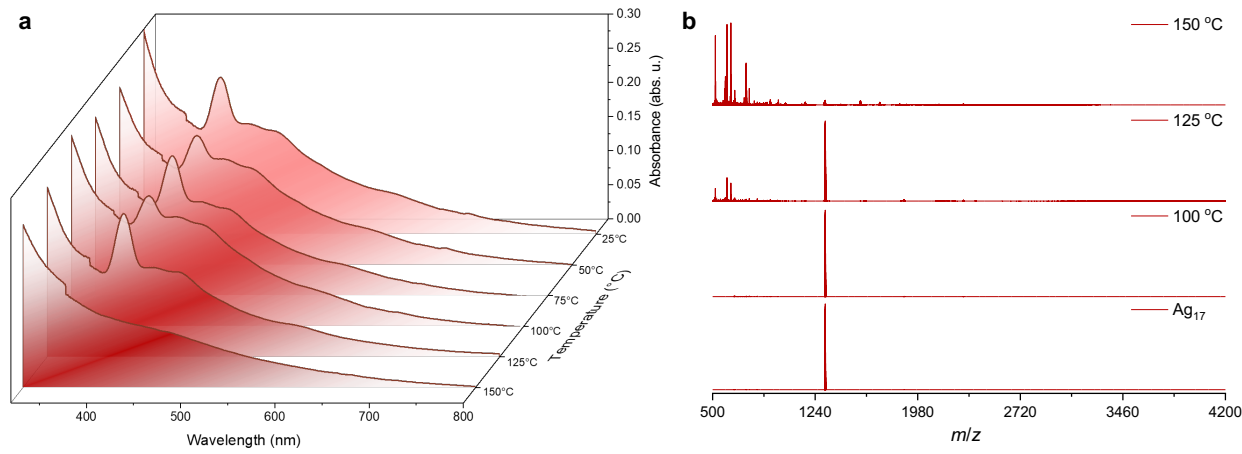
Supplementary Fig. 24 | a Positive ion mode ESI-MS spectrum of the as synthesized crude of Ag_{17} , AuAg_{16} , $\text{Ag}_{13}\text{Cu}_4$ and $\text{AuAg}_{12}\text{Cu}_4$. Ag_{17} , didn't show the any peaks with DPPE whereas AuAg_{16} , showed $[\text{Au(DPPE)}_2]^+$ peak, $\text{Ag}_{13}\text{Cu}_4$ showed $[\text{Cu(DPPE)}_2]^+$ peak and $\text{AuAg}_{12}\text{Cu}_4$ showed both $[\text{Au(DPPE)}_2]^+$ and $[\text{Cu(DPPE)}_2]^+$ peaks in the crude sample. **b,c** Comparative isotopic distribution of the experimental and simulated (Cyan) peaks for **b** $[\text{Cu(DPPE)}_2]^+$ and **c** $[\text{Au(DPPE)}_2]^+$ peaks.



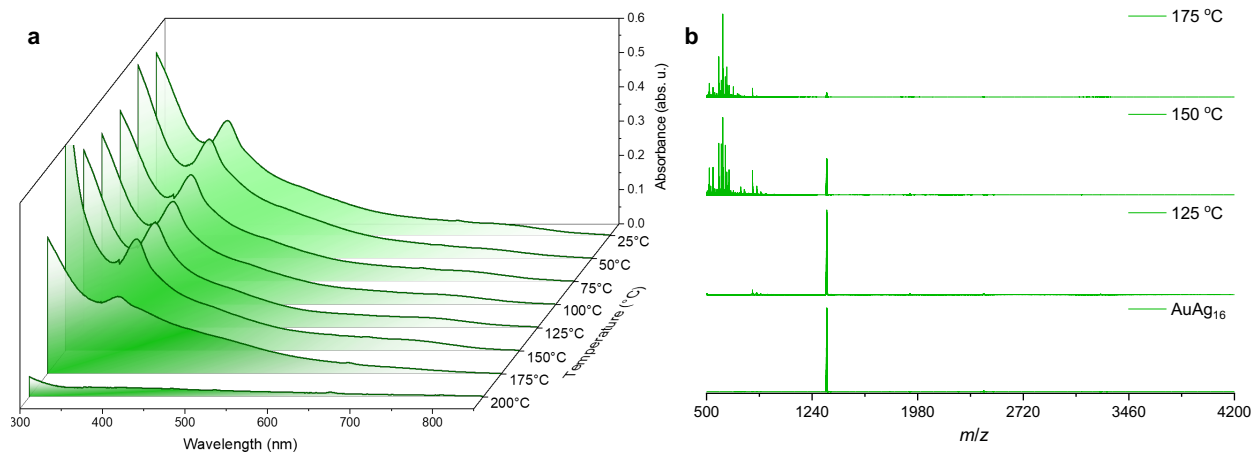
Supplementary Fig. 25 | Positive ion mode ESI-MS spectrum of different crystals of $\text{AuAg}_{12}\text{Cu}_4$. ESI-MS of the crystals of $\text{AuAg}_{12}\text{Cu}_4$ did not show any peaks corresponding to $[\text{Au}(\text{DPPE})_2]^+$ and $[\text{Cu}(\text{DPPE})_2]^+$ expected at m/z 993.24 and 859.20, respectively.



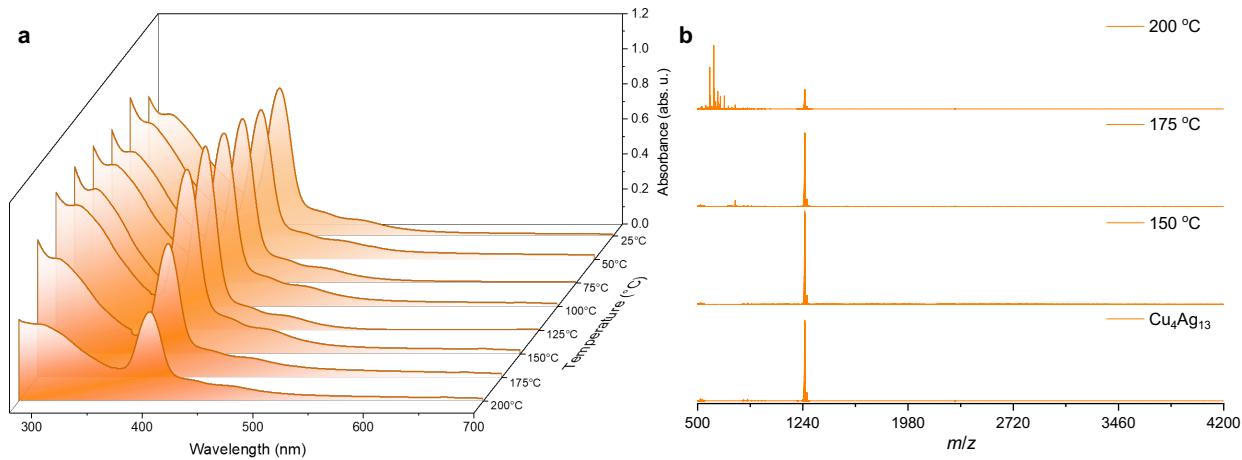
Supplementary Fig. 26 | Time dependent stability UV-Vis absorption spectra of **a** Ag_{17} , **b** AuAg_{16} , **c** $\text{Ag}_{13}\text{Cu}_4$ and **d** $\text{AuAg}_{12}\text{Cu}_4$ in DCM solution. During this study, clusters are saved in a closed Eppendorf vial in dark condition at 4 °C.



Supplementary Fig. 27 | Thermal Stability of Ag₁₇ NC at different temperatures. Comparative **a** UV-Vis absorption spectra and **b** ESI-MS data of Ag₁₇ after heating the cluster at different temperatures. After 90 min of heating, the powder sample was dissolved in DCM for UV-Vis and ESI-MS measurements.

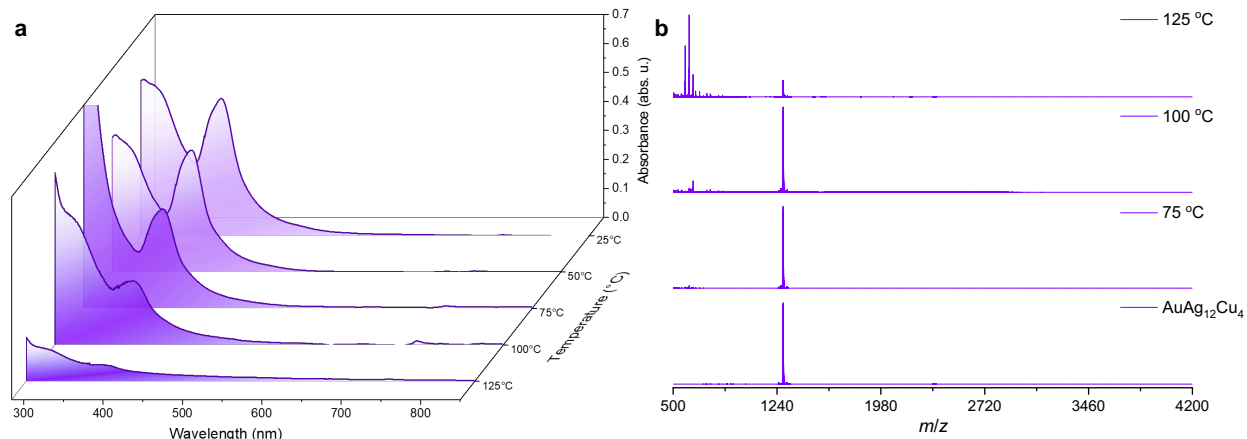


Supplementary Fig. 28 | Thermal Stability of AuAg₁₆ NC at different temperatures. Comparative **a** UV-Vis absorption spectra and **b** ESI-MS data of AuAg₁₆ after heating the cluster at different temperatures. After 90 min of heating, the powder sample was dissolved in DCM for UV-Vis and ESI-MS measurements.



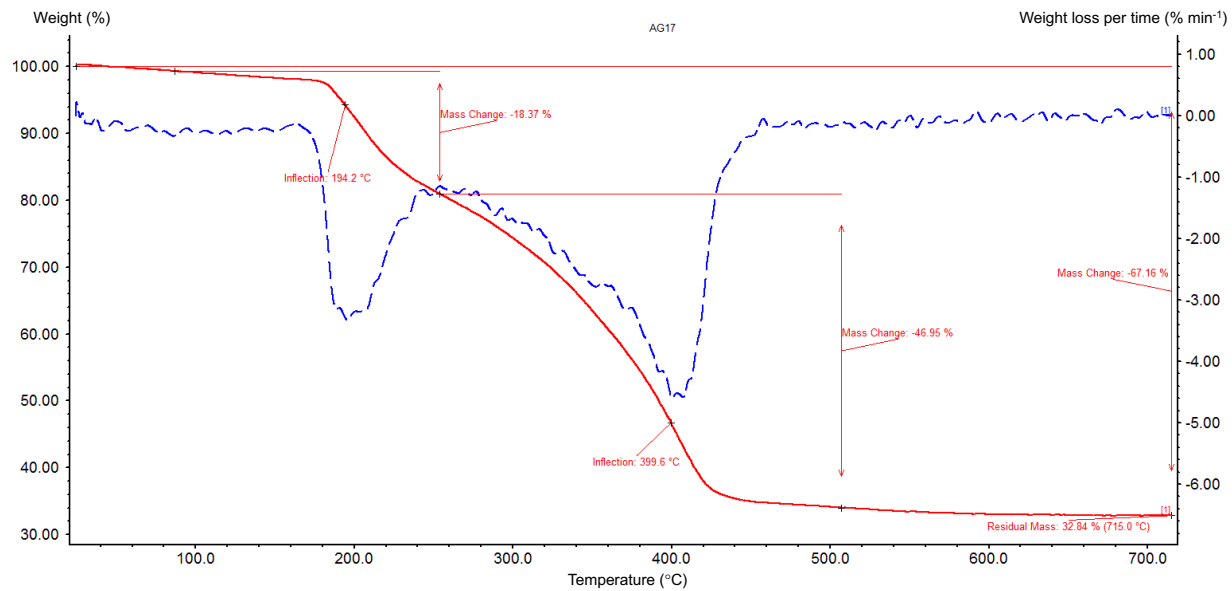
Supplementary Fig. 29 | Thermal Stability of $\text{Ag}_{13}\text{Cu}_4$ NC at different temperatures.

Comparative **a** UV-Vis absorption spectra and **b** ESI-MS data of $\text{Ag}_{13}\text{Cu}_4$ after heating the cluster at different temperatures. After 90 min of heating, after 90 min of heating, the powder sample was dissolved in DCM for UV-Vis and ESI-MS measurements.

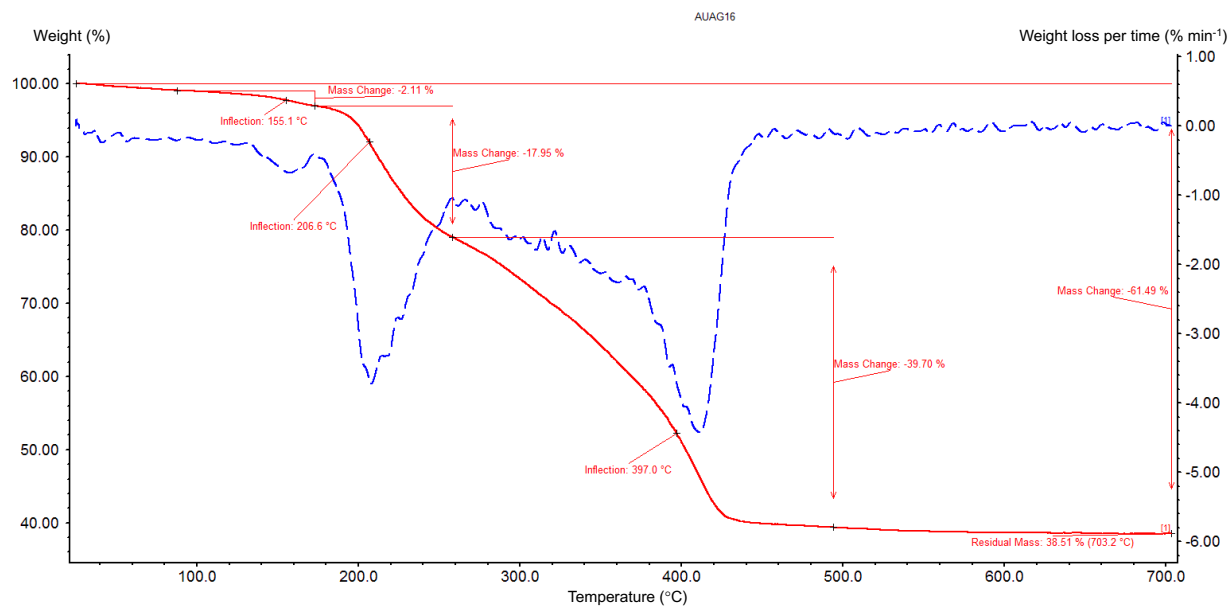


Supplementary Fig. 30 | Thermal Stability of $\text{AuAg}_{12}\text{Cu}_4$ NC at different temperatures.

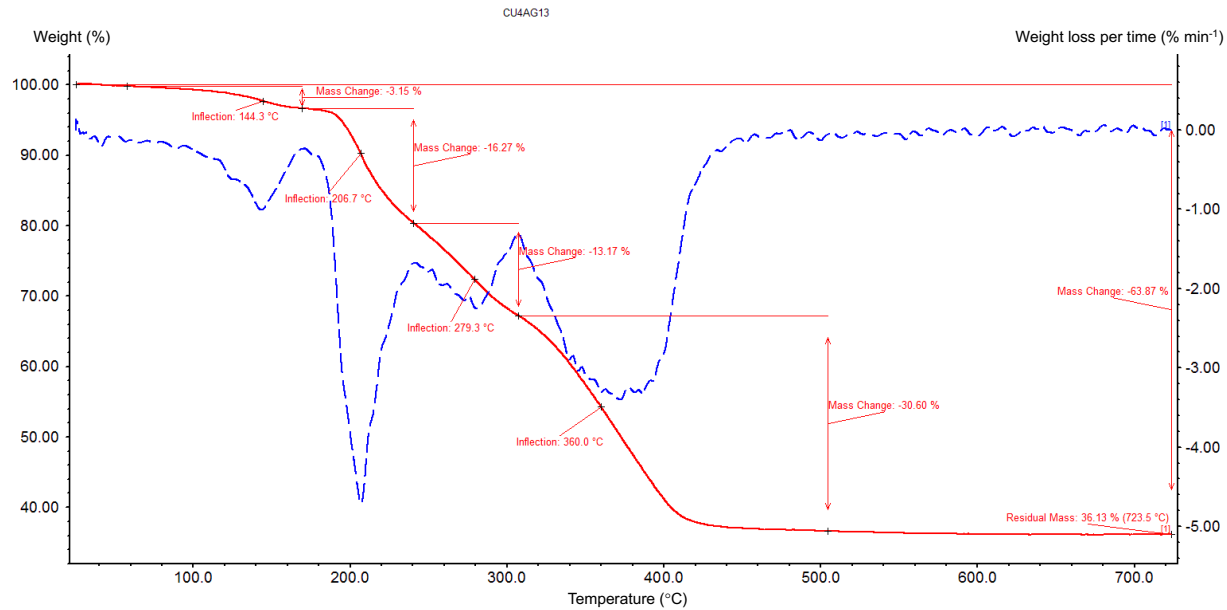
Comparative **a** UV-Vis absorption spectra and **b** ESI-MS data of $\text{AuAg}_{12}\text{Cu}_4$ after heating the cluster at different temperatures. After 90 min of heating, the powder sample was dissolved in DCM for UV-Vis and ESI-MS measurements.



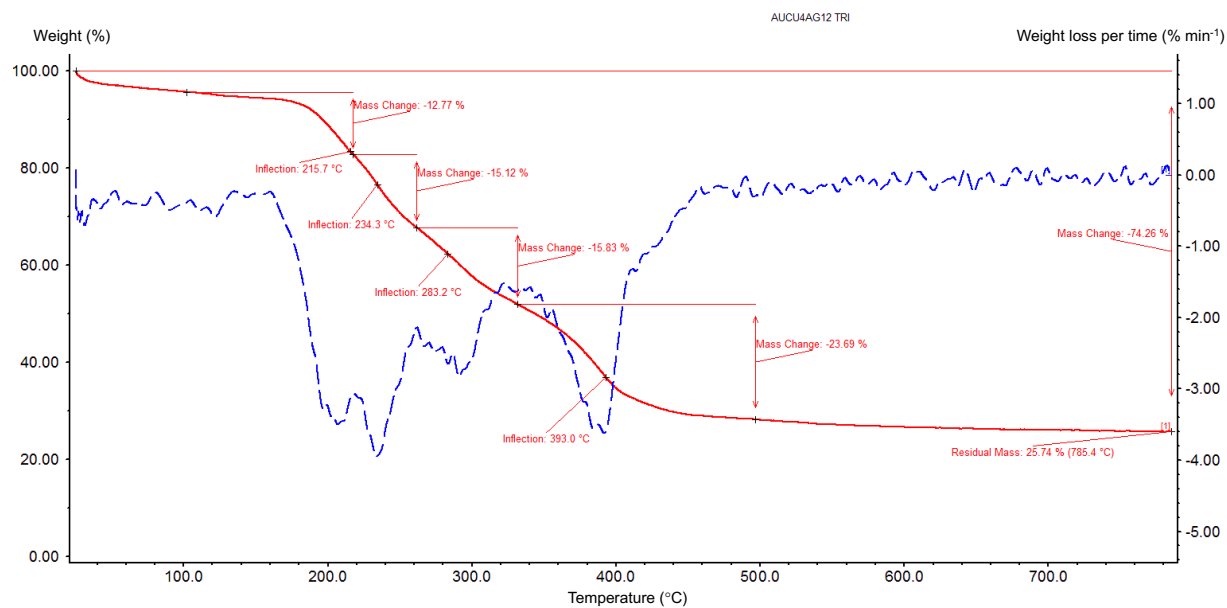
Supplementary Fig. 31 | TG and DTG plots of microcrystalline Ag₁₇ solids.



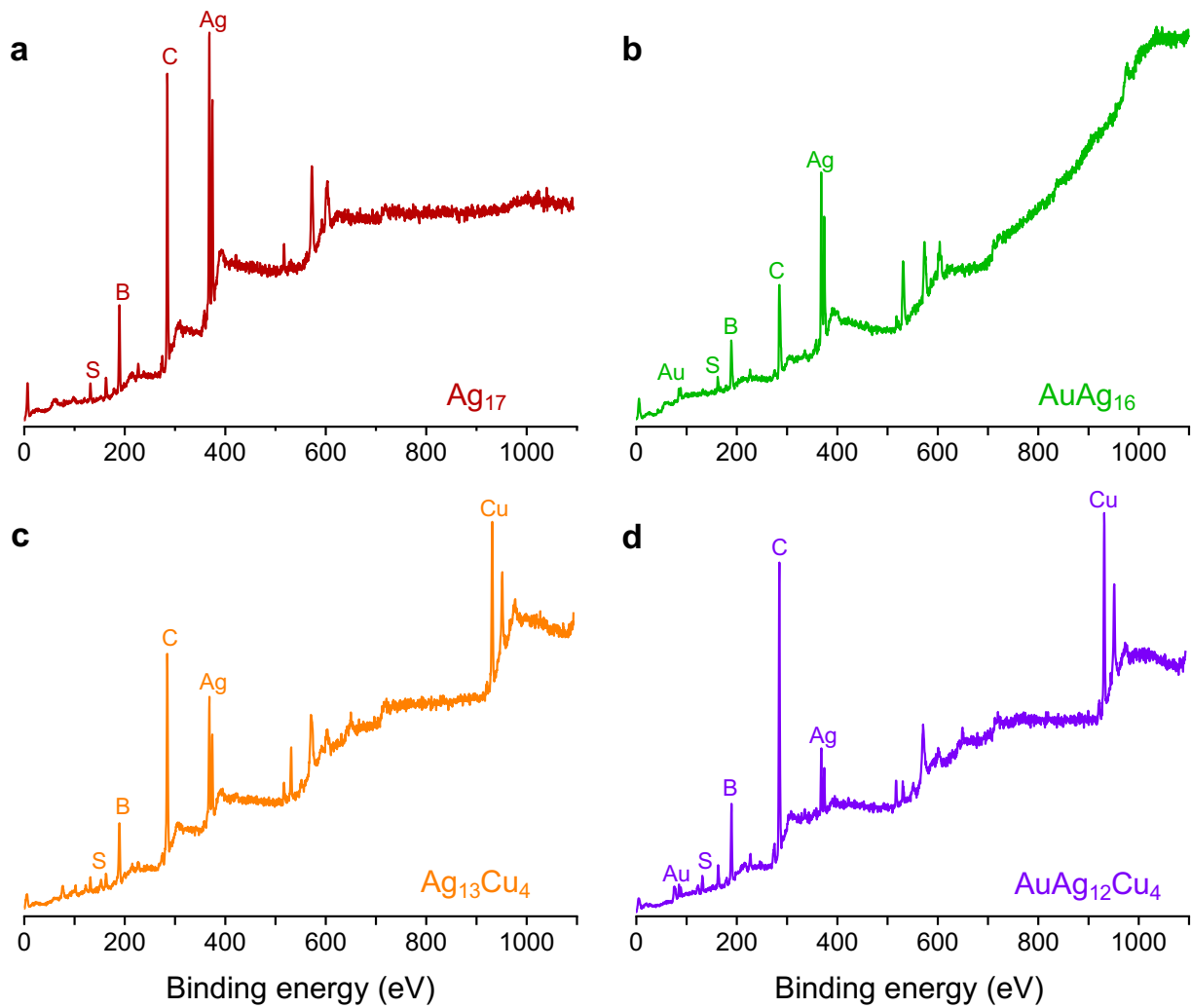
Supplementary Fig. 32 | TG and DTG plots of microcrystalline AuAg₁₆ solids.



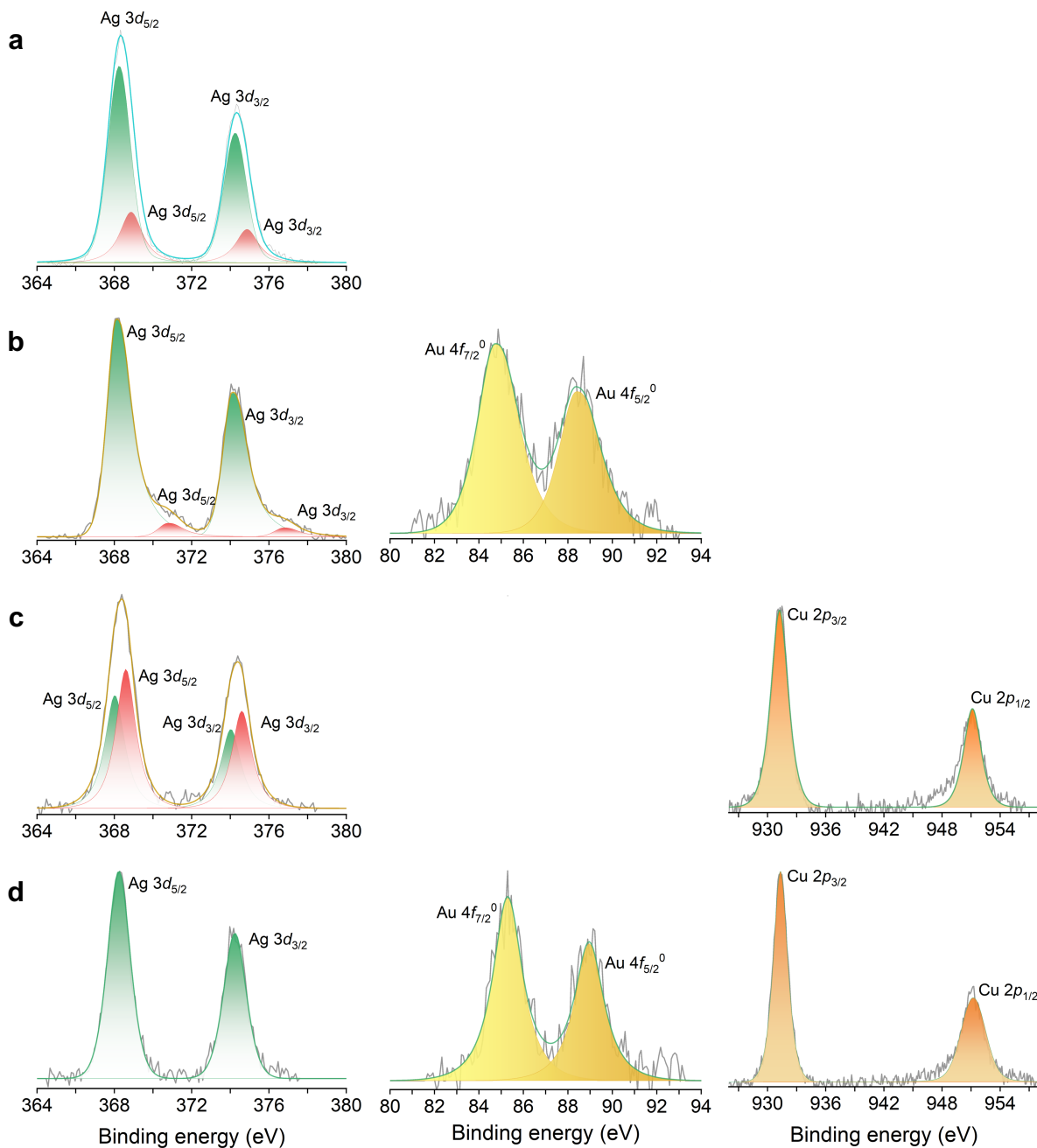
Supplementary Fig. 33 | TG and DTG plots of microcrystalline $\text{Ag}_{13}\text{Cu}_4$ solids.



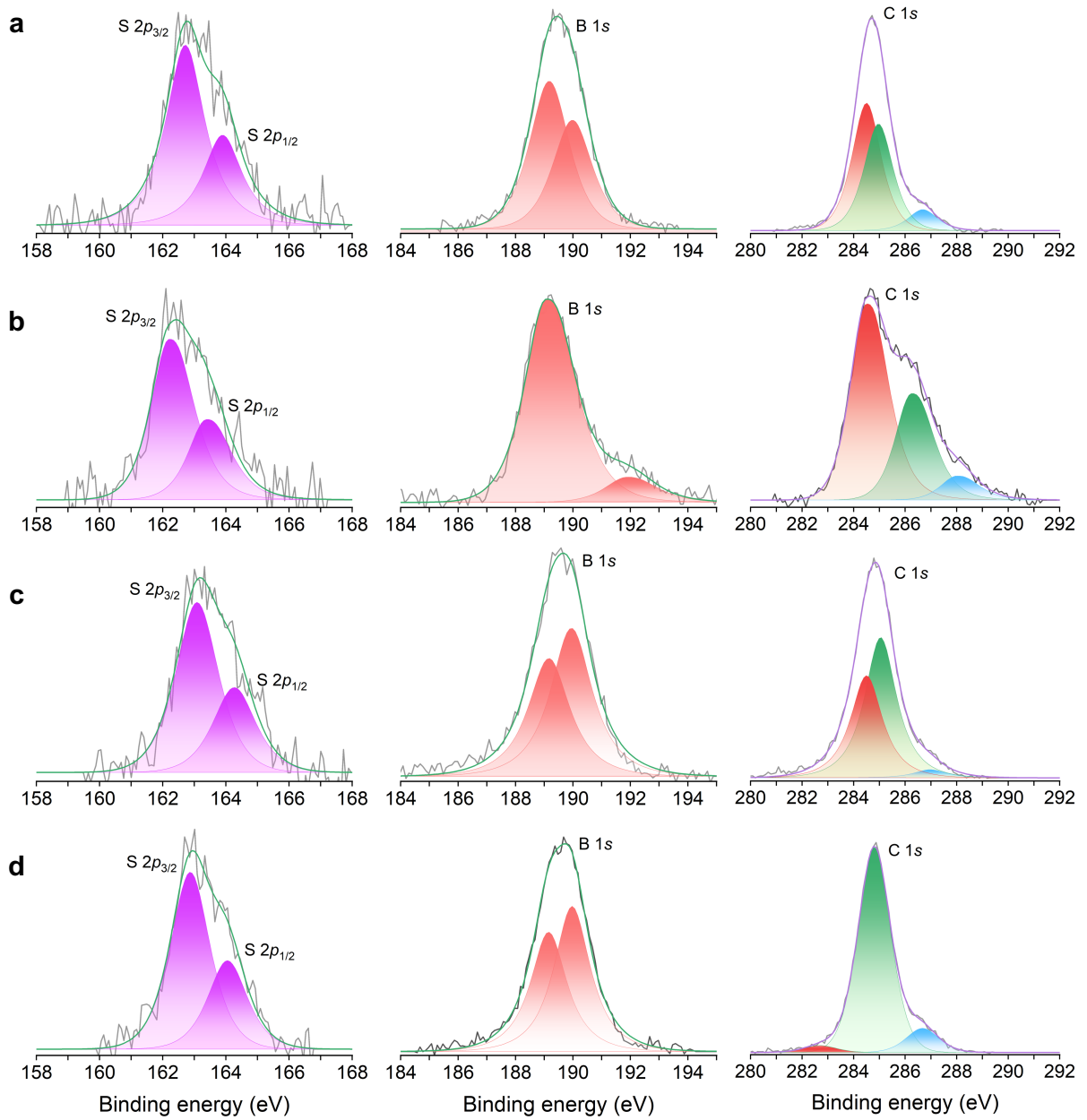
Supplementary Fig. 34 | TG and DTG plots of microcrystalline $\text{AuAg}_{12}\text{Cu}_4$ solids.



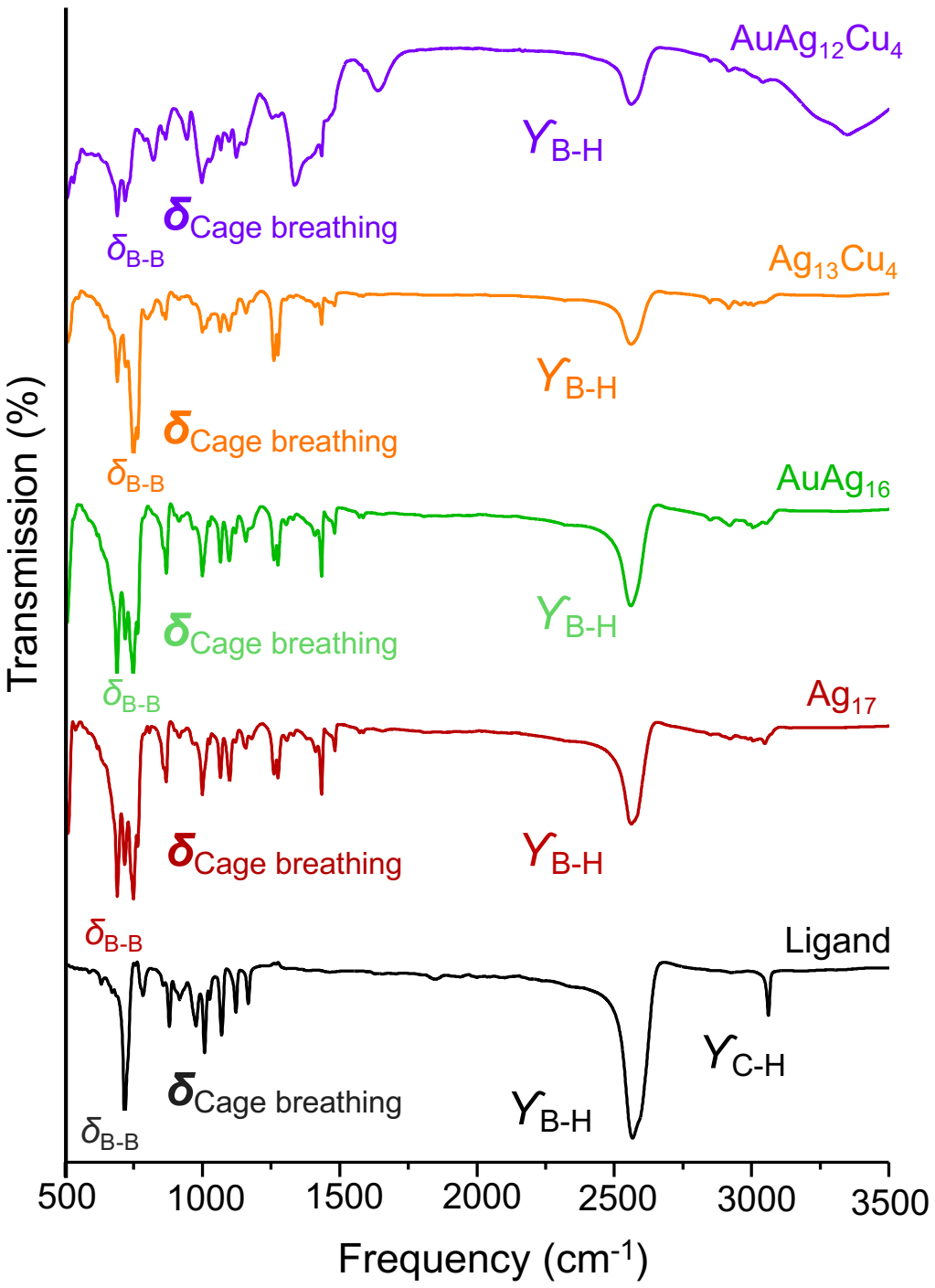
Supplementary Fig. 35 | XPS survey scan of **a** Ag₁₇, **b** AuAg₁₆, **c** Ag₁₃Cu₄ and **d** AuAg₁₂Cu₄. Binding energy of the respective elements are marked here.



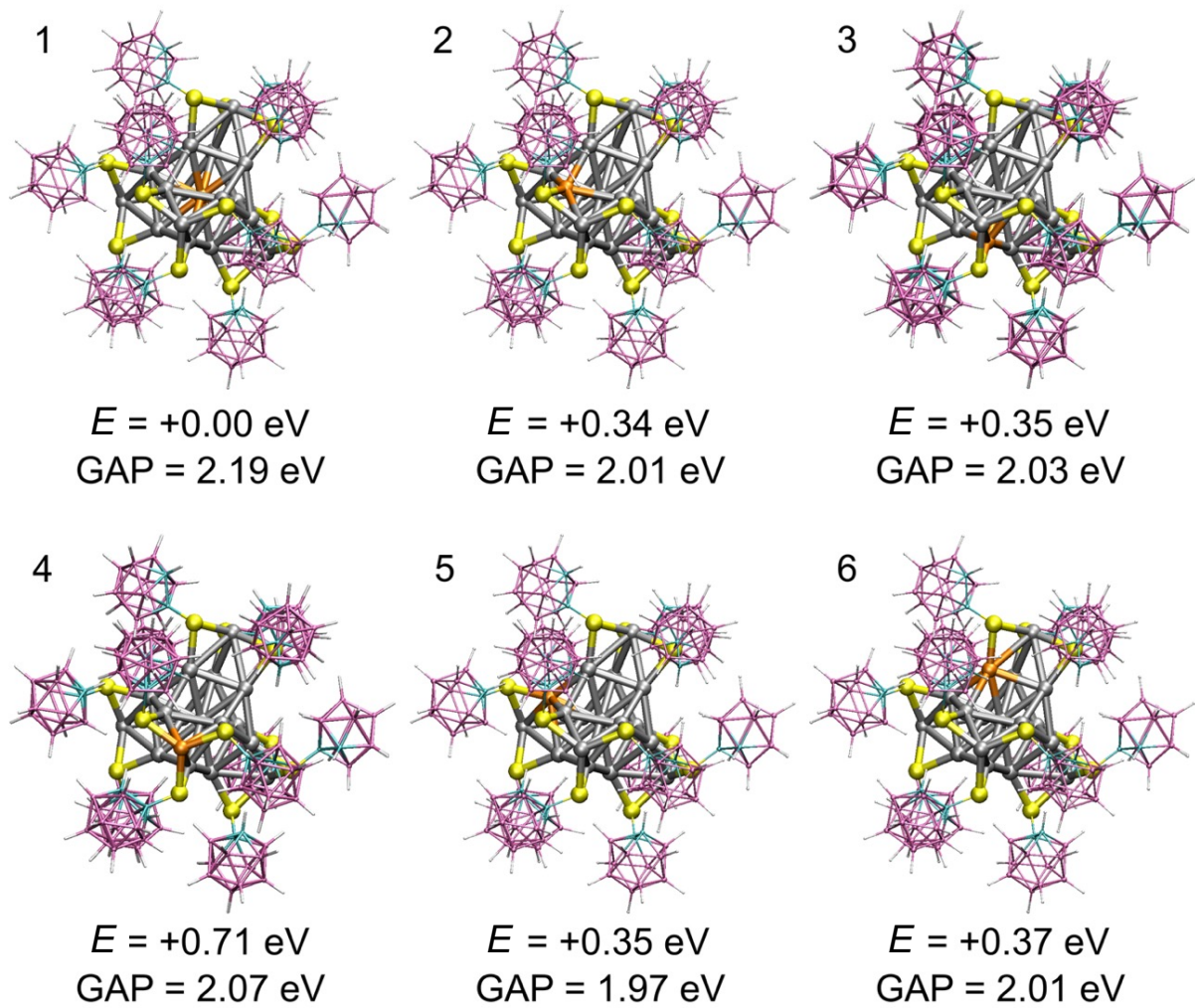
Supplementary Fig. 36 | Selected scan with respective peak fittings of **a** Ag₁₇, **b** AuAg₁₆, **c** Ag₁₃Cu₄ and **d** AuAg₁₂Cu₄.



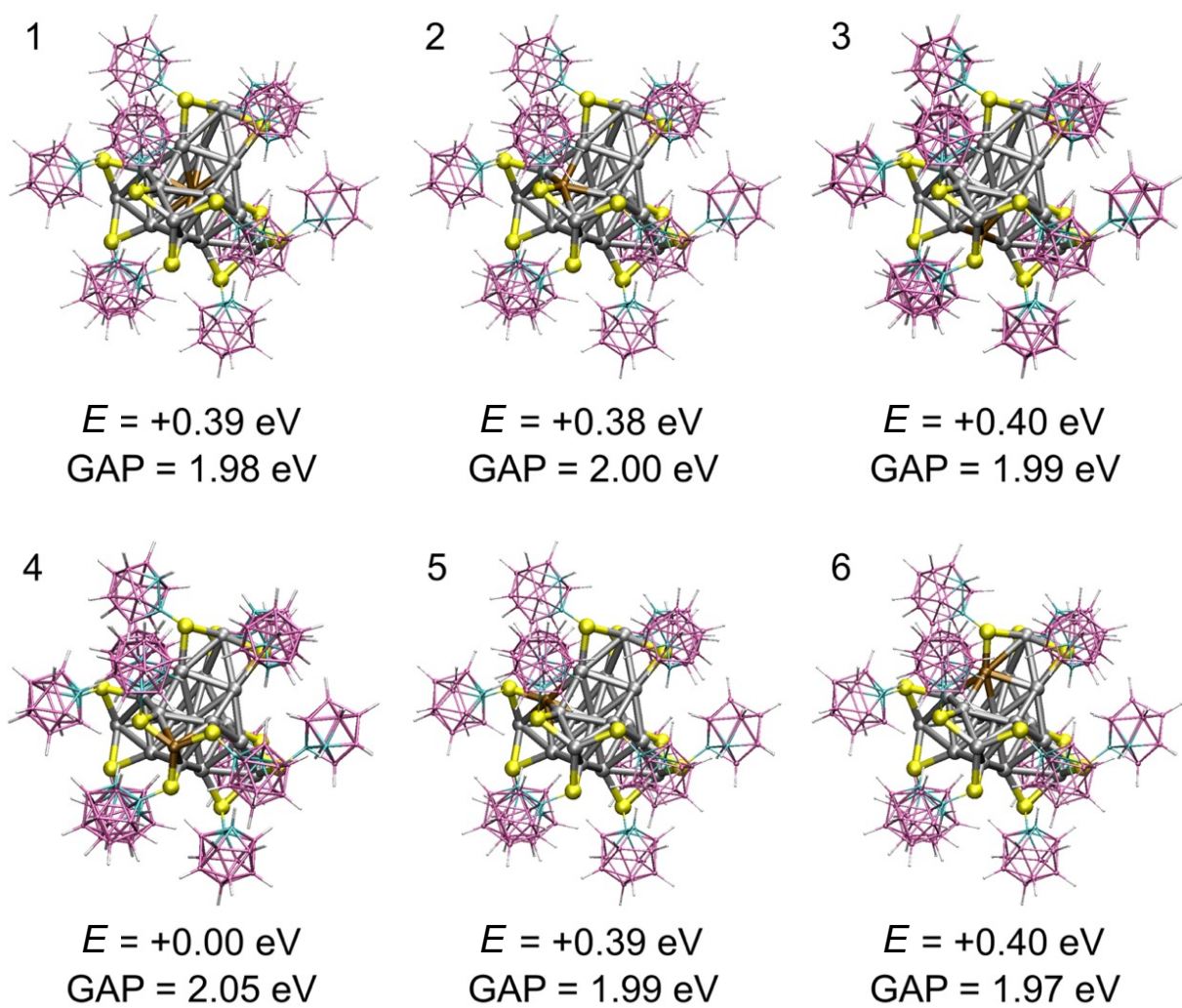
Supplementary Fig. 37 | Selected scan with respective peaks i.e., S 2p, B 1s and C 1s of **a** Ag₁₇, **b** AuAg₁₆, **c** Ag₁₃Cu₄ and **d** AuAg₁₂Cu₄.



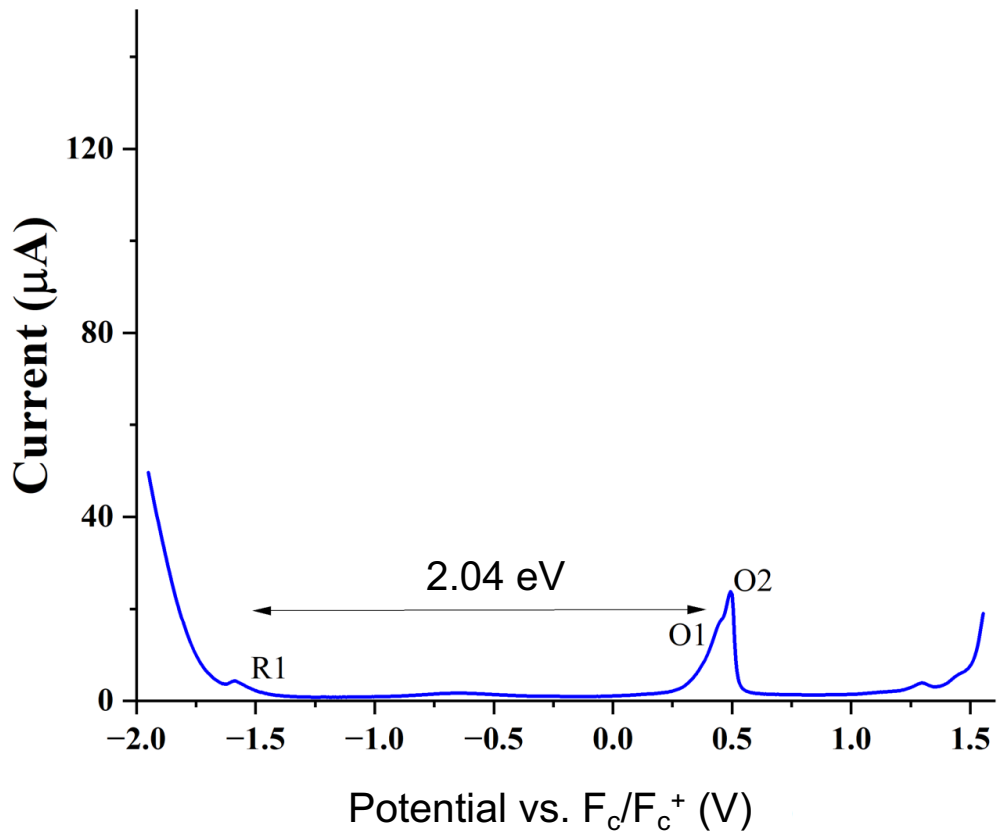
Supplementary Fig. 38 | Combined FT-IR spectra of the *o*1-CBT ligand, Ag_{17} , AuAg_{16} , $\text{Ag}_{13}\text{Cu}_4$ and $\text{AuAg}_{12}\text{Cu}_4$.



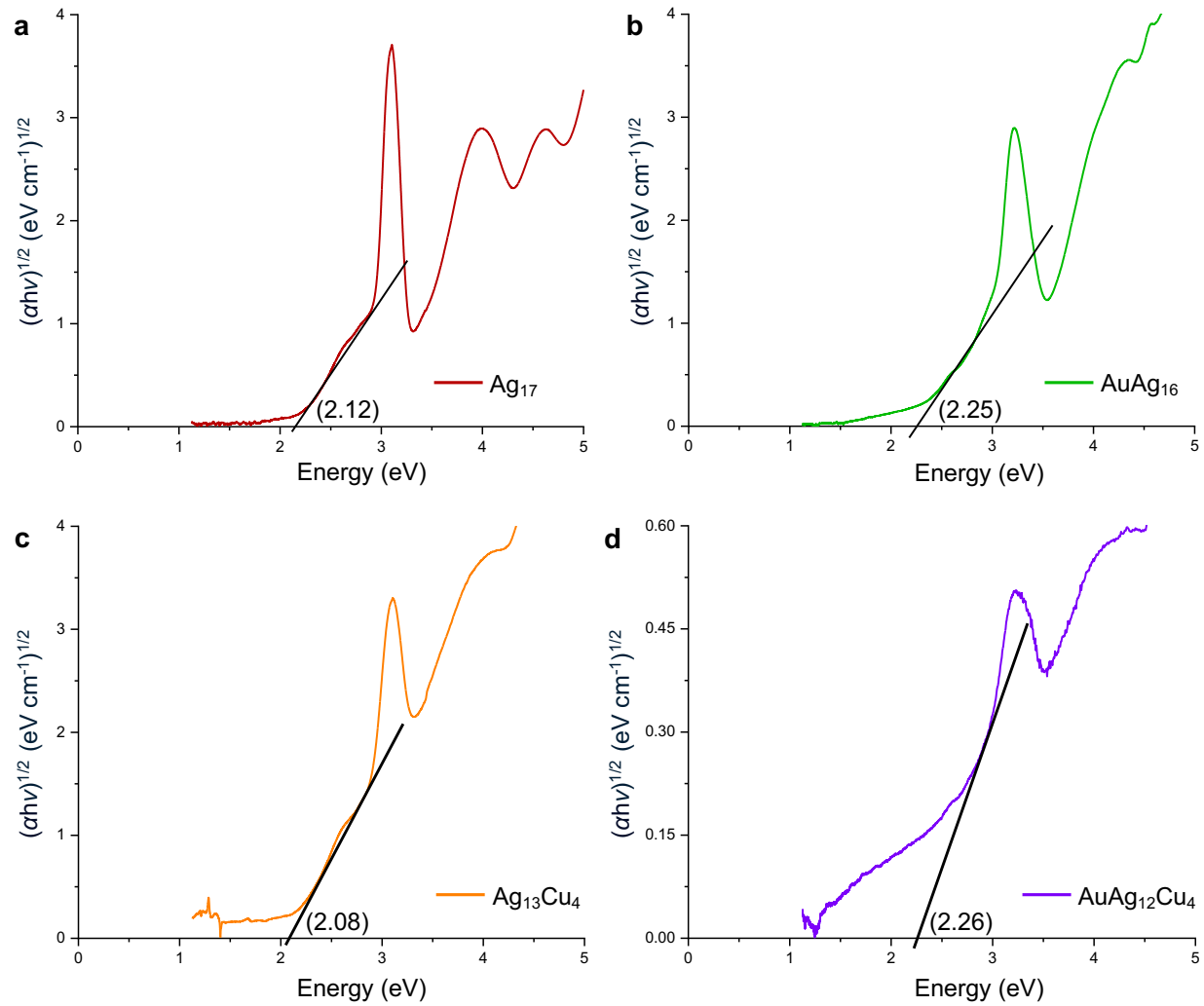
Supplementary Fig. 39 | Optimized structures and relative energies of cluster when Au is added in all symmetrically different metal atom positions.



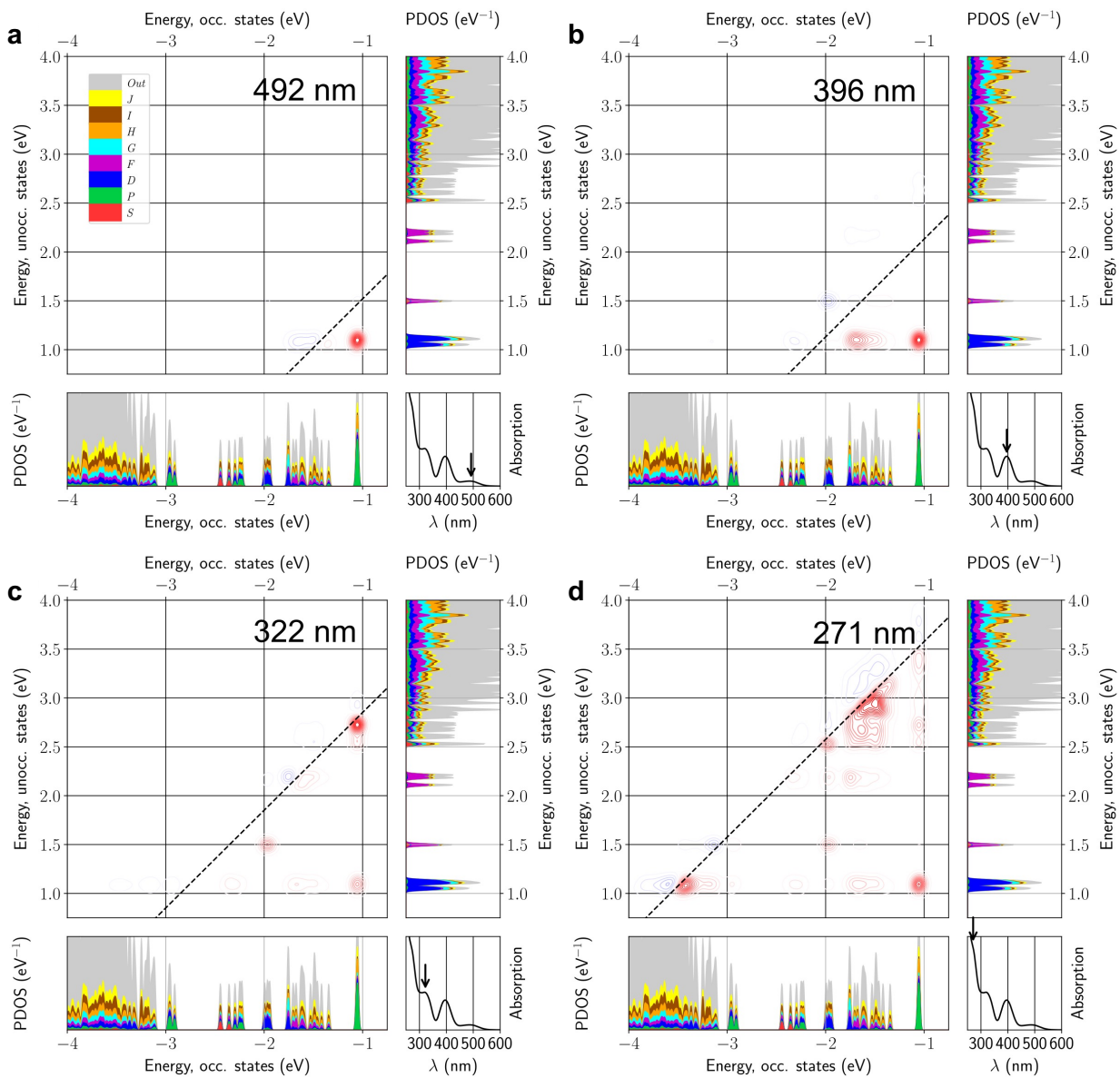
Supplementary Fig. 40 | Optimized structures and relative energies of cluster when Cu is added in all symmetrically different metal atom positions.



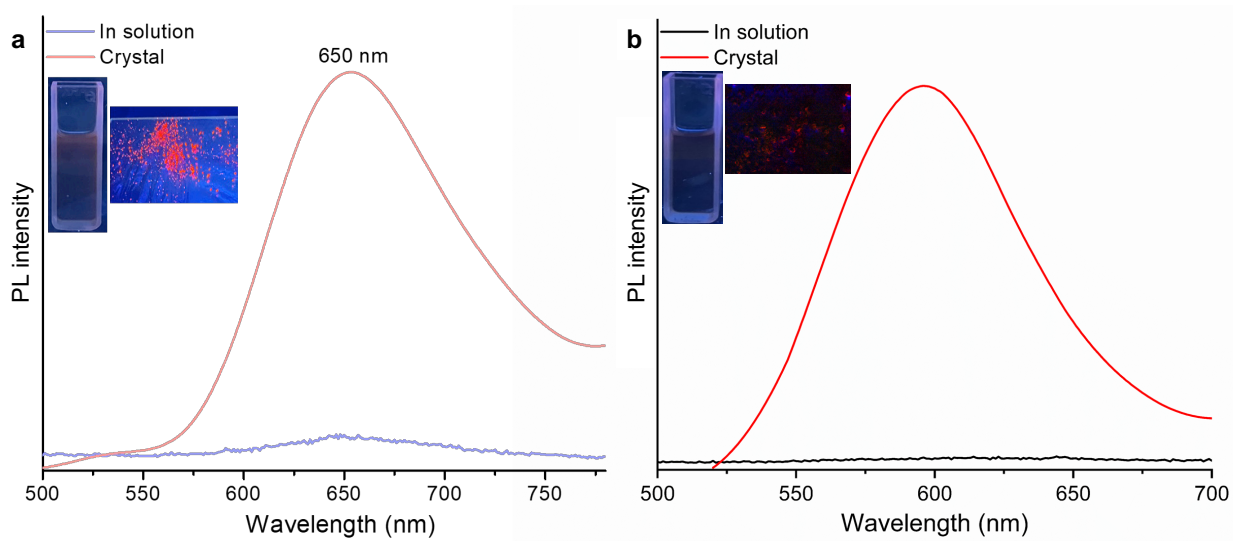
Supplementary Fig. 41 | DPV studies with Ag_{17} NC showing the experimental band gap of 2.04 eV.



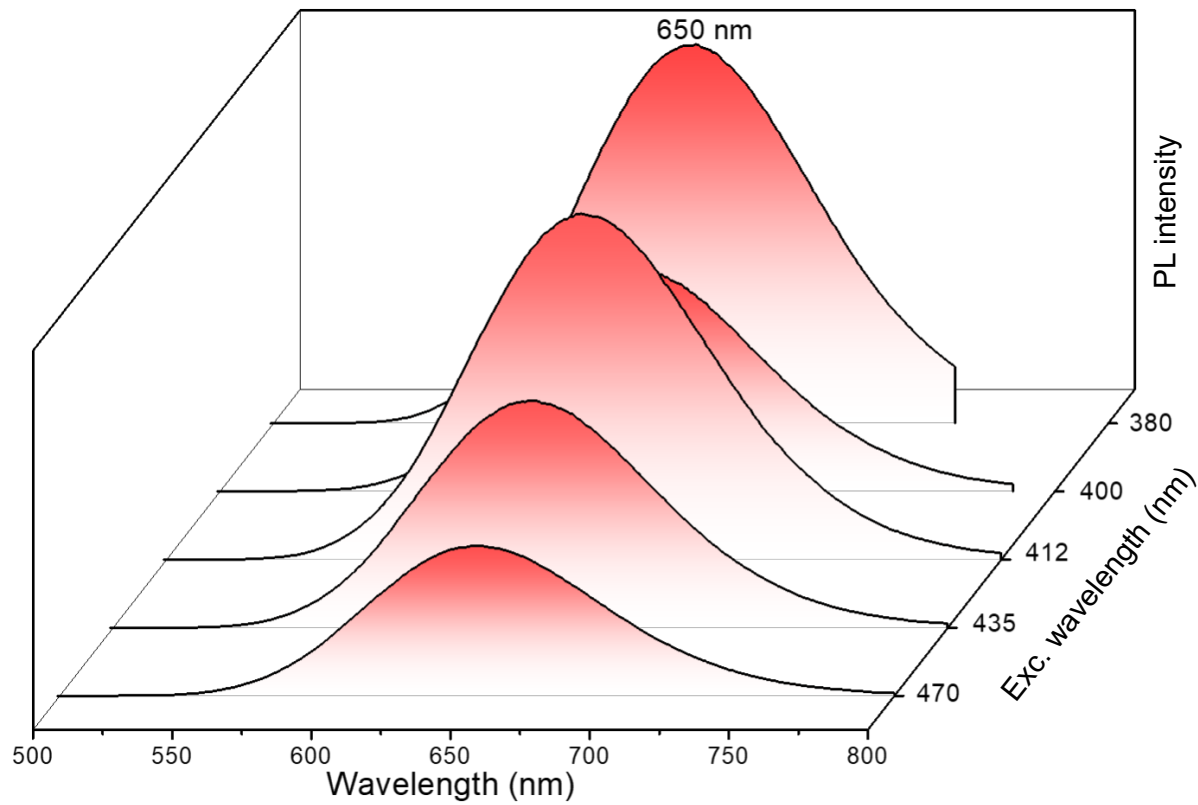
Supplementary Fig. 42 | Tauc's plots for the energy band gap of the **a** Ag₁₇, **b** AuAg₁₆, **c** Ag₁₃Cu₄ and **d** AuAg₁₂Cu₄ nanoclusters.



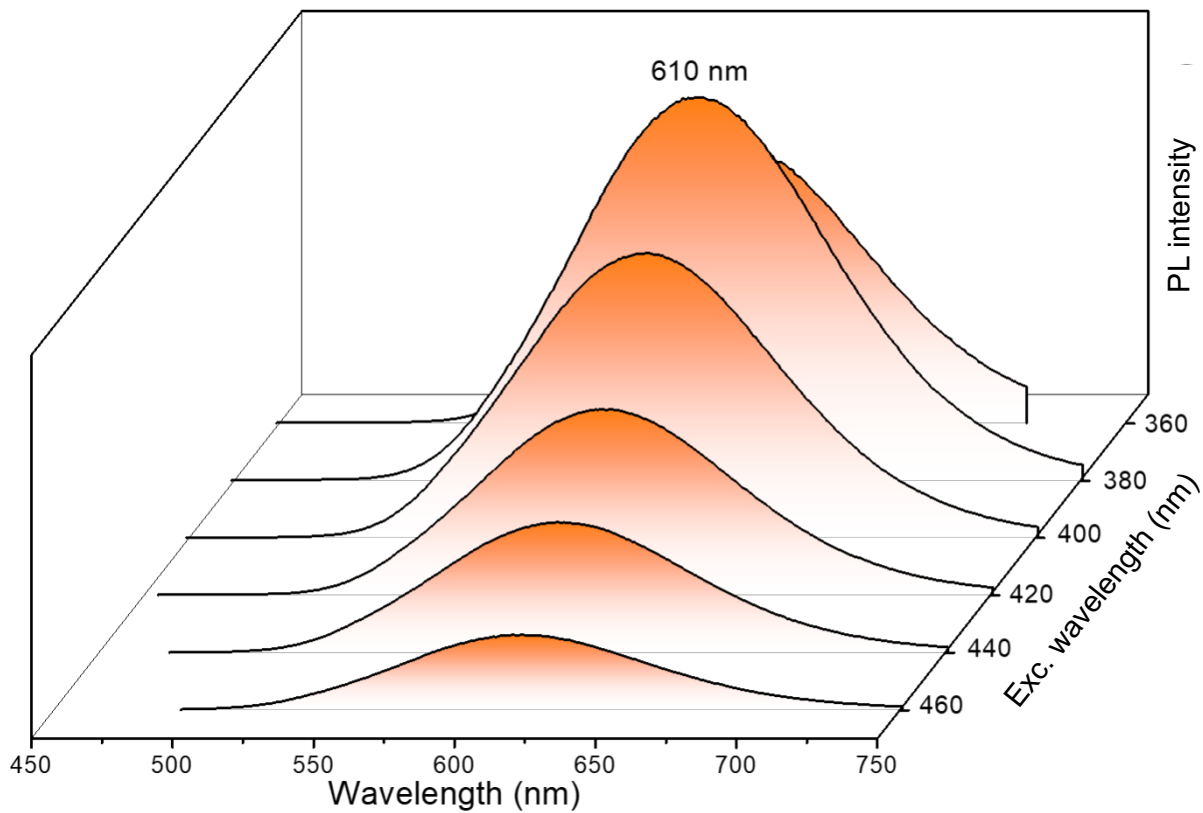
Supplementary Fig. 43 | Dipole transition contribution maps (DTCMs) showing the strengthening and screening contributions in Kohn-Sham basis for Ag_{17} at the energy of **a** 492 nm **b** 396 nm **c** 322 nm **d** 271 nm absorption peaks.



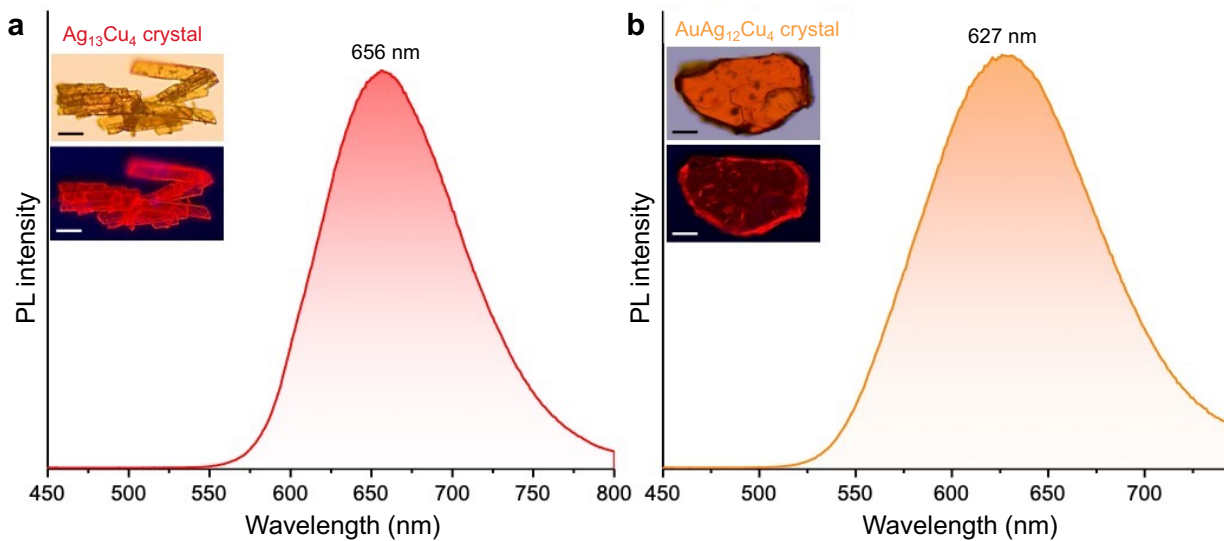
Supplementary Fig. 44 | Crystallization induced emission (CIE) behavior of **a** Ag_{17} and **b** AuAg_{16} . Inset shows the photographs of the respective cluster under UV light in solution and crystals.



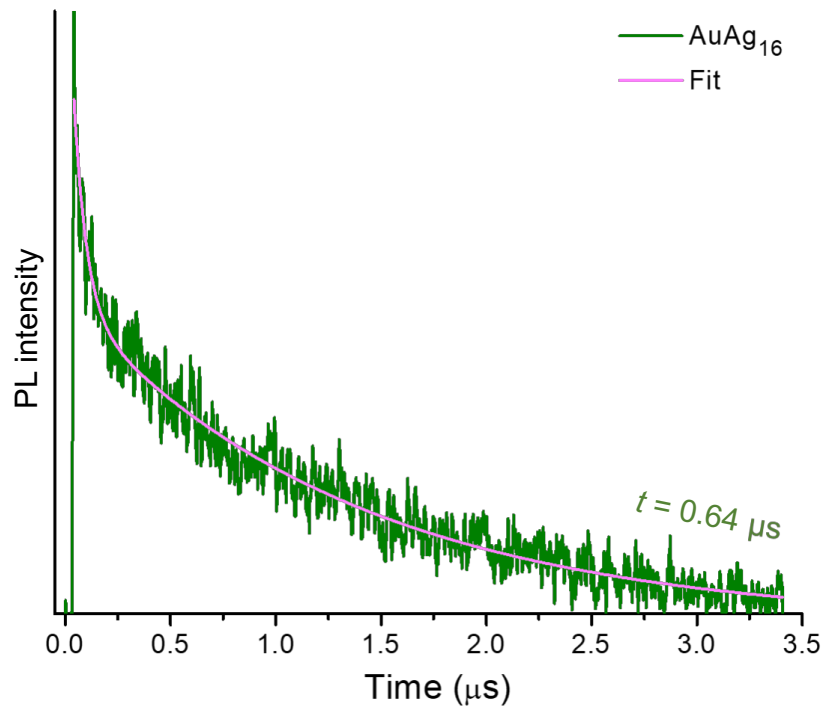
Supplementary Fig. 45 | Excitation-dependent emission spectra of $\text{Ag}_{13}\text{Cu}_4$ in DCM solution.



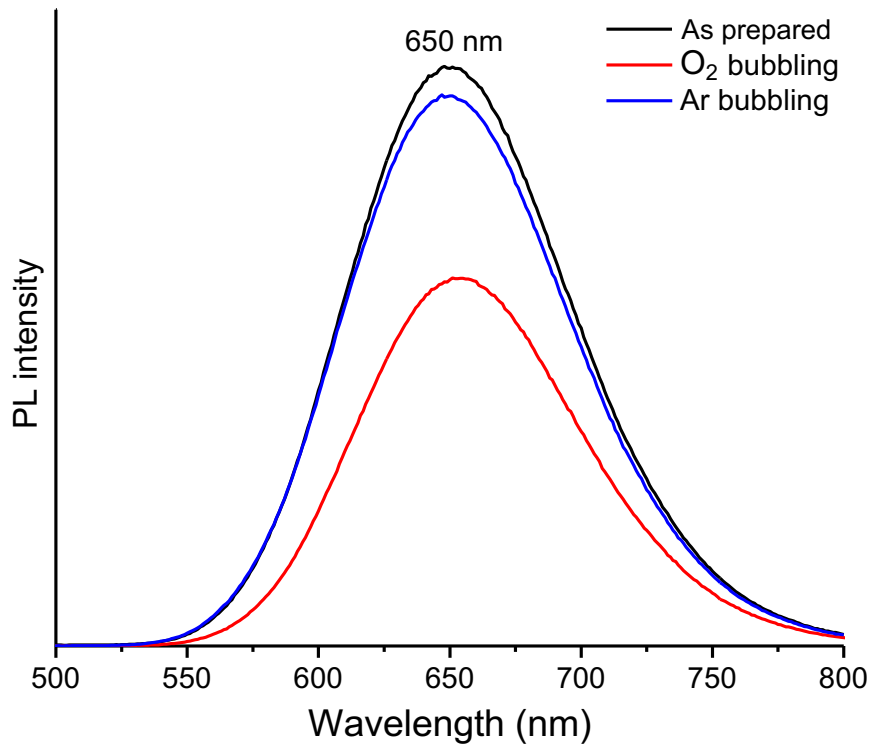
Supplementary Fig. 46 | Excitation-dependent emission spectra of $\text{AuAg}_{12}\text{Cu}_4$ in DCM solution.



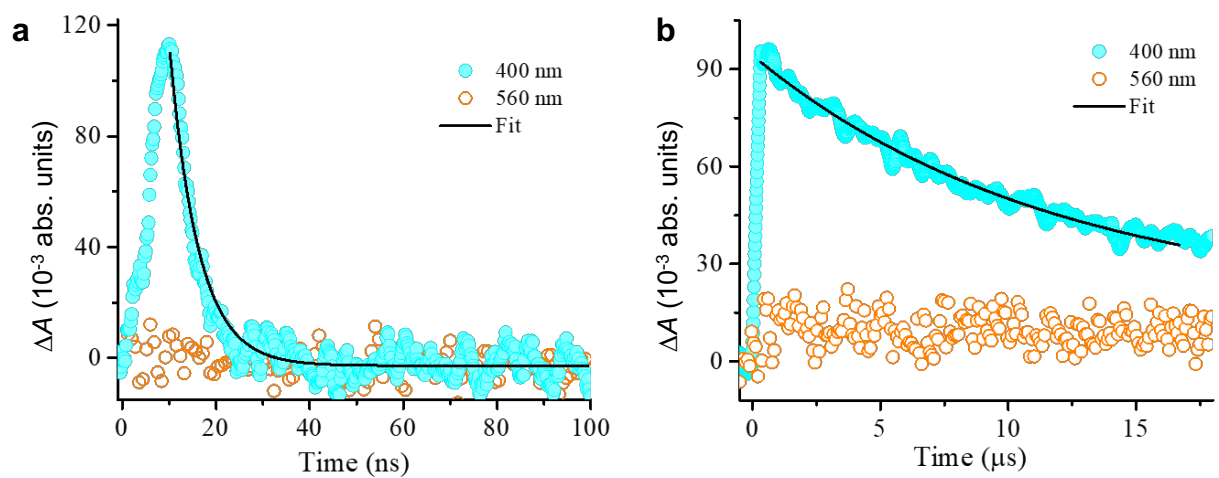
Supplementary Fig. 47 | Photoluminescence emission spectra of **a** $\text{Ag}_{13}\text{Cu}_4$ and **b** trimetallic $\text{AuAg}_{12}\text{Cu}_4$ crystals. Inset shows the optical micrographs of the respective crystals. Top: daylight, down: UV light. Scale bar 50 μm .



Supplementary Fig. 48 | Photoluminescence decay profile of AuAg_{16} .



Supplementary Fig. 49 | Photoluminescence emission spectra of $\text{Ag}_{13}\text{Cu}_4$ in DCM solution after oxygen and argon bubbling indicating phosphorescence emission originating from triplet state. Excitation wavelength was 412 nm.



Supplementary Fig. 50 | Nanosecond transient absorption decay kinetics for **a** $\text{Ag}_{13}\text{Cu}_4$ and **b** $\text{AuAg}_{12}\text{Cu}_4$. The solid line in the figures represents the single exponential fit.

Supplementary Tables

Supplementary Table 1 | Peak positions of the experimental and calculated absorption spectra. Possible additional non-assigned peaks are given in parenthesis at the next closest assigned peak.

Cluster	Absorption peak positions (nm)				
Ag ₁₇ , exp.	-	400	312	269	241
Ag ₁₇ , calc.	492	396	322	271	-
AuAg ₁₆ , exp.	-	385	288	271	-
AuAg ₁₆ , calc.	458	389	328	276	-
Ag ₁₃ Cu ₄ , exp.	475	400	307	-	-
Ag ₁₃ Cu ₄ , calc.	499	428	320 (364)	281	-
AuAg ₁₂ Cu ₄ , exp.	-	385	303	265	-
AuAg ₁₂ Cu ₄ , calc.	477	423	317 (356)	281	-

Supplementary Table 2 | Crystallographic information of Ag₁₇, AuAg₁₆, Ag₁₃Cu₄ and AuAg₁₂Cu₄ cluster crystals.

	Ag ₁₇	AuAg ₁₆	Ag ₁₃ Cu ₄	AuAg ₁₂ Cu ₄
Chemical formula	C ₂₄ H ₁₃₂ Ag ₁₇ B ₁₂₀ S ₁₂	C ₁₈₀ H ₂₇₆ Ag ₁₆ Au ₄ B ₁₂₀ P ₁₂ S ₁₂	C ₁₈₀ H ₂₇₆ Ag ₁₃ B ₁₂₀ Cu ₇ P ₁₂ S ₁₂	C ₂₄ H ₁₃₂ Ag ₁₂ AuB ₁₂₀ Cu ₄ S ₁₂
Formula weight	3937.00	7007.34	6340.64	3848.77
Temperature	173(2) K	296(2) K	273(2) K	129(2) K
Crystal system	Orthorhombic	Trigonal	Triclinic	Cubic
Space group	Pbcn	R -3	P-1	F d -3
Crystal Size (mm ³)	0.178 x 0.115 x 0.078	0.121 x 0.092 x 0.017	0.261 x 0.115 x 0.088	0.090 x 0.095 x 0.075
a (Å)	51.188(2)	30.0358(11)	22.4896(10)	38.364(17)
b (Å)	21.0030(9)	30.0358(11)	23.7297(12)	38.364(17)
c (Å)	33.3626(18)	59.198(4)	30.8515(14)	38.364(17)
α (°)	90	90	94.853(3)	90
β (°)	90	90	94.104(2)	90

γ (°)	90	120	103.94(3)	90
V (Å) ³	35868(2)	46250(5)	15850.2(13)	56464(8)
Z	8	6	2	8
Density calc. (mg m ⁻³)	1.458	1.510	1.329	0.905
Absorption coefficient	15.976 mm ⁻¹	13.055 mm ⁻¹	8.359 mm ⁻¹	8.700 mm ⁻¹
F(000)	14936	20376	6284	14616
Theta range for data collection	1.726 to 51.241°.	1.855 to 44.408°.	2.285 to 66.000°.	1.995 to 65.909°
Index ranges	-51<=h<=47, -11<=k<=20, -33<=l<=32	-21<=h<=25, -25<=k<=27, -29<=l<=53	-26<=h<=26, -28<=k<=28, -36<=l<=36	-44<=h<=45, -42<=k<=44, -43<=l<=40
Reflections collected	148451	29799	361230	96882
Independent reflections	18940 [R(int) = 0.1333] 0.1631]	7828 [R(int) = 0.1333] 0.1731	53869 [R(int) = 0.1469]	4113 [R(int) = 0.0805]
Completeness to theta	97.5 %	97.1 %	97.5	100.0 %
Max. and min. transmission	0.3030 and 0.0912	0.5041 and 0.1731	0.5210 and 0.2208	0.5872 and 0.3571
Data / restraints / parameters	18940 / 3142 / 1558	7828 / 1899 / 937	53869 / 2009 / 3074	4113 / 0 / 131
Goodness-of-fit on F ²	1.030	1.481	1.036	1.085
Final R indices [I>2sigma(I)]	R1 = 0.0949, wR2 = 0.2658	R1 = 0.1726, wR2 = 0.4085	R1 = 0.0765, wR2 = 0.2069	R1 = 0.0782, wR2 = 0.2469
R indices (all data)	R1 = 0.1989, wR2 = 0.3665	R1 = 0.3348, wR2 = 0.5357	R1 = 0.1787, wR2 = 0.3161	R1 = 0.1015, wR2 = 0.2895

Largest diff. peak and hole	1.515 and -0.642 $\text{e } \text{\AA}^{-3}$	4.161 and -0.930 $\text{e } \text{\AA}^{-3}$	1.131 and -1.276 $\text{e } \text{\AA}^{-3}$	2.445 and - 0.764 $\text{e } \text{\AA}^{-3}$
CCDC No.	2356804	2356806	2356807	2356892

Supplementary Table 3 | Atomic coordinates ($x \times 10^4$) and equivalent isotropic displacement parameters ($\text{\AA}^2 \times 10^3$) for Ag_{17} cluster. $U(\text{eq})$ is defined as one third of the trace of the orthogonalized U_{ij}^{eq} tensor. Check CIF justifications of level A and level B alerts.

	x	y	z	$U(\text{eq})$
Ag(1)	6338(1)	7418(1)	6317(1)	140(1)
Ag(2)	6354(1)	8608(1)	6696(1)	151(1)
Ag(3)	6767(1)	7640(1)	6814(1)	150(1)
Ag(4)	6562(1)	6393(1)	6715(1)	152(1)
Ag(5)	6925(1)	9043(1)	6728(1)	159(1)
Ag(6)	6298(1)	6240(1)	5930(1)	156(1)
Ag(7)	6709(1)	8266(1)	6024(1)	153(1)
Ag(8)	5881(1)	7934(1)	6639(1)	153(1)
Ag(9)	6277(1)	7309(1)	7150(1)	151(1)
Ag(10)	6800(1)	6941(1)	5983(1)	155(1)
Ag(11)	6801(1)	5491(1)	6093(1)	169(1)
Ag(12)	6115(1)	8470(1)	5942(1)	155(1)
Ag(13)	5964(1)	6544(1)	6579(1)	155(1)
Ag(14)	6419(1)	7510(1)	5486(1)	158(1)
Ag(15)	5904(1)	7170(1)	5838(1)	157(1)
Ag(16)	5704(1)	7067(1)	7336(1)	163(1)
Ag(17)	5930(1)	8054(1)	5109(1)	175(1)
C(1)	6995(5)	8351(13)	7693(10)	157(4)
C(2)	6683(5)	8589(13)	7791(10)	167(6)
B(1)	6690(8)	9057(18)	8235(12)	176(7)
B(2)	6826(8)	8637(17)	8630(13)	182(7)
B(3)	6818(6)	7803(17)	7946(12)	161(6)
B(4)	6935(7)	9073(17)	7838(13)	169(6)
B(5)	7129(7)	7913(17)	8080(12)	167(5)

B(6)	7217(8)	8697(17)	8004(12)	173(6)
B(7)	6619(8)	8234(17)	8286(12)	172(7)
B(8)	6888(8)	7847(18)	8460(13)	181(7)
B(9)	7012(8)	9191(19)	8329(12)	183(8)
B(10)	7147(8)	8353(18)	8473(13)	185(7)
C(3)	7366(5)	8671(12)	5947(10)	166(5)
C(4)	7413(6)	7972(14)	5684(11)	189(7)
B(11)	7701(8)	8021(19)	5479(15)	196(8)
B(12)	7653(7)	7556(18)	5895(14)	190(8)
B(13)	7448(7)	8006(16)	6236(14)	176(7)
B(14)	7863(7)	8732(17)	5591(14)	189(8)
B(15)	7770(7)	7977(19)	6306(14)	188(7)
B(16)	7921(8)	7947(17)	5856(14)	185(8)
B(17)	7882(7)	8705(18)	6101(14)	186(8)
B(18)	7586(6)	8682(17)	6345(14)	175(6)
B(19)	7510(8)	8673(18)	5449(14)	191(7)
B(20)	7645(7)	9120(18)	5922(12)	178(7)
C(5)	7294(5)	6262(13)	6824(11)	179(6)
C(6)	7130(5)	5650(13)	7014(11)	164(5)
B(21)	7503(7)	5317(17)	7548(14)	185(7)
B(22)	7655(7)	5317(17)	7091(13)	183(8)
B(23)	7327(6)	5028(17)	7184(12)	172(7)
B(24)	7179(7)	5544(16)	7477(14)	173(6)
B(25)	7160(7)	6297(16)	7296(13)	175(6)
B(26)	7496(7)	6604(18)	7229(13)	193(8)
B(27)	7642(7)	6062(17)	6873(15)	189(8)
B(28)	7704(8)	5980(18)	7402(15)	199(9)
B(29)	7415(7)	6137(17)	7676(14)	192(8)
B(30)	7399(6)	5440(17)	6778(13)	174(6)
C(7)	6488(6)	10154(14)	6100(11)	182(6)
C(8)	6456(5)	10240(13)	6609(11)	166(6)
B(31)	6272(8)	10640(18)	5846(15)	198(8)
B(32)	6175(7)	10271(17)	6320(13)	182(7)
B(33)	6233(7)	10833(17)	6724(15)	191(7)
B(34)	6558(8)	10987(16)	6733(15)	197(8)
B(35)	6702(7)	10589(17)	6345(14)	187(7)

B(36)	6583(7)	10827(17)	5887(15)	195(7)
B(37)	6629(8)	11375(18)	6259(15)	207(9)
B(38)	6349(7)	11464(18)	5975(16)	201(9)
B(39)	6331(8)	11517(19)	6508(17)	215(9)
B(40)	6099(8)	11076(18)	6278(15)	200(8)
C(9)	5548(6)	9184(15)	5641(11)	179(6)
C(10)	5353(6)	9635(18)	5316(12)	219(9)
B(41)	5492(8)	9311(18)	6084(14)	185(7)
B(42)	5469(8)	9940(20)	5813(14)	202(8)
B(43)	5135(8)	10040(30)	5706(16)	236(10)
B(44)	5242(8)	9860(20)	6171(16)	224(10)
B(45)	5308(7)	8810(20)	5381(14)	205(8)
B(46)	5375(7)	8610(20)	5864(13)	188(8)
B(47)	5186(8)	9010(20)	6225(15)	211(9)
B(48)	5047(8)	8680(30)	5732(15)	223(10)
B(49)	4951(9)	9430(20)	5902(15)	232(10)
B(50)	5023(8)	9350(30)	5417(16)	241(10)
C(11)	5760(6)	9340(14)	7327(11)	191(7)
C(12)	5596(5)	8696(14)	7438(11)	172(6)
B(51)	5633(8)	9990(20)	7608(16)	217(9)
B(52)	5650(6)	8520(20)	7917(13)	185(6)
B(53)	5369(7)	8883(18)	7802(13)	181(7)
B(54)	5421(7)	9395(18)	7404(14)	189(7)
B(55)	5901(7)	8800(20)	7608(13)	186(7)
B(56)	5851(8)	9070(20)	8098(15)	211(9)
B(57)	5522(8)	9090(20)	8232(15)	210(8)
B(58)	5400(8)	9650(20)	7899(14)	202(8)
B(59)	5930(8)	9610(20)	7715(15)	213(9)
B(60)	5697(8)	9790(20)	8106(16)	226(11)
C(13)	5307(6)	6174(16)	6690(10)	174(6)
C(14)	5238(6)	6922(16)	6459(10)	183(7)
B(61)	4889(7)	7080(20)	6470(13)	203(8)
B(62)	5075(7)	6710(20)	6887(14)	183(7)
B(63)	5029(7)	5870(20)	6910(13)	190(7)
B(64)	5179(8)	5540(20)	6448(12)	194(7)
B(65)	5298(8)	6230(20)	6207(13)	189(7)

B(66)	5030(8)	6720(20)	6032(14)	201(8)
B(67)	4754(8)	6430(20)	6767(14)	214(9)
B(68)	4722(9)	6400(30)	6222(15)	225(10)
B(69)	4826(8)	5700(20)	6481(14)	220(9)
B(70)	4963(9)	5870(20)	6040(15)	217(10)
C(15)	6296(7)	3789(14)	5934(12)	210(8)
C(16)	6229(6)	4596(14)	6056(12)	180(6)
B(71)	6370(8)	4183(17)	6391(14)	193(7)
B(72)	5899(8)	4684(19)	6171(14)	203(8)
B(73)	6168(8)	4741(18)	6492(14)	190(7)
B(74)	6250(9)	3470(19)	6439(16)	216(9)
B(75)	5980(9)	4110(20)	5808(17)	217(9)
B(76)	5784(10)	3930(20)	6147(17)	235(10)
B(77)	5868(9)	4282(19)	6629(17)	222(9)
B(78)	6170(9)	4021(19)	6803(17)	213(8)
B(79)	5936(9)	3490(20)	6547(18)	235(10)
B(80)	6007(10)	3350(20)	6045(18)	246(11)
C(17)	6159(5)	6290(14)	7974(10)	168(5)
C(18)	6470(6)	5964(14)	7842(10)	185(7)
B(81)	6414(8)	5165(18)	7825(13)	186(7)
B(82)	6191(7)	5684(17)	7631(13)	175(6)
B(83)	5940(7)	5715(18)	7974(12)	171(7)
B(84)	6028(7)	6060(20)	8392(13)	181(7)
B(85)	6362(7)	6210(20)	8385(13)	191(7)
B(86)	6536(8)	5470(20)	8312(13)	196(8)
B(87)	6261(7)	5500(20)	8608(14)	195(8)
B(88)	6266(7)	4870(20)	8259(13)	188(8)
B(89)	5982(7)	5200(20)	8345(13)	186(8)
B(90)	6079(7)	4997(19)	7872(13)	183(8)
C(19)	6525(7)	8487(15)	4653(11)	191(6)
C(20)	6824(6)	8710(15)	4863(12)	198(7)
B(91)	6560(7)	9134(16)	4992(14)	183(7)
B(92)	6569(8)	9870(20)	4765(14)	204(9)
B(93)	6787(9)	8460(20)	4381(15)	215(8)
B(94)	7016(9)	9090(20)	4469(15)	222(10)
B(95)	6800(10)	9150(20)	4033(16)	231(10)

B(96)	6876(9)	9790(20)	4360(14)	221(10)
B(97)	6525(9)	9730(20)	4264(15)	220(10)
B(98)	6353(9)	9260(19)	4578(13)	200(8)
B(99)	6868(8)	9512(19)	4901(14)	200(9)
B(100)	6513(10)	8760(20)	4155(15)	217(9)
C(21)	5648(6)	6549(16)	4965(11)	189(6)
C(22)	5399(8)	6415(19)	4623(11)	226(8)
B(101)	5892(10)	5430(20)	4770(15)	218(9)
B(102)	5692(11)	5190(30)	4390(17)	265(14)
B(103)	5441(9)	5930(20)	5029(15)	210(8)
B(104)	5744(8)	5829(18)	5201(15)	197(8)
B(105)	5941(9)	6191(19)	4886(14)	199(8)
B(106)	5913(11)	5860(20)	4376(17)	236(10)
B(107)	5584(10)	5250(20)	4938(16)	231(10)
B(108)	5389(11)	5580(30)	4552(17)	260(12)
B(109)	5610(12)	6000(30)	4179(17)	261(12)
B(110)	5750(9)	6560(20)	4463(15)	219(8)
C(23)	7105(6)	6072(12)	5245(11)	168(6)
B(113)	7021(8)	6672(19)	4927(13)	191(8)
B(111)	6829(9)	6023(19)	4972(14)	194(7)
B(112)	6898(11)	6380(20)	4503(15)	231(10)
C(24)	7337(7)	6414(17)	4929(11)	209(8)
B(114)	7186(11)	6500(30)	4449(16)	230(10)
B(115)	7395(12)	5900(20)	4519(15)	248(11)
B(116)	7160(13)	5320(30)	4588(17)	267(12)
B(117)	7114(13)	5880(30)	4160(19)	286(15)
B(118)	7346(10)	5620(20)	5034(15)	220(9)
B(119)	6990(10)	5370(19)	5006(15)	214(9)
B(120)	6872(13)	5540(30)	4556(17)	261(12)
S(1)	7061(1)	9082(3)	6011(3)	158(2)
S(2)	6078(1)	7083(4)	7818(3)	160(2)
S(3)	7111(1)	8222(3)	7195(3)	155(2)
S(4)	6814(1)	5401(3)	6839(3)	162(2)
S(5)	6530(1)	9636(3)	6960(3)	162(2)
S(6)	5882(2)	9124(4)	5440(3)	164(2)
S(7)	5504(1)	8097(4)	7102(3)	162(2)

S(8)	6405(2)	5126(4)	5718(3)	176(3)
S(9)	5600(2)	6065(4)	6971(3)	170(3)
S(10)	6348(2)	7793(4)	4772(3)	174(2)
S(11)	7136(2)	6158(4)	5751(3)	165(3)
S(12)	5590(2)	7247(4)	5269(3)	172(2)

checkCIF/PLATON report (justification)

Alert level A

THETM01_ALERT_3_A The value of sine(theta_max)/wavelength is less than 0.550

Calculated sin(theta_max)/wavelength = 0.5058

Response: The crystal was not diffracting at higher Brag angles.

Hence a resolution cut was made during data integration in order to omit weak higher reflections.

Alert level B

PLAT084_ALERT_3_B High wR2 Value (i.e. > 0.25) 0.37 Report

Response: Due to weak higher angle reflections. Also, the carborane moieties disordered in the lattice. This contributes high wR2 values.

PLAT342_ALERT_3_B Low Bond Precision on C-C Bonds 0.04556 Ang.

Response: Due to poor resolution of the crystal, the accuracies of C-C bonds are low.

Supplementary Table 4 | Atomic coordinates ($\times 10^4$) and equivalent isotropic displacement parameters ($\text{\AA}^2 \times 10^3$) for $\text{Ag}_{13}\text{Cu}_4$ cluster. $U(\text{eq})$ is defined as one third of the trace of the orthogonalized U^{ij} tensor. Check CIF justifications of level A and level B alerts.

	<i>x</i>	<i>y</i>	<i>z</i>	<i>U</i> (eq)
Ag(1)	8144(1)	2594(1)	7794(1)	82(1)
Ag(2)	7346(1)	3291(1)	8006(1)	90(1)
Ag(3)	8577(1)	3376(1)	8537(1)	91(1)
Ag(4)	7573(1)	2405(1)	8561(1)	91(1)
Ag(5)	8464(1)	3779(1)	7668(1)	92(1)
Ag(6)	7511(1)	2979(1)	7123(1)	91(1)
Ag(7)	6901(1)	2041(1)	7684(1)	90(1)
Ag(8)	9396(1)	3132(1)	7882(1)	94(1)
Ag(9)	7685(1)	1787(1)	7056(1)	93(1)
Ag(10)	8770(1)	2235(1)	8485(1)	94(1)

Ag(11)	8749(1)	2797(1)	7045(1)	94(1)
Ag(12)	8975(1)	1942(1)	7574(1)	96(1)
Ag(13)	7788(1)	1410(1)	7902(1)	94(1)
Cu(1)	6300(1)	2563(1)	8397(1)	84(1)
Cu(2)	9563(1)	4350(1)	8285(1)	89(1)
Cu(3)	7805(1)	2431(1)	6276(1)	89(1)
Cu(4)	8898(1)	1030(1)	8216(1)	95(1)
C(1)	5928(6)	3557(6)	7752(4)	86(3)
C(2)	5239(7)	3095(8)	7604(5)	114(4)
C(3)	6959(6)	3040(6)	9443(4)	89(3)
C(4)	6595(7)	3579(7)	9440(6)	109(3)
C(5)	6520(6)	1320(6)	6189(4)	92(3)
C(6)	6129(7)	588(7)	6136(5)	113(4)
C(7)	7647(7)	3817(7)	6252(4)	96(3)
C(8)	7246(8)	4322(8)	6231(6)	127(4)
C(9)	5743(6)	1099(6)	8106(5)	92(3)
C(10)	6174(8)	628(7)	7961(5)	111(3)
C(11)	9207(6)	2173(6)	6123(4)	87(3)
C(12)	9400(7)	2138(7)	5602(5)	106(3)
C(13)	9808(6)	3963(6)	9298(4)	85(3)
C(14)	10138(7)	3438(7)	9113(5)	108(4)
C(15)	10545(7)	4176(7)	7533(5)	103(3)
C(16)	10555(8)	4874(8)	7417(6)	119(4)
C(17)	8582(6)	5212(6)	8108(5)	92(3)
C(18)	8280(9)	5674(9)	7833(6)	137(4)
C(19)	10334(7)	1563(7)	7890(5)	109(4)
C(20)	10702(9)	2211(9)	7748(7)	147(4)
C(21)	7868(7)	19(6)	7512(5)	97(3)
C(22)	7210(8)	-482(8)	7346(6)	130(4)
C(23)	8705(7)	1318(6)	9296(5)	97(3)
C(24)	8352(9)	598(8)	9338(7)	140(5)
S(1)	6378(2)	3503(2)	8248(1)	92(1)
S(2)	6729(2)	2404(2)	9052(1)	92(1)
S(3)	7349(2)	1470(2)	6258(1)	96(1)
S(4)	7233(2)	3101(2)	6348(1)	93(1)
S(5)	5829(2)	1792(2)	7895(1)	93(1)

S(6)	8834(2)	2748(2)	6245(1)	93(1)
S(7)	9273(2)	4239(2)	8972(1)	94(1)
S(8)	10330(2)	3957(2)	8049(1)	101(1)
S(9)	9053(2)	4818(2)	7828(1)	97(1)
S(10)	9563(2)	1199(2)	7686(1)	102(1)
S(11)	7947(2)	427(2)	8037(1)	101(1)
S(12)	9210(2)	1536(2)	8886(1)	103(1)
B(1)	5287(8)	3795(9)	7805(7)	108(4)
B(2)	4752(9)	3487(10)	7361(7)	123(5)
B(3)	5130(8)	3042(10)	7030(6)	112(4)
B(4)	5869(8)	3078(8)	7296(5)	96(4)
B(5)	5936(9)	4236(8)	7639(6)	105(4)
B(6)	5215(10)	4201(11)	7371(7)	132(5)
B(7)	5127(9)	3724(11)	6895(7)	128(5)
B(8)	5778(8)	3476(9)	6849(6)	107(4)
B(9)	6272(8)	3778(8)	7314(6)	97(4)
B(10)	5838(10)	4201(10)	7064(7)	125(5)
B(11)	6491(10)	3101(9)	9834(6)	109(4)
B(12)	7196(10)	2938(9)	9948(6)	114(4)
B(13)	7731(9)	3324(9)	9610(7)	112(4)
B(14)	7332(9)	3707(8)	9307(7)	103(4)
B(15)	7103(9)	4233(9)	9636(7)	118(4)
B(16)	7829(10)	4085(9)	9742(7)	120(5)
B(17)	7735(11)	3628(10)	10162(7)	138(5)
B(18)	6952(12)	3467(10)	10305(7)	140(6)
B(19)	6576(11)	3872(10)	9968(8)	134(5)
B(20)	7370(11)	4171(10)	10169(7)	134(5)
B(21)	6159(8)	1710(9)	5876(6)	106(4)
B(22)	6183(8)	1014(8)	5687(6)	105(4)
B(23)	6115(8)	1742(9)	6433(6)	103(4)
B(24)	6105(8)	1084(9)	6600(6)	106(4)
B(25)	5416(8)	1283(9)	6544(7)	112(4)
B(26)	5416(8)	560(9)	6344(7)	112(4)
B(27)	5459(9)	553(9)	5782(7)	120(5)
B(28)	5481(9)	1250(9)	5631(7)	118(5)
B(29)	5469(8)	1717(9)	6100(7)	114(4)

B(30)	5027(9)	990(8)	6032(6)	109(4)
B(31)	7796(10)	4365(8)	6660(7)	110(4)
B(32)	8395(8)	4136(9)	6443(7)	107(4)
B(33)	8194(9)	3920(10)	5893(7)	118(4)
B(34)	7450(10)	4010(11)	5755(7)	129(5)
B(35)	7559(12)	4770(12)	5811(9)	165(7)
B(36)	8150(13)	4533(12)	5637(8)	156(6)
B(37)	8709(11)	4588(10)	6060(7)	125(5)
B(38)	8467(10)	4873(10)	6531(7)	121(5)
B(39)	7757(10)	5000(10)	6406(9)	138(5)
B(40)	8309(11)	5119(11)	6037(8)	140(5)
B(41)	5384(9)	482(8)	7781(6)	105(4)
B(42)	5017(9)	755(9)	8204(6)	108(4)
B(43)	5583(8)	1038(8)	8618(6)	97(3)
B(44)	6278(8)	977(8)	8485(6)	101(4)
B(45)	6258(9)	226(8)	8402(6)	103(4)
B(46)	5701(9)	-83(9)	7959(7)	114(4)
B(47)	4999(9)	-1(9)	8124(7)	121(5)
B(48)	5092(9)	352(9)	8660(7)	115(4)
B(49)	5894(9)	508(9)	8829(7)	110(4)
B(50)	5523(9)	-159(9)	8512(7)	114(4)
B(51)	9715(8)	2013(8)	6496(6)	97(4)
B(52)	9002(8)	1502(8)	6310(6)	94(3)
B(53)	8862(8)	1573(8)	5770(5)	94(3)
B(54)	9956(7)	2378(9)	6049(6)	95(3)
B(55)	9683(9)	1267(9)	6356(7)	108(4)
B(56)	10282(9)	1818(9)	6181(6)	112(4)
B(57)	10104(9)	1904(9)	5628(7)	110(4)
B(58)	9391(8)	1392(9)	5453(6)	110(4)
B(59)	9142(9)	1020(9)	5895(6)	106(4)
B(60)	9931(9)	1189(9)	5828(6)	112(4)
B(61)	10561(8)	4147(8)	9234(6)	96(3)
B(62)	10299(7)	4452(9)	9660(5)	96(4)
B(63)	9704(9)	3943(9)	9838(6)	106(4)
B(64)	9619(9)	3287(9)	9482(6)	108(4)
B(65)	10048(10)	3394(11)	10015(7)	126(5)

B(66)	10309(9)	3076(10)	9551(6)	111(4)
B(67)	10905(9)	3602(9)	9377(7)	115(4)
B(68)	10988(9)	4261(9)	9721(6)	113(4)
B(69)	10466(9)	4131(10)	10117(6)	121(5)
B(70)	10829(9)	3582(9)	9937(6)	118(5)
B(71)	10392(9)	3709(9)	7072(6)	109(4)
B(72)	11137(8)	3963(9)	7324(7)	110(4)
B(73)	11227(9)	4682(9)	7537(7)	117(4)
B(74)	10011(9)	4269(9)	7129(6)	110(4)
B(75)	10305(9)	4141(9)	6645(7)	116(4)
B(76)	10398(10)	4885(10)	6852(7)	125(5)
B(77)	11150(10)	5123(10)	7115(7)	125(5)
B(78)	11533(10)	4555(10)	7058(7)	124(5)
B(79)	11011(10)	3950(10)	6757(7)	123(5)
B(80)	11015(10)	4678(10)	6623(7)	126(5)
B(81)	7804(9)	5048(10)	7999(7)	117(4)
B(82)	7604(12)	5730(11)	8072(7)	140(6)
B(83)	8306(12)	6276(11)	8226(8)	143(5)
B(84)	8923(11)	5942(8)	8230(7)	114(4)
B(85)	8628(10)	6139(9)	8720(7)	122(5)
B(86)	7834(11)	6022(10)	8617(7)	125(5)
B(87)	7532(9)	5252(10)	8495(7)	119(5)
B(88)	8148(7)	4944(8)	8500(6)	96(3)
B(89)	8775(8)	5492(7)	8627(5)	89(3)
B(90)	8168(9)	5534(9)	8887(7)	109(4)
B(91)	10515(9)	2151(10)	8282(7)	126(4)
B(92)	11256(10)	2575(12)	8200(8)	144(4)
B(93)	11486(11)	2207(13)	7739(9)	162(5)
B(94)	10900(10)	1556(12)	7574(9)	151(4)
B(95)	11539(10)	1512(13)	7905(7)	162(4)
B(96)	11756(10)	2094(10)	8277(8)	152(4)
B(97)	11154(10)	2080(10)	8595(8)	140(4)
B(98)	10586(8)	1504(11)	8403(7)	126(4)
B(99)	10814(9)	1107(12)	7981(8)	143(4)
B(100)	11332(8)	1445(9)	8429(7)	152(4)
B(101)	8205(8)	317(9)	7067(6)	100(4)

B(102)	7417(8)	174(9)	7076(6)	107(4)
B(103)	7885(10)	-683(9)	7515(8)	123(4)
B(104)	8465(9)	-193(8)	7321(7)	108(4)
B(105)	7769(9)	-14(9)	6603(7)	114(4)
B(106)	7126(11)	-533(11)	6760(8)	141(6)
B(107)	7412(13)	-1052(10)	7037(8)	148(6)
B(108)	8227(13)	-856(10)	7043(8)	141(5)
B(109)	8426(11)	-221(9)	6773(7)	121(4)
B(110)	7768(12)	-770(10)	6587(8)	139(5)
B(111)	8965(12)	988(11)	9703(7)	133(5)
B(112)	8888(9)	1681(9)	9795(6)	113(4)
B(113)	8296(9)	1773(9)	9486(6)	104(4)
B(114)	7935(9)	1092(9)	9203(7)	116(4)
B(115)	8330(15)	529(12)	9917(10)	175(7)
B(116)	8677(13)	1219(13)	10180(8)	153(6)
B(117)	8249(11)	1724(11)	10043(7)	133(5)
B(118)	7626(11)	1330(10)	9692(7)	127(5)
B(119)	7658(13)	623(11)	9592(9)	153(6)
B(120)	7876(13)	993(12)	10107(9)	153(6)
Cu(5)	3761(1)	2228(1)	10417(1)	97(1)
Cu(6)	7942(1)	262(1)	3685(1)	93(1)
Cu(7)	6087(1)	3616(1)	3785(1)	103(1)
C(25)	3462(8)	908(8)	9692(6)	118(4)
C(26)	3624(9)	472(9)	9462(6)	150(5)
C(27)	3271(11)	160(10)	9097(7)	176(6)
C(28)	2711(11)	257(11)	8963(8)	178(7)
C(29)	2516(9)	676(10)	9194(7)	155(6)
C(30)	2883(8)	1026(8)	9565(6)	131(5)
C(31)	4652(7)	1191(7)	10149(5)	97(4)
C(32)	4837(8)	778(8)	10377(5)	115(5)
C(33)	5439(9)	708(8)	10351(6)	129(6)
C(34)	5836(8)	1045(8)	10080(6)	116(5)
C(35)	5634(8)	1417(7)	9863(5)	108(4)
C(36)	5039(7)	1513(7)	9884(5)	101(4)
C(37)	3570(7)	921(7)	10618(5)	107(4)
C(38)	2928(6)	1012(7)	10701(6)	108(4)

C(39)	3267(11)	1743(10)	11618(7)	162(5)
C(40)	3292(13)	1935(11)	12065(8)	184(6)
C(41)	3046(15)	2355(13)	12213(9)	210(7)
C(42)	2620(15)	2516(12)	11930(9)	212(7)
C(43)	2579(13)	2380(10)	11476(8)	187(6)
C(44)	2912(12)	1963(9)	11324(7)	156(5)
C(45)	2155(9)	1776(9)	10486(7)	181(6)
C(46)	2097(9)	2198(9)	10211(6)	175(6)
C(47)	1527(9)	2197(10)	10002(8)	206(7)
C(48)	1015(10)	1784(11)	10075(10)	234(8)
C(49)	1067(10)	1338(12)	10338(10)	245(8)
C(50)	1641(9)	1332(11)	10553(9)	224(7)
C(51)	4562(8)	3276(7)	11285(5)	109(4)
C(52)	4001(10)	3386(10)	11346(7)	155(8)
C(53)	3944(13)	3835(13)	11641(9)	201(12)
C(54)	4426(16)	4154(14)	11892(10)	204(13)
C(55)	4994(13)	4092(11)	11837(8)	176(9)
C(56)	5085(9)	3623(8)	11533(6)	136(6)
C(57)	5149(8)	2343(7)	11116(6)	117(5)
C(58)	4950(10)	2055(8)	11477(7)	141(6)
C(59)	5318(12)	1731(10)	11671(9)	174(9)
C(60)	5843(14)	1674(13)	11491(11)	196(12)
C(61)	6040(12)	1941(12)	11127(10)	187(10)
C(62)	5679(8)	2287(9)	10931(6)	141(6)
C(63)	5066(7)	3174(7)	10476(5)	102(4)
C(64)	4631(7)	3463(7)	10233(5)	106(4)
C(65)	3429(8)	3379(8)	9820(6)	114(4)
C(66)	3261(9)	3475(9)	9407(7)	148(5)
C(67)	2853(10)	3818(11)	9325(8)	170(6)
C(68)	2614(10)	4067(10)	9647(9)	158(6)
C(69)	2756(9)	3983(9)	10039(8)	144(5)
C(70)	3171(8)	3630(8)	10153(7)	129(5)
C(71)	4186(7)	2694(7)	9430(5)	99(4)
C(72)	3814(11)	2210(8)	9194(6)	147(7)
C(73)	4013(14)	1979(11)	8813(7)	188(11)
C(74)	4550(12)	2259(13)	8661(7)	163(8)

C(75)	4910(10)	2715(13)	8887(7)	179(10)
C(76)	4726(9)	2968(11)	9267(6)	154(8)
C(77)	4761(8)	4204(7)	3832(6)	120(4)
C(78)	4531(9)	3771(9)	4096(8)	151(7)
C(79)	3961(11)	3701(12)	4247(10)	194(10)
C(80)	3586(12)	4059(13)	4097(11)	204(12)
C(81)	3813(11)	4475(12)	3834(11)	204(12)
C(82)	4402(9)	4573(10)	3706(7)	152(7)
C(83)	5855(8)	5043(8)	3688(7)	121(5)
C(84)	5872(9)	5333(9)	4099(7)	139(6)
C(85)	6166(12)	5908(11)	4199(10)	183(10)
C(86)	6426(14)	6206(10)	3904(12)	188(12)
C(87)	6442(12)	5962(12)	3469(10)	186(10)
C(88)	6141(10)	5362(10)	3376(8)	156(7)
C(89)	5317(8)	4093(8)	3031(6)	130(5)
C(90)	5148(7)	3446(8)	2909(6)	121(5)
C(91)	6312(5)	3367(6)	2663(4)	119(4)
C(92)	6782(6)	3875(6)	2753(4)	162(8)
C(93)	7149(6)	4079(6)	2428(5)	198(12)
C(94)	7046(7)	3777(8)	2013(4)	195(11)
C(95)	6576(7)	3270(7)	1922(3)	182(10)
C(96)	6209(6)	3065(5)	2248(4)	157(7)
C(97)	5560(10)	2373(8)	2995(7)	136(5)
C(98)	4982(11)	2059(9)	3020(7)	158(6)
C(99)	4807(12)	1431(10)	3001(8)	170(6)
C(100)	5253(12)	1156(10)	2928(8)	162(6)
C(101)	5832(11)	1428(9)	2876(7)	163(6)
C(102)	5989(10)	2057(9)	2909(7)	155(5)
C(103)	5416(8)	2296(8)	4282(6)	122(4)
C(104)	4803(9)	2191(9)	4185(7)	152(5)
C(105)	4404(10)	1652(9)	4123(8)	170(6)
C(106)	4638(10)	1178(9)	4158(8)	155(6)
C(107)	5262(10)	1231(8)	4243(8)	153(5)
C(108)	5642(9)	1817(8)	4314(7)	139(5)
C(109)	5691(8)	3377(8)	4847(6)	108(4)
C(110)	5764(9)	3967(8)	4905(6)	130(6)

C(111)	5638(12)	4230(10)	5300(6)	160(8)
C(112)	5435(12)	3899(11)	5622(7)	162(9)
C(113)	5365(12)	3336(11)	5573(8)	166(9)
C(114)	5493(9)	3047(9)	5193(6)	131(6)
C(115)	7555(8)	4632(8)	4176(6)	147(5)
C(116)	7441(8)	5073(7)	3944(6)	145(5)
C(117)	7765(8)	5654(8)	4027(7)	159(6)
C(118)	8178(11)	5800(11)	4389(8)	203(7)
C(119)	8397(12)	5363(9)	4582(7)	208(8)
C(120)	8076(10)	4776(9)	4481(7)	197(7)
C(121)	7628(8)	3555(10)	3722(6)	135(5)
C(122)	8255(10)	3783(11)	3719(8)	165(6)
C(123)	8578(11)	3459(12)	3474(9)	179(7)
C(124)	8342(12)	2950(13)	3266(9)	188(7)
C(125)	7747(11)	2711(12)	3281(8)	174(6)
C(126)	7359(10)	2989(10)	3530(7)	151(5)
C(127)	6675(7)	2978(7)	4522(5)	105(4)
C(128)	7138(8)	3568(7)	4560(5)	115(5)
C(129)	6756(4)	-623(4)	2872(3)	95(4)
C(130)	6166(4)	-938(5)	2932(3)	118(5)
C(131)	5926(4)	-1488(5)	2707(4)	137(7)
C(132)	6275(5)	-1723(4)	2421(4)	127(6)
C(133)	6864(5)	-1408(6)	2360(4)	165(9)
C(134)	7105(4)	-858(5)	2586(4)	145(7)
C(135)	7149(7)	568(8)	2747(6)	117(5)
C(136)	7577(9)	1096(8)	2776(6)	131(6)
C(137)	7631(10)	1483(10)	2466(8)	159(8)
C(138)	7251(11)	1346(11)	2082(8)	181(10)
C(139)	6835(11)	781(11)	2025(7)	166(8)
C(140)	6789(8)	428(9)	2348(6)	141(7)
C(141)	6512(6)	246(7)	3493(5)	105(4)
C(142)	6768(7)	806(7)	3812(5)	107(4)
C(143)	7739(7)	1493(7)	4418(5)	100(4)
C(144)	8132(10)	1905(8)	4225(6)	138(6)
C(145)	8381(10)	2478(8)	4414(7)	141(7)
C(146)	8212(9)	2640(9)	4818(7)	131(6)

C(147)	7825(8)	2236(8)	4997(6)	121(5)
C(148)	7560(7)	1678(7)	4823(5)	106(4)
C(149)	7175(7)	333(7)	4592(5)	101(4)
C(150)	7594(8)	247(8)	4919(5)	115(5)
C(151)	7415(9)	-95(8)	5251(6)	125(5)
C(152)	6800(10)	-364(8)	5268(6)	134(6)
C(153)	6376(9)	-295(9)	4941(6)	134(6)
C(154)	6552(7)	77(8)	4613(6)	118(5)
C(155)	8479(7)	-672(7)	4370(5)	95(4)
C(156)	8866(7)	-185(7)	4599(5)	106(4)
C(157)	9185(8)	-186(9)	4994(6)	125(6)
C(158)	9093(8)	-687(9)	5187(6)	127(6)
C(159)	8692(8)	-1184(9)	4982(6)	136(6)
C(160)	8382(7)	-1173(8)	4571(5)	115(5)
C(161)	6940(9)	-1273(9)	3988(7)	145(5)
C(162)	6418(9)	-1737(9)	3973(8)	154(6)
C(163)	6431(10)	-2215(10)	3686(8)	157(6)
C(164)	6885(11)	-2238(9)	3437(7)	155(6)
C(165)	7446(10)	-1779(8)	3497(7)	153(6)
C(166)	7451(8)	-1295(7)	3765(6)	116(4)
C(167)	8621(7)	-753(7)	3465(5)	109(4)
C(168)	9152(7)	-212(7)	3464(5)	111(4)
C(169)	8957(8)	638(8)	2883(6)	111(4)
C(170)	8719(8)	204(9)	2531(6)	132(6)
C(171)	8692(11)	320(12)	2107(7)	166(8)
C(172)	8913(15)	903(15)	2008(9)	207(12)
C(173)	9132(14)	1364(13)	2355(9)	207(12)
C(174)	9155(11)	1202(10)	2779(8)	165(8)
C(175)	9554(7)	1013(7)	3733(5)	100(4)
C(176)	10156(8)	1070(9)	3594(6)	136(7)
C(177)	10657(9)	1479(9)	3803(7)	145(7)
C(178)	10571(9)	1845(9)	4150(7)	139(7)
C(179)	9992(9)	1785(8)	4291(6)	136(6)
C(180)	9490(8)	1363(8)	4081(5)	116(5)
P(1)	3892(2)	1327(2)	10182(1)	98(1)
P(2)	4623(2)	2721(2)	10859(1)	101(1)

P(3)	3948(2)	2938(2)	9955(1)	95(1)
P(4)	2918(2)	1785(2)	10738(2)	115(1)
P(5)	5520(2)	4268(2)	3624(2)	112(1)
P(6)	5813(2)	3159(2)	3089(2)	112(1)
P(7)	7112(2)	3889(2)	4034(1)	108(1)
P(8)	5904(2)	3035(2)	4344(2)	104(1)
P(9)	7455(2)	754(2)	4156(1)	98(1)
P(10)	7111(2)	93(2)	3166(1)	95(1)
P(11)	8901(2)	475(2)	3443(1)	101(1)
P(12)	8077(2)	-623(2)	3855(1)	98(1)

checkCIF/PLATON report (justification)

Alert level B

PLAT342_ALERT_3_B Low Bond Precision on C-C Bonds 0.02913 Ang.

Response: The structure contains disordered phenyl moieties. This caused low accuracies in C-C bonds

PLAT973_ALERT_2_B Check Calcd Positive Resid. Density on Ag1 1.93 eA-3

Response: These are Fourier truncation ripples around the heavy atoms.

Supplementary Table 5 | Atomic coordinates ($\times 10^4$) and equivalent isotropic displacement parameters ($\text{\AA}^2 \times 10^3$) for AuAg₁₆ nanocluster. $U(\text{eq})$ is defined as one third of the trace of the orthogonalized U_{ij}^2 tensor. Check CIF justifications of level A and level B alerts.

	<i>x</i>	<i>y</i>	<i>z</i>	$U(\text{eq})$
Au(1)	6667	3333	5573(1)	164(2)
Ag(1)	7283(2)	3818(2)	5951(1)	169(2)
Ag(2)	6783(2)	3929(2)	5195(1)	176(2)
Ag(3)	6980(2)	4364(2)	5650(1)	172(2)
Ag(4)	7690(2)	4070(2)	5505(1)	172(2)

Ag(5)	6667	3333	6374(2)	180(3)
Ag(6)	6440(2)	4707(2)	5308(1)	187(2)
S(1)	7591(6)	4060(6)	6348(3)	182(5)
S(2)	6767(6)	4558(6)	4921(3)	183(5)
S(3)	7092(6)	5227(6)	5613(3)	182(5)
S(4)	8617(6)	4475(6)	5422(3)	189(6)
C(1)	7572(18)	4631(17)	6396(9)	188(9)
C(2)	7660(20)	5098(19)	6206(9)	188(9)
B(1)	8140(20)	5185(18)	6394(11)	188(9)
B(2)	7800(20)	4936(19)	6645(10)	190(9)
B(3)	7190(20)	4656(19)	6603(10)	190(9)
B(4)	7120(20)	4790(20)	6332(11)	189(9)
B(5)	8010(20)	5660(20)	6335(10)	189(10)
B(6)	8120(20)	5583(19)	6598(11)	189(10)
B(7)	7490(20)	5240(19)	6732(9)	191(10)
B(8)	7110(20)	5156(18)	6549(11)	190(9)
B(9)	7380(20)	5430(20)	6300(10)	190(9)
B(10)	7657(19)	5734(18)	6547(9)	191(9)
C(3)	6200(14)	4191(15)	4754(7)	196(9)
C(4)	6363(19)	4261(18)	4479(8)	209(11)
B(11)	5643(17)	3641(15)	4805(7)	197(11)
B(12)	5651(17)	4211(16)	4793(7)	195(10)
B(13)	6081(16)	4589(14)	4591(8)	201(10)
B(14)	5850(20)	3710(20)	4330(10)	212(12)
B(15)	5860(20)	4282(17)	4338(8)	211(12)
B(16)	5440(16)	4262(16)	4535(8)	203(11)
B(17)	5160(13)	3678(16)	4669(8)	200(11)
B(18)	5390(20)	3312(16)	4558(9)	201(12)
B(19)	5300(17)	3719(17)	4387(8)	204(12)
B(20)	6043(19)	3662(16)	4595(9)	204(10)
C(5)	7683(14)	5653(15)	5473(8)	200(10)
C(6)	7840(20)	6263(17)	5406(10)	209(11)
B(21)	7670(30)	5820(20)	5199(8)	208(11)
B(22)	7930(30)	5440(30)	5269(10)	211(11)
B(23)	8210(20)	5600(20)	5529(12)	205(11)
B(24)	8210(20)	6160(20)	5589(12)	208(12)

B(25)	8800(30)	6350(30)	5498(10)	218(13)
B(26)	8470(30)	6640(30)	5410(10)	217(12)
B(28)	8280(30)	5930(20)	5075(12)	217(13)
B(27)	8180(20)	6420(30)	5155(12)	218(12)
B(29)	8550(30)	5860(20)	5315(12)	216(11)
B(30)	8754(16)	6450(20)	5216(9)	221(13)
C(7)	8967(13)	4611(15)	5684(6)	172(9)
C(8)	9173(16)	4189(15)	5728(9)	174(9)
B(31)	8730(20)	4192(18)	5904(9)	172(10)
B(32)	8850(20)	4802(18)	5935(9)	179(9)
B(33)	9368(18)	5216(14)	5781(11)	181(10)
B(34)	9611(13)	4834(16)	5702(13)	179(10)
B(35)	8982(16)	4520(19)	6155(12)	181(11)
B(36)	9420(20)	5128(19)	6068(12)	188(11)
B(37)	9920(20)	5150(18)	5923(11)	187(11)
B(38)	9770(20)	4531(19)	5883(10)	183(10)
B(39)	9170(17)	4165(18)	5998(11)	179(10)
B(40)	9614(15)	4704(17)	6129(7)	189(11)
Au(2)	4924(1)	4733(1)	7277(1)	213(2)
P(1)	4542(7)	4490(7)	6904(4)	219(6)
P(2)	5682(7)	4807(7)	7108(4)	212(7)
P(3)	4822(9)	5337(9)	7503(5)	280(8)
P(4)	4427(8)	4117(8)	7566(4)	254(7)
C(15)	5590(20)	4820(20)	6827(11)	234(16)
C(16)	4990(20)	4370(20)	6809(10)	206(15)
C(9)	5830(20)	4273(14)	7177(11)	256(13)
C(10)	6106(17)	4141(19)	7032(7)	262(15)
C(11)	6125(15)	3690(20)	7069(9)	261(15)
C(12)	5860(20)	3379(12)	7252(11)	281(18)
C(13)	5585(17)	3510(20)	7397(7)	291(17)
C(14)	5566(16)	3960(20)	7359(9)	278(15)
C(17)	6296(14)	5464(16)	7142(10)	256(13)
C(18)	6630(30)	5416(17)	7286(9)	290(17)
C(19)	7100(20)	5850(30)	7346(7)	311(19)
C(20)	7218(13)	6330(20)	7261(10)	320(20)
C(21)	6880(20)	6376(14)	7117(9)	308(19)

C(22)	6418(19)	5940(30)	7057(7)	303(17)
C(23)	4490(20)	4990(20)	6723(9)	243(14)
C(24)	4226(15)	4855(13)	6519(11)	250(15)
C(25)	4257(16)	5230(30)	6374(6)	261(16)
C(26)	4560(20)	5750(20)	6432(9)	269(18)
C(27)	4823(15)	5887(14)	6635(11)	261(17)
C(28)	4792(17)	5510(30)	6781(6)	248(15)
C(29)	3884(12)	3906(14)	6861(8)	216(12)
C(30)	3806(15)	3460(20)	6754(7)	244(16)
C(31)	3310(20)	3040(13)	6735(7)	247(16)
C(32)	2896(11)	3066(15)	6822(8)	247(17)
C(33)	2974(16)	3510(20)	6928(7)	229(16)
C(34)	3470(20)	3932(13)	6948(6)	221(15)
C(35)	3991(10)	3420(11)	7481(7)	272(13)
C(36)	3467(10)	3191(12)	7522(7)	281(17)
C(37)	3126(12)	2736(13)	7413(8)	296(18)
C(38)	3309(17)	2509(13)	7263(7)	310(20)
C(39)	3834(18)	2738(13)	7222(7)	323(19)
C(40)	4175(14)	3193(13)	7330(7)	305(17)
C(41)	4810(30)	4050(30)	7809(6)	304(16)
C(42)	4467(16)	3600(20)	7920(14)	326(19)
C(43)	4590(30)	3496(17)	8133(14)	330(20)
C(44)	5050(30)	3850(30)	8235(6)	330(20)
C(45)	5387(17)	4300(20)	8125(11)	320(20)
C(46)	5270(20)	4403(18)	7912(11)	305(19)
C(47)	4420(30)	5570(30)	7349(7)	290(13)
C(48)	4717(14)	6100(30)	7361(8)	303(16)
C(49)	4560(30)	6411(15)	7252(11)	317(17)
C(50)	4100(30)	6190(30)	7131(8)	308(18)
C(51)	3801(16)	5650(30)	7120(6)	297(17)
C(52)	3960(20)	5347(14)	7228(9)	302(16)
C(53)	5320(20)	5857(16)	7698(10)	322(14)
C(54)	5304(18)	6140(20)	7881(11)	335(18)
C(55)	5750(30)	6464(18)	7998(7)	344(19)
C(56)	6217(19)	6510(19)	7932(12)	360(20)
C(57)	6230(20)	6230(30)	7749(13)	364(19)

C(58)	5790(40)	5900(20)	7632(8)	351(17)
C(59)	4290(30)	4820(30)	7726(13)	305(14)
C(60)	3920(30)	4240(30)	7685(13)	295(14)

checkCIF/PLATON report (justification)

Alert level A

THETM01_ALERT_3_A The value of sine(theta_max)/wavelength is less than 0.550

Calculated sin(theta_max)/wavelength = 0.4539

Response: The crystal is very weakly diffracting at higher angles. Even though data was collected up to 0.82 Å resolution, the crystal did not diffract at higher angles. Hence a resolution cut was applied during data integration. This is the only crystal that we could obtain after several repeated crystallization.

PLAT084_ALERT_3_A High wR2 Value (i.e. > 0.25) 0.54 Report

Response: The crystal diffracted extremely weakly. Also the peripheral moieties are highly disordered. Inclusion of very weak reflections above 35 degrees caused high wR2.

PLAT973_ALERT_2_A Check Calcd Positive Resid. Density on Au1 5.12 eA-3

Response: The electron density is observed near a heavy atom. Due to poor quality of the data, absorption correction is not adequate.

PLAT973_ALERT_2_A Check Calcd Positive Resid. Density on Au2 3.11 eA-3

Response: The electron density is observed near a heavy atom. Due to poor quality of the data, absorption correction is not adequate.

PLAT973_ALERT_2_A Check Calcd Positive Resid. Density on Ag1 3.04 eA-3

Response: The electron density is observed near a heavy atom. Due to poor quality of the data, absorption correction is not adequate.

PLAT973_ALERT_2_A Check Calcd Positive Resid. Density on Ag3 2.92 eA-3

Response: The electron density is observed near a heavy atom. Due to poor quality of the data, absorption correction is not adequate. PLAT973_ALERT_2_A Check Calcd Positive Resid. Density on Ag4 2.82 eA-3

Response: The electron density is observed near a heavy atom. Due to poor quality of the data, absorption correction is not adequate.

PLAT973_ALERT_2_A Check Calcd Positive Resid. Density on Ag2 2.76 eA-3

Response: The electron density is observed near a heavy atom. Due to poor quality of the data, absorption correction is not adequate.

PLAT973_ALERT_2_A Check Calcd Positive Resid. Density on Ag5 2.60 eA-3

Response: The electron density is observed near a heavy atom. Due to poor quality of the data, absorption correction is not adequate.

PLAT973_ALERT_2_A Check Calcd Positive Resid. Density on Ag6 2.54 eA-3

Response: The electron density is observed near a heavy atom. Due to poor quality of the data, absorption correction is not adequate.

Alert level B

PLAT026_ALERT_3_B Ratio Observed / Unique Reflections (too) Low .. 30% Check

Response: The data quality is very poor due to very weak diffraction of the crystal. Several attempts were made to prepare the crystal during a period of 6-7 months and we could get this crystal specimen only for the data collection. A total of 21 runs performed by an optimized data collection strategy, however only 5 runs contain diffraction spots.

PLAT082_ALERT_2_B High R1 Value 0.17 Report

Response: Data quality is very poor and also the structure contains disordered moieties. All the carborane moieties are refined using DFIX, SIMU and ISOR restraints. Due to poor resolution of the crystal, AFIX 66 was used to generate idealized coordinates for all phenyl moieties. All these factors contributed to high R1 values. The data presented here is only used for representation purpose and to show that the molecule has been formed with the support of other experimental observations.

PLAT094_ALERT_2_B Ratio of Maximum / Minimum Residual Density 4.47 Report

Response: The residual electron density is observed near a heavy atom. Due to poor quality of the data, absorption correction is not adequate.

PLAT342_ALERT_3_B Low Bond Precision on C-C Bonds 0.08463 Ang.

Response: Due to poor resolution of the crystal and disorder in phenyl moieties, the accuracies in C-C bonds are low.

Supplementary Table 6 | Atomic coordinates ($\times 10^4$) and equivalent isotropic displacement parameters ($\text{\AA}^2 \times 10^3$) for AuAg₁₂Cu₄ nanocluster. $U(\text{eq})$ is defined as one third of the trace of the orthogonalized U_{ij}^{ij} tensor. Check CIF justifications of level A and level B alerts.

	x	y	z	$U(\text{eq})$
Cu(1)	6946(1)	1946(1)	6946(1)	82(1)
Ag(1)	6849(1)	1654(1)	6242(1)	66(1)
Au(1)	6250	1250	6250	58(1)
S(1)	7279(1)	2072(1)	6481(1)	88(1)
C(1)	7172(4)	2489(4)	6307(4)	96(4)
C(2)	7042(5)	2820(4)	6573(5)	125(5)
B(1)	7466(8)	2816(6)	6365(8)	160(10)
B(2)	7418(5)	2635(4)	5976(5)	105(5)
B(3)	6994(5)	2525(4)	5899(4)	93(4)
B(4)	6768(5)	2640(4)	6272(4)	95(5)
B(5)	7225(8)	3215(5)	6381(8)	155(10)
B(6)	6811(8)	3105(5)	6308(7)	139(8)
B(7)	6748(6)	2913(4)	5886(5)	112(6)
B(8)	7171(6)	2916(5)	5732(6)	134(8)
B(9)	7441(8)	3097(6)	6017(8)	156(10)
B(10)	7040(7)	3259(5)	5981(7)	143(8)

checkCIF/PLATON report (justification)

Alert level B

PLAT973_ALERT_2_B Check Calcd Positive Resid. Density on Ag1 1.76 eA-3

Response: Residual electron density is found near the metal atoms as

expected for heavy atom structures, which are probably due to absorption error or Fourier ripples around the heavy atom.

PLAT973_ALERT_2_B Check Calcd Positive Resid. Density on Au1 1.76 eA-3

Response: Residual electron density is found near the metal atoms as

expected for heavy atom structures, which are probably due to absorption error or Fourier ripples around the heavy atom.